

Mechanisms of Specificity in Neuronal Activity-regulated Gene Transcription

by

Liang-Fu Chen

Department of Neurobiology
Duke University

Date: _____

Approved:

Anne West, Supervisor

Jörg Grandl, Chair

Debra Silver

Jeremy Kay

Dissertation submitted in partial fulfillment of
the requirements for the degree of Doctor
of Philosophy in the Department of
Neurobiology in the Graduate School
of Duke University

2017

ABSTRACT

Mechanisms of Specificity in Neuronal Activity-regulated Gene Transcription

by

Liang-Fu Chen

Department of Neurobiology
Duke University

Date: _____

Approved:

Anne West, Supervisor

Jörg Grandl, Chair

Debra Silver

Jeremy Kay

An abstract of a dissertation submitted in partial fulfillment of the requirements for the degree of Doctor of Philosophy in the Department of Neurobiology in the Graduate School of Duke University

2017

Copyright by
Liang-Fu Chen
2017

Abstract

The ability to convert sensory stimuli into long-lasting changes in brain function is essential for animals to interact with and learn from their environment. This process is achieved by encoding sensory stimuli into temporal patterns of neuronal activity, which in turn modulate the connectivity and strength of neural circuits in the brain. These long-term plastic changes in the brain are known to depend on the neuronal activity-regulated transcription of new gene products. My dissertation research sought to elucidate how the timing and level of transcriptional responses following neuronal activity can be precisely regulated to form proper neuronal connections. In the first part of this dissertation, I investigated the role of the developmentally regulated GluN3A subunit in NMDAR-induced transcription. I observed that neurons lacking the transcription factor CaRF showed enhanced NMDAR-induced expression of *Bdnf* and *Arc* both in cultured neurons and following sensory stimulation in the developing brain in vivo. I identified GluN3A as a regulatory target of CaRF and found that neurons lacking GluN3A showed selective enhancement of NMDAR-induced transcription. GluN3A limited synaptic activity-induced transcription by inhibiting both NMDAR-induced nuclear translocation of the p38 MAP kinase and activation of the transcription factor MEF2C. These data demonstrate that GluN3A negatively regulates NMDAR-dependent activation of gene transcription and reveal a novel mechanism that regulates the level of NMDAR-induced transcriptional response in the developing brain. In the second part of my dissertation, I examined the role of enhancer histone acetylation in neuronal activity-regulated gene transcription. I applied quantitative single-molecule fluorescence in situ hybridization to measure neuronal activity-induced gene transcription at the single neuron level, taking advantage of the intrinsic stochasticity of transcription to quantify the effects of enhancer regulation on the dynamics of promoter state transitions. Locally-induced enhancer histone acetylation by CRISPR-mediated epigenome editing was sufficient to increase *Fos* mRNA expression both under basal conditions and

following membrane depolarization in primary hippocampal neurons, via a mechanism that involves enhancer recruitment of Brd4, increased transcriptional elongation by the release of paused polymerase, and prolonged activation of *Fos* promoters. These data indicate that enhancer histone acetylation plays a causative role in the induction of neuronal activity-regulated gene transcription and open up the possibility to specifically control the level and timing of the neuronal activity-induced transcriptional response. Taken together my dissertation works elucidate mechanisms that control the specificity, timing, and amplitude of transcriptional responses to neuronal activity, revealing novel information about the dynamic range of this fundamental cellular process.

Contents

Abstract.....	i
List of Tables	ix
List of Figures	x
Acknowledgement	iv
1. Introduction	1
1.1 Mechanisms of neuronal activity-regulated transcription	2
1.2 Receptors and stimulus specificity.....	6
1.3 Transcription Factors and Synapse Specificity.....	7
1.3.1 Npas4: An activity-dependent, cell-type specific master regulator of inhibitory/excitatory balance.....	8
1.3.2 MEF2: activation, repression, transcription, translation—MEF2 does it all.....	12
1.4 Chromatin Regulation in neuronal activity-regulated gene transcription.....	16
1.4.1 ATP-dependent chromatin remodelers.	16
1.4.2 CHD4: timing transcriptional repression.....	19
1.4.3 Epigenome editing by CRISRP-based method.....	22
2. The transcription factor CaRF limits NMDAR-dependent transcription in the developing brain	23
2.1 Summary	23
2.2 Introduction	23
2.3 Materials and Methods.....	25
2.3.1 Dissociated Neuron Cultures	25
2.3.2 Quantitative PCR.....	26
2.3.3 RNAi and Lentiviral Infection	26
2.3.4 Immunofluorescence	27
2.3.5 Western Blotting.....	27
2.3.6 Electrophoretic Mobility Shift Assays (EMSA)	28
2.3.7 BDNF ELISA.....	28
2.3.8 Pilocarpine-induced Seizure.....	28
2.3.9 Dark Adaptation and Light Exposure	29
2.3.10 Quantification of inhibitory synapse density	29
2.3.11 Statistical Analyses.....	30
2.4 Results.....	30
2.4.1 Loss of CaRF results in potentiation of NMDAR-dependent transcription.....	30

2.4.2 The NMDAR subunit gene Grin3a is a regulatory target of CaRF	34
2.4.3 Enhanced sensory experience induced gene transcription in the developing cortex of CaRF knockout mice.....	40
2.4.4 Enhanced BDNF expression in CaRF-knockdown neurons accelerates inhibitory synapse development.....	42
2.5 Discussion.....	44
2.5.2 Modulation of NMDAR-dependent transcription.....	46
2.5.3 Activity-dependent transcription in the developing brain	47
3. The NMDA receptor subunit GluN3A inhibits synaptic activity-induced and MEF2C-dependent transcription.....	49
3.1 Summary	49
3.2 Introduction	49
3.3 Materials and Methods.....	51
3.3.1 Plasmids	51
3.3.2 Dissociated Neuron Cultures	51
3.3.3 Lentiviral Infection	52
3.3.4 Neuronal Transfection for Luciferase Assays.....	52
3.3.5 Western Blotting.....	53
3.3.6 Immunofluorescence	53
3.3.7 Antibodies.....	53
3.3.8 Quantitative PCR.....	54
3.3.9 Statistical Analyses.....	54
3.4 Results.....	54
3.4.1 The NMDAR subunit GluN3A inhibits NMDAR-induced MEF2 transcriptional program	54
3.4.2 GluN3A inhibits NMDAR-dependent gene transcription via a p38MAPK-MEF2C pathway	57
3.4.3 Enhanced NMDAR-dependent nuclear activation of p38 MAPK in GluN3A knockdown neurons	63
3.5 Discussion.....	65
4. Histone acetylation at enhancers prolongs the activation of neuronal activity-inducible gene transcription.....	70
4.1 Summary	70
4.2 Introduction	70
4.3 Materials and Methods.....	73

4.3.1 Plasmids	73
4.3.2 Dissociated Neuron Cultures	73
4.3.3 Cell Culture.....	74
4.3.4 Immunofluorescence	74
4.3.5 Immunofluorescence image acquisition and analysis	74
4.3.6 Reverse transcription and quantitative PCR.....	74
4.3.7 Chromatin Immunoprecipitation-Qpcr.....	75
4.3.8 Single molecule fluorescence in situ hybridization.....	75
4.3.9 smFISH image acquisition and analysis.....	76
4.3.10 Mathematical modeling.....	76
4.3.11 Calcium Imaging.....	77
4.3.12 Electrophysiology and analysis	77
4.3.13 Statistical Analyses.....	77
4.4 Results.....	78
4.4.1 Local induction of H3K27ac at Fos enhancers is sufficient to drive transcription via Brd4 recruitment and activation of transcriptional elongation.....	78
4.4.2 Transient membrane depolarization drives dynamic H3K27 acetylation at Fos regulatory elements that matches the time course of Fos transcription.....	83
4.4.3 Single neuron analysis of gene expression reveals gene-local, probabilistic regulation of neuronal activity-dependent transcription	85
4.4.4 Local induction of H3K27ac at Fos enhancers alters the dynamics of Fos promoter state transitions, increasing Fos protein expression and driving functional neuronal adaptations	90
4.5 Discussion.....	95
5. Conclusion and Discussion	99
5.1 CaRF: a context-specific regulator of Bdnf transcription and GABAergic synapse formation	99
5.2 Single cell analysis of neuronal activity-regulated gene transcription	102
5.3 Epigenome editing in neuronal activity-regulated gene transcription.....	105
Appendix A.....	107
Appendix B.....	109
Reference.....	110
Biography.....	125

List of Tables

Table1: The best fit parameters in k_{ON} -sensitive two-state promoter model.....	92
---	----

List of Figures

Figure 1: Mechanisms that regulate activity-dependent transcription of <i>Fos</i>	3
Figure 2: Genomic views of neuronal activity dependent gene transcription.....	5
Figure 3: <i>Npas4</i> expression is induced rapidly by neuronal activity.....	9
Figure 4: Neuronal activity induces MEF2-dependent gene transcription.....	14
Figure 5: Specificity in BAF complex.....	18
Figure 6: NuRD controls the timing of gene expression by turning genes off both on a developmental timescale and in response to transient neuronal activity.....	20
Figure 7: Stimulus-specific induction of <i>Bdnf</i> exon IV transcription.....	30
Figure 8: Validation of <i>Carf</i> shRNA.....	31
Figure 9: <i>Carf</i> knock down potentiates NMDARs dependent <i>Bdnf</i> exon IV transcription.....	32
Figure 10: Levels of <i>Arc</i> and <i>Fos</i> mRNA in <i>Carf</i> knock down neurons following TTX WD.....	33
Figure 11: mRNA levels of NMDAR subunits in cultured mouse cortical neurons.....	34
Figure 12: GluN3A level in <i>Carf</i> knock down and knock out neurons.....	34
Figure 13: <i>Carf</i> and <i>Grin3a</i> expression are inversely regulated by neuronal activity.....	36
Figure 14: CaRF does not bind to <i>Grin3a</i> promoter directly.....	37
Figure 15: Schematic diagram showing the protein domain organization of CaRF and the targeting sites of <i>Carf</i> shRNAs.....	37
Figure 16: <i>Grin3a</i> expression is regulated by a specific CaRF isoform.....	38
Figure 17: GluN3A rescues the potentiated <i>Bdnf</i> and <i>Arc</i> expression in <i>Carf</i> knock down neurons.....	39
Figure 18: BDNF expression is potentiated in visual cortex of <i>Carf</i> knock down mice following light stimulation.....	40
Figure 19: Light exposure does not induce gene transcription in somatosensory cortex.....	41
Figure 20: Accelerated inhibitory synapse formation in <i>Carf</i> knock down neurons.....	43
Figure 21: Validation of <i>Grin3a</i> shRNA viruses.....	54
Figure 22: NMDARs dependent gene transcription is potentiated in <i>Grin3a</i> knock down neurons.....	55

Figure 23: Validation of GluN3A overexpression virus.....	56
Figure 24: MEF2 transcriptional activity is potentiated in <i>Grin3a</i> knock down neurons.....	57
Figure 25: MEF2C is required for the potentiated <i>Bdnf</i> transcription in <i>Grin3a</i> knock down neurons.....	58
Figure 26: Validation of Mef2 shRNA viruses.....	59
Figure 27: MEF2C is sufficient to drive the potentiated <i>Bdnf</i> transcription in <i>Grin3a</i> knock down.....	60
Figure 28: Identification of kinase that mediates the potentiated MEF2 activity in <i>Grin3a</i> knock down neurons.....	61
Figure 29: Ser-387 of MEF2C is phosphorylated in <i>Grin3a</i> knock down neurons following NMDARs activation.....	62
Figure 30: p38 kinase inhibitor, SB203580, inhibits the potentiated of <i>Bdnf</i> transcription in <i>Grin3a</i> knock down neurons.....	62
Figure 31: Potentiation of activated p38 in the nucleus of neurons lacking <i>Grin3a</i> following TTX WD.....	64
Figure 32: Phosphorylated p38 is accumulated in the nucleus of neurons lacking <i>Grin3a</i> following TTX WD.....	65
Figure 33: The epigenetic landscape of the <i>Fos</i> genomic locus in embryonic 16.5 day mouse forebrain.....	78
Figure 34: Locations of gRNAs used in this study.....	78
Figure 35: Induction of <i>Fos</i> transcription by dCas9-p300 in N2A cell.....	79
Figure 36: Recruitment of dCas9-p300 to <i>Fos</i> enhancers.....	80
Figure 37: Induction of histone acetylation at <i>Fos</i> enhancer by dCas9-p300.....	81
Figure 38: Enhanced Brd4 dependent transcriptional activation by histone acetylation at enhancers.....	82
Figure 39: Induction of histone acetylation and <i>Fos</i> transcription by a short pulse of membrane depolarization.....	84
Figure 40: Induction of <i>Fos</i> transcription by TSA.....	85
Figure 41: Variation of intracellular calcium and <i>Fos</i> protein expression following membrane depolarization.....	86
Figure 42: Distribution of <i>Fos</i> mRNA and active transcription sites by smFISH.....	86

Figure 43: The induction of <i>Fos</i> and <i>Npas4</i> following membrane depolarization by RT-qPCR and smFISH.....	87
Figure 44: Fraction of excitatory (GAD65-) and inhibitory (GAD65+) neurons (MAP2+) in primary cultured hippocampal neurons.....	88
Figure 45: Distribution of <i>Fos</i> and <i>Npas4</i> mRNA and active transcription sites by two color smFISH.....	89
Figure 46: Average distance between two active TSs of indicated genes at 20 min following 5min 55mM KCl.....	89
Figure 47: Distribution of <i>Fos</i> mRNA and active transcription sites in primary hippocampal neurons transfected with dCas9-p300 and indicated gRNAs.....	90
Figure 48: Diagram of the two-state promoter model.....	91
Figure 49: Enhanced <i>Fos</i> protein expression in primary neurons transfected with dCas9-p300 and <i>Enh2</i> gRNAs.....	93
Figure 50: increased AP1 transcriptional activity and reduced resting membrane potential in neurons transfected with dCas9-p300 and <i>Enh2</i> gRNAs.....	94
Figure 51: Regulation of <i>Bdnf</i> transcription by CaRF.....	99
Figure 52: Diagram of control activity-regulated gene transcription by epigenetic editing.....	105

Acknowledgement

I am very grateful to my adviser, Anne West, for her constant support and enthusiasm. She gave me freedom to explore and do anything I deem important, but in the meantime provided me with guidance whenever I need it. I would like also thanks my thesis committee, Jörg Grandl, Debra Silver, Jeremy Kay for their helpful insights and constructive criticisms.

I would like to thank the previous and current members in West lab for making the lab a fun place to work. I would also like to thank everyone who helped on my research projects: Michelle for starting projects in Chapter 2 and 3. Andreas for the identification of CaRF targets in Chapter 2. Aditi, Jie and Kelli for their assistance in the experiments in Chapter 2 and 3. David for his assistance in the experiments in Chapter 4. Bre and Jorg for the recording in Chapter 4. Mariana and Nick for the mathematical model and critical discussion in Chapter 4. Finally, I would like to thank the undergraduate students worked with me, Caitlin, Marty and Allen, for working hard and help on my projects.

Last, but definitely not least, I would like to thank everyone in Duke community who discussed ideas, shared reagents and provided technical assistance.

1. Introduction

The mammalian brain is a paragon of complexity. The average human brain contains tens of billions of neurons and hundreds of trillions of synaptic connections (Bargmann and Marder, 2013; DeFelipe, 2010). Yet every day, legions of new brains are assembled from scratch in developing embryos, and for the most part they work as intended. As is true for all developmental programs, the fundamental instructions for wiring the brain are encoded in DNA. Those plans are executed in concert with signals from the environment that guide and refine the developmental process. Importantly, during the prenatal period both the intrinsic and extrinsic regulatory mechanisms that drive brain development are highly robust, such that - barring mutations in key regulatory genes - the total number of neurons, their relative position in the brain, and their primary connections are grossly similar between individual members of a species.

By contrast, in the period after birth a new variable comes into play in the form of sensory experience, which adds dynamic range to the final state of any given connectome. Activation of sensory neurons drives patterned neural activity in the cortex that initiates critical period stages of synapse development and maturation (Katz and Shatz, 1996; Wiesel, 1982). Neural activity regulates excitatory and inhibitory synapse development in this time window in large part by converging on the regulation of environmentally-sensitive transcription factors that coordinate the expression of gene products required for synapse formation, elimination, and plasticity (Majdan and Shatz, 2006; West and Greenberg, 2011). Depending on the environment into which any given animal is born, the nature, timing, and extent of this sensory experience will differ and thus the experience-dependent development of synapses will vary between these organisms as well. For proper brain development, the timing and level of transcriptional response following neuronal activity must be precisely regulated.

My dissertation research has been directed toward identifying the key molecular regulatory mechanisms that mediate this process. In this section, I first use the regulation of a

neuronal activity-regulated gene, *Fos*, as an example to elaborate upon what is known about the molecular mechanisms in neuronal activity-dependent gene transcription. Next, I discuss how neurons can encode the specificity of specific receptor signaling from the synapse to the nucleus. Then, I highlight new insights into the conundrum of synapse specificity, by reviewing studies that elucidate how transcriptional processes occurring in the nucleus of the neuron can promote the development of specific subsets of synapses in the cell periphery. Finally, I discuss how chromatin regulatory factors can serve as modulators of the postnatal experience dependent stages of synapse development.

1.1 Mechanisms of neuronal activity-regulated transcription

Neurons encode perceptions, movements, decisions and memories by firing sequences of action potentials in precise temporal patterns. Furthermore, these patterns of neuronal activity modify the connectivity and strength of neural circuits in the brain by modulating neural functions such as neurotrophin release (Balkowiec and Katz, 2000), neuronal differentiation (Gu and Spitzer, 1997), dendritic spine stability (Wyatt et al., 2012), and synaptic strength (Nelson and Turrigiano, 2008). One well-studied example of the consequences of different neural patterns for the specificity of plasticity is long-term potentiation (LTP) and depression (LTD), as long-term potentiation can be induced by delivering repetitive trains of high frequency stimulation whereas long-term depression can be induced by delivering a train of low frequency stimulation.

One way neuronal activity modulates neural plasticity is via neuronal activity-regulated gene transcription. The idea that neuronal activity regulates gene transcription first came from the observation that neurotransmitters can induce *Fos* transcription in PC12 cells (Greenberg et al., 1986). This observation was quickly extended to neurons when it was demonstrated that *Fos* transcription is robustly induced following seizure in post-mitotic neurons of the central nervous system (CNS) (Morgan et al., 1987). A whole program of activity regulated genes was identified in a series of following studies (Nedivi et al., 1993; Qian et al., 1993) and many of these gene products act to directly modulate synaptic function (Lyons and West, 2011; West and

Greenberg, 2011). Subsequently, neuronal activity-dependent gene transcription has been shown to be a fundamental process needed for certain forms of long-term plastic changes in the brain (Nguyen et al., 1994; Wang et al., 2006).

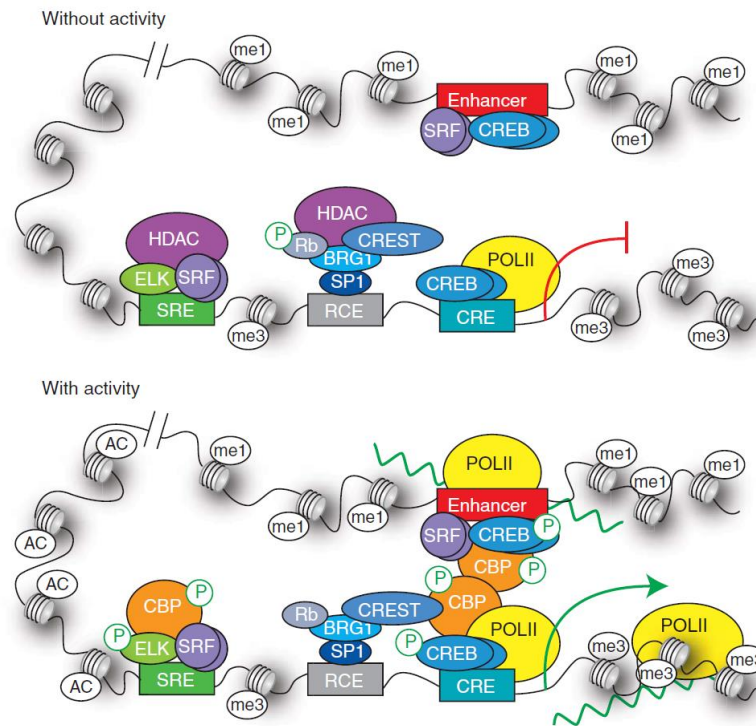


Figure 1: Mechanisms that regulate activity-dependent transcription of *Fos*. Adapted from Cold Spring Harb Perspect Biol. 2011 Jun 1;3(6).

Because *Fos* transcription is so widely and strongly induced, the molecular mechanisms that regulate its transcription have been characterized in detail and provide general concepts into how neuronal activity regulates multiple steps of transcription (**Fig. 1**). Transcription is a tightly regulated process that is comprised of a series of biochemical steps. First, nucleosome position or higher-order chromatin structures must be regulated to control the accessibility of the promoter region, then the assembly of generalized transcription factors and PolII happens at the start site, and then subsequent elongation produces nascent mRNA transcripts. In neurons under basal conditions, the *Fos* promoter is already transcriptionally permissive, with transcription factors SRF and CREB and the RNA polymerase II complex pre-bound (Kim et al., 2010). However, the promoter is held in a repressed state as reflected by the deacetylation of promoter histones, which

depends at least in part on the presence of histone deacetylases (HDACs) (Qiu and Ghosh, 2008). Neuronal activity induced signaling events impact proteins at the *Fos* promoter to relieve this repression. These promoter regulatory events include 1) the phosphorylation of CREB at Ser133, which facilitates recruitment of the histone acetyltransferase CBP to the *Fos* promoter (Chrivia et al., 1993; Sheng et al., 1991), 2) Activation of SRF-dependent transcription of *Fos* (Xia et al., 1996), 3) Release of HDACs from the promoter and their export to the cytoplasm (Qiu and Ghosh, 2008), and 4) Recruitment of the transcriptional cofactor CBP as well as RNA polymerase II to distal *cis* enhancer elements that interact with the *Fos* promoter by looping (Kim et al., 2010). In addition to the regulation of transcriptional initiation, evidence suggests that *Fos* transcription is regulated at the level of transcriptional elongation. Regulated phosphorylation of RNA polymerase II causes the polymerase complex to undergo promoter proximal stalling following initiation until activity-dependent elongation is cued (Saha and Dudek, 2013).

Neuronal activity patterns are transduced into transcriptional activation using intracellular calcium signals (Greenberg et al., 1986). One of the most important calcium adaptors in the cell is the protein CaM, which can coordinate up to four calcium ions with its four EF hand domains (Clapham, 2007). The Ca²⁺/CaM complex is then capable of activating several different downstream kinases pathways, including the family of CaMKs, MAPK and PKA. These kinases are then linked to gene expression through the phosphorylation of intermediate signaling targets that culminate in the promoter regulatory events described in **Fig. 1**. The analysis of calcium regulated promoters led to the identification of the cAMP response element (CRE) as a major calcium-responsive transcriptional element (Ginty, 1997). It has been proposed that the CRE binding protein (CREB) transcription factor family couples temporal signals to long-term changes in synaptic strength (Nelson and Turrigiano, 2008) and cross talk between MAPK and PKA is required for calcium stimulation of CREB-dependent transcription (Impey et al., 1998). While CREB is an important calcium responsive transcription factor for *Fos* transcription, internal deletions within the *Fos* gene that abolish CREB binding do not preclude calcium activation of

Fos transcription. This finding, together with the observation that calcium activates serum response factor-dependent transcription via CaMK dependent pathway (Miranti et al., 1995), indicates that the SRE is also a calcium response element.

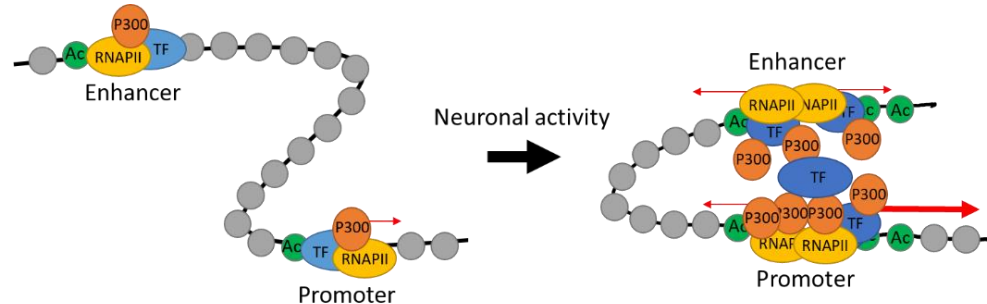


Figure 2: Genomic views of neuronal activity dependent gene transcription.

In addition to gene promoters, which lie in close proximity to the transcription start site of genes, distal enhancers also contribute to the activation of gene transcription (Banerji et al., 1981). Genome-level sequencing studies have revealed important roles for distal enhancers in the control of neuronal activity-regulated gene transcription (**Fig. 2**) (Joo et al., 2015; Kim et al., 2010; Malik et al., 2014; Schaukowitch et al., 2014). Neuronal activity-regulated enhancers were identified by enhancer mark, histone H3 monomethylated at lysine 4 (H3K4me1), and a strong inducibility of the transcriptional co-activator p300/CBP binding following membrane depolarization (Kim et al., 2010). Many of these enhancers show increased acetylation of histone H3 Lys27 (H3K27ac) after membrane depolarization (Malik et al., 2014) and transcription factors known activity-regulated such as CREB, Npas4 and SRF bind to these enhancers either constitutively or in an activity-regulated manner (Kim et al., 2010). There are five putative activity-regulated enhancers of the *Fos* gene. A recent study shows that distinct subsets of the enhancers are activated by different stimuli and the activation of specific enhancers are required for stimulus-specific induction of *Fos* transcription (Joo et al., 2016). Thus, in addition to direct regulations at gene promoters, differential use of distal enhancers can also confer the specificity of the transcriptional response to different extracellular stimuli.

1.2 Receptors and stimulus specificity

As mentioned in the section above, neurons transduce signals from synapse to nucleus mainly through calcium regulated signaling pathways. The two most physiologically relevant modes of calcium entry into neurons in terms of regulating changes in gene transcription are entry through NMDARs and L-type voltage-gated calcium channel (L-VGCCs) (Bading et al., 1993; Ghosh et al., 1994a). Presynaptic action potentials inducing the release of glutamate activate NMDA-, AMPA-, and kainate-type glutamate receptors postsynaptically. Activation of the NMDA-type glutamate receptor permits direct influx of calcium. In addition, activation of all these receptors results in a large sodium influx that drives postsynaptic membrane depolarization. This depolarization then induces the opening of VGCCs including L-type VGCCs. Calcium influx via L-VGCCs and NMDARs can activate a number of different signaling cascades leading the activation of specific gene program (Bading et al., 1993; Hardingham et al., 1997).

The specificity of receptor signaling is thought to arise through the nature of the specific protein-protein interactions between channels and components of intracellular signaling pathways. One well studied case in the distinct regulation of signaling pathway by receptor is NMDARs regulated transcription. NMDAR receptors are heterotetramers that are made up of different subunit compositions and the subunit composition of these receptors determines the specificity of the downstream signaling cascades initiated following receptor activation (Lau and Zukin, 2007; Sasaki et al., 2002). For example, activation of synaptic NMDARs which are predominantly GluN2A-containing, induces CREB Ser133 phosphorylation which leads transcriptional activation. By contrast, extrasynaptic NMDARs, which are predominantly GluN2B-containing, stimulation results in CREB Ser133 dephosphorylation, which is required for transcriptional deactivation (Hardingham and Bading, 2010; Hardingham et al., 2002). This differential regulation of CREB activity by the distinct pool of NMDARs is mediated by Erk1/2-Jacob pathway (Karpova et al., 2013). Jacob is a protein messenger of NMDAR signaling to the nucleus that effects CREB dependent transcription. Synaptic, but not extrasynaptic NMDARs activation

activates ERK1/2 mediates nucleus translocation of Jacob (Karpova et al., 2013). There are seven known NMDAR subunits GluN1, GluN2A-D, and GluN3A-B (Ciabarra et al., 1995; Dingledine et al., 1999; Matsuda et al., 2002; McBain and Mayer, 1994; Nishi et al., 2001; Sucher et al., 1995). Studies in NMDARs dependent signaling have been heavily focused on GluN2A and GluN2B and little is known about other subunits effect on NMDARs dependent transcription. In Chapter3, I will examine the role of a developmental regulated submit, GluN3A, in NMDARs dependent transcription.

1.3 Transcription Factors and Synapse Specificity

Transcription factors reside predominantly in the nucleus, where they are well-poised to integrate signaling information originating anywhere within the cell. This integrative capacity of stimulus-regulated transcription factors allows them to transduce reception of tiny amounts of growth factors into binary cell survival/cell death decisions (Brunet et al., 2001), and to drive homeostatic plasticity by summing neural activity levels into global synaptic scaling responses (Ibata et al., 2008). However, the central location of transcription factors raises the question of how they can have a meaningful impact on local synaptic connectivity, where the specificity of connections is essential to brain function. Previous studies from our lab on transcription factor CaRF provided some hints on how nuclear transcription factors encode specificity at synapse level. CaRF is a transcriptional activator and expression of exon IV-containing forms of *Bdnf* is significantly reduced in the cortex of CaRF knockout mice demonstrating that CaRF contributes to transcriptional activation of *Bdnf* promoter IV in vivo (McDowell et al., 2010; Tao et al., 2002). BDNF is known to regulate the formation of inhibitory synapse (Lyons and West, 2011) and indeed, the expression of GABAergic synaptic protein is altered in CaRF knockout mice (McDowell et al., 2010). Interestingly, while the transcriptional activity of CaRF is induced by membrane depolarization, CaRF is not required for the induction of *Bdnf* transcription that is driven by this stimulus (McDowell et al., 2010; Tao et al., 2002). I explored the role of CaRF in NMDARs dependent *Bdnf* transcription and will discuss my findings in Chapter 2. Together,

these findings demonstrate that transcription factor CaRF encodes specificity at the level of synapse type (e.g. excitatory, inhibitory). In the following section, I discuss two other examples of transcription factors that regulate specificity at synapse. These examples show that although nuclear transcription factors are unlikely to directly instruct the formation or elimination of individual synapses, they do encode specificity at subcellular synapse location (e.g. somatic, dendritic). Furthermore, by interacting functionally with local translational machinery they can have regulatory control over local activity-dependent synaptic plasticity.

1.3.1 Npas4: An activity-dependent, cell-type specific master regulator of inhibitory/excitatory balance

Npas4 belongs to the basic helix-loop-helix-Per-Arnt-Sim (bHLH-PAS) transcription factor family (Ooe et al., 2004), whose members share a bHLH DNA-binding domain, dual PAS domains, and a C-terminal activation domain (Partch and Gardner, 2010). These transcription regulators dimerize or form complexes with transcriptional coactivators through their bHLH and PAS domains to regulate diverse functions including development, circadian rhythms and cellular responses to hypoxia and environmental toxins (Gu et al., 2000; Kewley et al., 2004; Partch and Gardner, 2010). Among the bHLH-PAS family, Npas4 is unique for its restricted expression in neurons and the fact that its expression is selectively induced in neurons following membrane depolarization-induced calcium influx (Lin et al., 2008). Indeed, even compared with other immediate-early gene transcription factors such as Fos, Npas4 is far more selective for calcium signaling cascades, as its expression is induced only by calcium influx through L-type voltage gated calcium channels or NMDA receptors, but it is insensitive to the elevation of intracellular cAMP or the application of growth or neurotrophic factors (Lin et al., 2008). The mechanisms that confer this specificity upon Npas4 induction are not completely understood, though Npas4 seems to be a direct target of the activity-inducible transcription factor SRF (Kim et al., 2010; Kuzniewska et al., 2016).

Npas4 has been shown to play a prominent role in linking synaptic activity to inhibitory/excitatory synapse balance in a cell type- and subcellular-specific manner during brain development. The calcium-dependent induction of Npas4 was first discovered in excitatory glutamatergic neurons, and, interestingly, in these cells Npas4 was found to selectively promote the development of GABAergic synapses (Lin et al., 2008). Reduced numbers of GABAergic synapses were found in cultured hippocampal neurons when Npas4 was knocked down, whereas increased numbers of GABAergic synapses were found when Npas4 was overexpressed. In contrast, these manipulations did not affect glutamatergic synapses, indicating a selective role for Npas4 in inhibitory synapse development in these neurons. In addition to regulating the total number of inhibitory connections made during synapse formation, Npas4 appears to play an important role in the activity-dependent plasticity of GABAergic synapses in mature neural circuits. Npas4-knockout mice show decreased CA1 hippocampal neuron miniature inhibitory postsynaptic current (IPSC) frequency after exposure to an enriched environment compared with their wild-type littermates (Bloodgood et al., 2013), and Npas4 has also been found to underlie the activity-dependent increase in inhibition on newborn excitatory granule cells of the dentate gyrus as they integrate into the hippocampal circuitry (Sim et al., 2013). These studies together support a role for Npas4 in selectively upregulating inhibitory GABAergic synapse development in excitatory neurons following neuronal activity, suggesting that Npas4 diminishes future excitation and maintains homeostatic balance between inhibition and excitation.

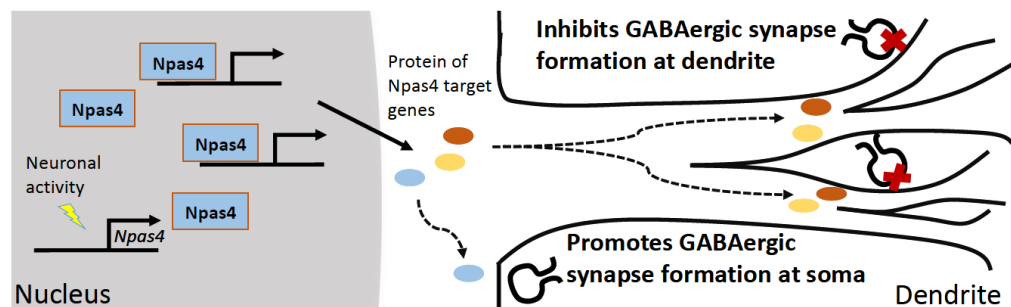


Figure 3: Npas4 expression is induced rapidly by neuronal activity. Npas4 target genes promote GABAergic synapse formation at the soma while also inhibiting GABAergic synapse formation at the apical dendritic spines.

Perhaps the most interesting and unexpected finding regarding the Npas4-dependent regulation of GABAergic synapses onto excitatory neurons is that there is subcellular specificity with respect to the effects of Npas4 manipulation on the synapses on the postsynaptic cell (**Fig. 3**). Bloodgood et al. (2013) used the spatial organization of synaptic inputs onto distinct regions of pyramidal neurons in the hippocampus to reveal this specificity in vivo. The authors found that exposure of mice to an enriched environment induced expression of Npas4 in the hippocampus. After this exposure, when a stimulating electrode was placed in the pyramidal layer to activate somatic inhibitory synapses onto nearby pyramidal neurons, the authors saw relatively smaller evoked inhibitory currents in Npas4-knockout neurons compared with Npas4 wild-type neurons, which is consistent with the culture experiments showing that Npas4 promotes inhibitory synapse formation. By contrast, when the authors stimulated stratum radiatum to activate inhibitory synapses on the distal apical dendrites of these pyramidal neurons they found significantly larger evoked inhibitory currents in the knockout neuron compared with wild type, suggesting that Npas4 actually inhibits the formation of distal inhibitory synapses, presumably in the same neurons where it promotes somatic inhibition (Bloodgood et al., 2013). Given that different classes of inhibitory interneurons are known to synapse onto different subcellular domains of hippocampal pyramidal neurons (Freund and Buzsaki, 1996) having distinct Npas4 regulation of these events is likely to be important for fine-tuning circuit plasticity in the hippocampus.

Excitatory neurons comprise the large majority of cells in the culture systems that are most often used to study activity-inducible transcription; thus until recently very little was known about the identity of activity-inducible genes in inhibitory neurons. To fill this gap in knowledge, Spiegel et al. (2014) cultured neurons from the embryonic medial ganglionic eminence, which gives rise to the GABAergic interneurons that populate the forebrain. Using this system, they discovered that Npas4 expression was indeed induced in inhibitory neurons by membrane depolarization and subsequent calcium influx, similar to its regulation in excitatory neurons. However, when the authors studied the effects of knocking out Npas4 on synapse formation, they

found that, rather than affecting GABAergic synapses, the loss of Npas4 reduced glutamatergic input to inhibitory neurons while having no effect on the GABAergic synapses made onto these neurons (Spiegel et al., 2014). Thus, in contrast to its effects in excitatory neurons, activity-inducible Npas4 expression appears to upregulate glutamatergic synapses in inhibitory neurons to increase their inhibitory output. This suggests a more complex role than previously thought for Npas4 in mediating neuronal inhibition/excitation balance across multiple cell types in the heterogeneous neural circuits that comprise the cortex. Overall, these studies suggest that Npas4 functions as a key homeostatic factor in the cortex, depressing network excitability following neuronal activity via a negative feedback mechanism that is spread across multiple cell types and synapses.

How it is possible for Npas4 to promote opposite types of synapses in two different classes of neurons? The expression of distinct cell type-specific programs of Npas4-regulated genes in excitatory and inhibitory neurons may underlie the differential effects of Npas4 in these two neuron types (Spiegel et al., 2014). Using a genetic method to identify activity-regulated genes that are selectively induced in inhibitory vs. excitatory neurons, Spiegel et al. (2014) identified a set of inhibitory neuron-specific genes whose induction is impaired in the absence of Npas4. These Npas4-regulated inhibitory neuron genes include *Kcna1*, *Frmpd3*, and *Nptx2*. These gene products have been reported previously to be postsynaptic at glutamatergic synapses and therefore may contribute to the Npas4-dependent enhancement of glutamatergic synapse formation in inhibitory neurons. With respect to the Npas4-regulated genes that drive GABAergic synapse formation in excitatory neurons, one possible target is *Bdnf*. *Bdnf* is selectively induced by activity only in excitatory and not inhibitory neurons and is well known to promote GABAergic synapse development in the postnatal cortex. Npas4 binds to three regulatory elements within the *Bdnf* gene, and knocking down *Bdnf* partly rescues the effects of Npas4 overexpression on increased GABAergic synapse number and function in hippocampal neurons (Lin et al. 2008). Interestingly, BDNF expression is reduced in the hippocampus of Npas4-

knockout mice, and disruption of BDNF function prevents Npas4-mediated increases in inhibition at the soma but does not affect Npas4's effects at the dendrites, thus providing a potential explanation for the subcellular specificity of Npas4-mediated inhibitory synapse formation (Bloodgood et al. 2013). Taken together, these data support the idea that Npas4's differential effects in these two cell types are due to distinct cell type-specific programs of Npas4-regulated gene expression. Further understanding of the distribution of Npas4 binding sites in different cell types by chromatin immunoprecipitation (ChIP) will help to elucidate our understanding of how broadly expressed transcription factors can generate cell type-specific biological consequences.

1.3.2 MEF2: activation, repression, transcription, translation—MEF2 does it all

Initially identified for their role in muscle cell differentiation (Gossett et al., 1989) the myocyte enhancer factor 2 (MEF2) family of transcription factors comprises four members, MEF2A–D, that are now understood to have essential functions in multiple tissues including the CNS (Dietrich, 2013; Pon and Marra, 2016). In the brain the MEF2A, -C, and -D proteins are highly expressed in distinct, yet overlapping brain regions, both during neuronal development and in the adult (Leifer et al., 1993; Lyons et al., 1995). MEF2B is found at much lower levels and is not discussed further here. Importantly, the MEF2s are known to be targets of activity-dependent calcium signaling in neurons, where they have been studied for their roles in activity-dependent neuronal survival (Mao, 1999; Okamoto et al., 2000) as well as stimulus-regulated glutamatergic synapse formation and elimination (Flavell et al., 2006). The MEF2 proteins are subject to multiple, stimulus-regulated posttranslational modifications that are thought to regulate MEF2's dual function as both a repressor and an activator (Lyons and West, 2011; McKinsey et al., 2002). In resting neurons, the MEF2s are sumoylated and they function primarily as transcriptional repressors (Shalizi et al., 2006). After neuronal activity, calcium influx through NMDARs and L-type voltage-gated calcium channels results in calcineurin-mediated dephosphorylation, MAP kinase-dependent phosphorylation, and a switch from sumoylation to acetylation at specific

residues on the MEF2s, all of which are associated with functional MEF2 activation (Flavell et al., 2006; Shalizi et al., 2006). Thus, MEF2 transcription factors are ideally poised to be important regulators of stimulus-inducible effects on neuronal development and function.

Both the transcriptional repressor and activator functions of the MEF2s have been implicated in synapse formation, with the accumulated evidence suggesting that the repressor forms regulate synapse formation and the activator forms promote synapse elimination. The repressor functions of the MEF2s have been studied in both the cerebellum and cortex, and repression by sumoylated MEF2A is particularly well characterized for its role in early cerebellar synapse development (Shalizi et al. 2006). In cerebellar granule neurons, sumoylated MEF2A enhances the formation of the mature claw morphology of granule neuron dendrites and knocking down MEF2A in cultured rat cerebellar slices impairs this dendritic differentiation. In cortical excitatory neurons, the repressor functions of MEF2C have similarly been shown to function in a cell-autonomous manner to regulate the development of glutamatergic synapses. Knocking out MEF2C in cortical neurons results in a mildly decreased frequency of miniature excitatory synaptic currents and significantly decreased dendritic spine density (Harrington et al., 2016). Spine density in the MEF2C-knockout neurons was rescued by expression of a fusion protein that links the DNA binding domain of MEF2C to the repressor domain of Engrailed (MEF2-En), indicating that the synapse-promoting effects of MEF2C in this context are mediated by its function as a transcriptional repressor. Interestingly, MEF2C also has a cell-autonomous effect on GABAergic synapses made onto cortical glutamatergic neurons, such that single-cell knockout of MEF2C is associated with increased amplitude and frequency of miniature inhibitory synaptic currents, and an increased number of GABAergic synapses, and this effect is again rescued by overexpression of MEF2C-En.

By contrast, the transcriptional activator functions of the MEF2 transcription factors have been implicated in the activity-dependent elimination of glutamatergic synapses in the hippocampus. Knocking down/out MEF2A, MEF2C, or MEF2D in hippocampal neurons was

found to increase excitatory synapse number, which first suggested a role for these factors in restricting synapse number (Barbosa et al., 2008; Flavell et al., 2006). The increase in glutamatergic synapses seen in MEF2A/D-knockdown neurons can be reversed by expressing a fusion protein that combines the DNA binding domain of MEF2 and the transcriptional activation domain of the viral transcription factor VP16 (MEF2-VP16), implicating the transcriptional activator function of MEF2 in this negative-regulatory effect on synapses.

A further level of MEF2-driven synapse specificity was revealed in a recent paper that showed that MEF2C differentially regulates local vs. long-range excitatory synaptic inputs onto neocortical neurons (Rajkovich et al., 2017). The authors found that knocking out *Mef2c* in a sparse population of layer 2/3 neurons in mouse barrel cortex weakened local excitatory synaptic input while enhancing long-range transcallosal excitatory inputs onto the same cells. Thus, even for the same type of synapses (excitatory) on a single type of neuron (also excitatory), MEF2C shows functional specificity in the direction of its regulatory effect depending on the source of the presynaptic input.

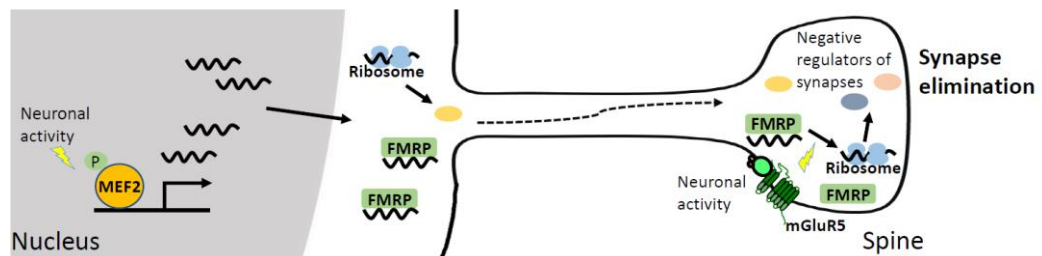


Figure 4: Neuronal activity induces MEF2-dependent gene transcription. FMRP traffics mRNAs from the nucleus to the synapses and represses local mRNA translation at the synapses until neuronal activation of mGluR5 receptors leads to target gene mRNA dissociation from FMRP. The ability of constitutively active MEF2-VP16 to drive synapse elimination is blocked in FMRP-knockout neurons, suggesting that these 2 pathways converge to locally regulate synapse pruning.

As in all cases where a transcription factor regulates synapses, it is natural to wonder how gene transcription in the nucleus of the neuron can be transduced into distal changes in synapse number in the periphery. Intriguingly, insights gleaned from studying a mouse model of fragile X syndrome (FXS), a genetic form of autism and mental retardation that occurs because of loss-of-function mutations in the *Fmr1* gene (Abrahams and Geschwind, 2008; Bassell and Warren,

2008), have suggested that the Fragile X Mental Retardation Protein (FMRP) encoded by *Fmr1* may link MEF2 in the nucleus and its effects at synapses (**Fig. 4**). FMRP is an RNA binding protein that mediates RNA trafficking from the nucleus to synapses and regulates local mRNA translation at synapses. FMRP is required for MEF2-dependent synapse elimination because MEF2-VP16 overexpression fails to drive excitatory synapse elimination in the absence of FMRP expression (Pfeiffer et al., 2010).

An explanation for the requirement for FMRP in MEF2-dependent synaptic changes may be that FMRP regulates translation of MEF2-induced transcripts at synapses. In hippocampal neurons, MEF2 promotes excitatory synapse elimination by inducing degradation of postsynaptic density protein 95 (PSD-95) at the dendrites, a process requiring Mdm2-dependent ubiquitination and Pcdh10-dependent degradation of PSD-95. *Pcdh10* is a target of both MEF2- and activity-dependent transcription and FMRP-dependent translational repression (Morrow et al., 2008; Tsai et al., 2012), and inhibition of Pcdh10 function inhibits MEF2-dependent synapse elimination. MEF2 and FMRP also cooperate to regulate the synaptic localization and activation of Mdm2. As a result of this dual regulatory circuit, even though Pcdh10 levels are elevated in *Fmr1*-knockout neurons, MEF2-dependent degradation of PSD-95 is blocked in the absence of FMRP because of a failure of PSD-95 at synapses to be ubiquitinated. Dendritic FMRP is also known to regulate the transport and translation of specific mRNAs in response to metabotropic glutamate receptor (mGluR) activation, and blocking dendritic mGluR5 activity also results in loss of MEF2-induced glutamatergic synapse elimination in cultured hippocampal neurons (Wilkerson et al., 2014). One potential mediator of synapse elimination in this context is the cytoskeletal protein Arc, which plays important roles in dendritic spine plasticity and glutamate receptor trafficking (Korb and Finkbeiner, 2011). *Arc* transcription is induced in an activity- and MEF2-dependent manner, and it is required for MEF2 and dendritic mGluR5-induced synapse elimination (Wilkerson et al., 2014). Dendritic mGluR5 activation promotes local translation of Arc mRNA, and Arc is also a known translational target of FMRP in dendrites (Park et al., 2008). Thus, through coordinate

transcriptional and translational control of a program of synapse regulatory gene products, MEF2 and FMRP work together to shape synaptic activity-dependent changes in glutamatergic synapses.

1.4 Chromatin Regulation in neuronal activity-regulated gene transcription.

Sequence-specific transcription factors are the primary determinants of gene expression programs in cells because they directly mediate the recruitment of RNA polymerase II onto gene promoters. However, there are many more potential binding sites across the genome for any given transcription factor than are used, and it is the biochemical state and physical structure of DNA and its associated histone proteins, a complex called chromatin, that determine which of the potential sites are available to be bound (Sheffield et al., 2013). In this manner chromatin state functions to establish the potential range of transcription factor action in any given cell. Although chromatin structure is one step upstream from transcription factor binding, loss-of-function phenotypes and pharmacological inhibition of several chromatin regulatory factors have revealed important and specific roles for many of these proteins in neuronal activity-regulated gene transcription, synapse development and cognitive performance (Gräff and Tsai, 2013; Ronan et al., 2013; West and Greenberg, 2011). In Chapter 4, I investigate the role of histone acetylation at enhancer in neuronal activity-regulated gene transcription. Here, I review two chromatin regulatory factors that regulate neuronal activity-regulated gene transcription and synapse development in the brain.

1.4.1 ATP-dependent chromatin remodelers.

ATP-dependent chromatin remodelers use the energy of ATP hydrolysis to alter nucleosome positions along genomic DNA or to exchange nucleosomes on chromatin. By moving nucleosomes into or out of transcription factor binding sites and clearing chromatin of nucleosomes marked with regulatory histone modifications, chromatin remodelers have the ability to modulate gene transcription. There are four families of ATP-dependent chromatin remodeling complexes defined by the ATPase they contain: 1) BAF, 2) INO80/SWR1, 3) ISWI,

and 4) CHD (Hargreaves and Crabtree, 2011). Recently several specific members of the BAF and CHD families have been shown to play important roles in synapse development, and those factors are reviewed here.

Brg1/Brm-associated factor (BAF) complexes are mammalian SWI/SNF-like, ATP-dependent chromatin-remodeling complexes that are comprised of an assembly of at least 15 subunits encoded by 29 genes. The core ATPase subunit of these ~2-MDa protein complexes can be either Brg1 (also known as SmarA4) or Brm (also known as SmarA2) (Kadoch and Crabtree, 2015; Ronan et al., 2013; Vogel-Ciernia and Wood, 2014). Some accessory subunits of the BAF complexes are tissue specific, and the particular subunit composition of a given BAF complex affects both its genome targeting and functions. For example, in neural progenitors BAF complexes contain primarily BAF45a and BAF53a, and in these cells BAF complexes are required for cell proliferation. By contrast, when progenitors exit the cell cycle to become postmitotic neurons, BAF45a and BAF53a are replaced by BAF45b, BAF45c, and BAF53b, and blocking this subunit switch inhibits neural differentiation (Lessard et al., 2007). Study of the functions and protein interactions of neural-specific subunits of the BAF complex has helped explain how these chromatin-remodeling complexes regulate neuronal and synaptic development.

In postmitotic neurons, the BAF complexes have been implicated as regulators of both dendrite outgrowth and synapse maturation. For example, neurons lacking Brm show increased numbers of mature, mushroom-shaped spines (Loe-Mie et al., 2010) whereas neurons lacking Brg1 show increased numbers of immature, thin spines (Zhang et al., 2015), and Brg1 is required for activity-dependent dendritic outgrowth (Wu et al., 2007). Although BAF complexes can still assemble without the neural-specific subunit BAF53b, hippocampal neurons lacking BAF53b show defects similar to neurons lacking Brg1 including reduced activity-dependent dendritic outgrowth (Wu et al. 2007). Profiling gene expression in mice with heterozygous knockout of BAF53b revealed altered expression of genes involved in actin cytoskeletal remodeling and postsynaptic density, suggesting that the BA53b-mediated recruitment of the BAF complex to

these genes may play an important role in regulation of synapse functions (Vogel-Ciernia et al., 2013). ChIP studies also show that BAF53b is required for the recruitment of BAF complexes to the promoter region of genes involved in dendritic outgrowth (Wu et al. 2007). Taken together, these studies indicate that BAF complexes regulate genes that are important for synaptic functions and suggest that neural-specific subunits are important for targeting the complexes to their genes.

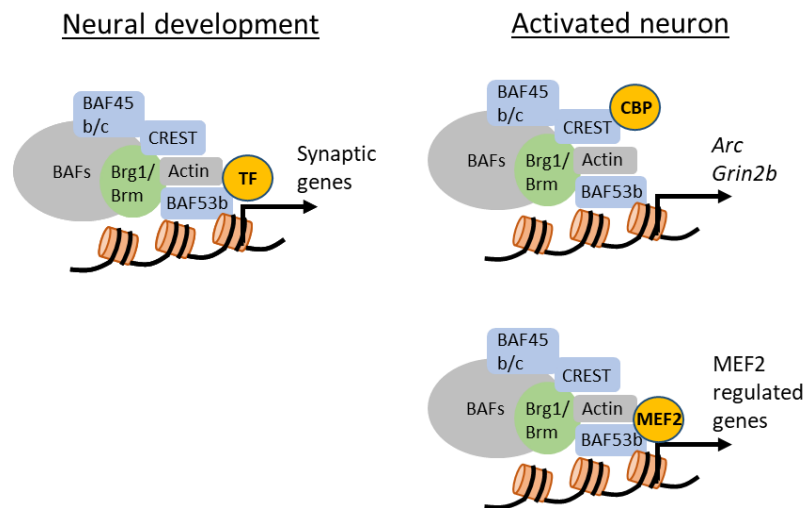


Figure 5: Tissue specific BAF subunits interact with distinct transcription factors or transcriptional coactivators resulting in activation of different gene programs during neural development. BAF complexes regulate a group of synaptic genes and mediates synapse formation and maturation. In activated neurons, BAF complexes regulate *Arc* and *Grin2b* expression by interacting with CBP. BAF complexes also interact with MEF2C and are required for MEF2C mediated synapse elimination.

How do distinct BAF complexes achieve functional biological specificity? It is well established that BAF complexes are recruited to target genes via their interaction with sequence-specific transcription factors, and if these interactions differ between cell types or conditions, then the function of the BAF complex will differ as well (Cosma et al., 1999). For example, under basal conditions in neural progenitors Brg1 interacts with the transcription factor Gli3 and functions as a transcriptional repressor to suppress the expression of Shh target genes (Zhan et al., 2011). However, after exposure to Shh Brg1 interacts with the transcription factor Gli1 and is required for Shh-induced gene activation. In postmitotic neurons, BAF complex subunit-specific interactions with transcription factors and other chromatin regulators may define the specific

function of BAF complexes in synapse development (**Fig. 5**). For example, the neural-specific BAF subunit CREST has been shown to regulate dendrite development via its interactions with the transcriptional coactivator and histone acetyltransferase CBP (Aizawa, 2004). BAF complexes containing CREST are found bound to the promoters of genes related to synapse functions including *Arc* and *Grin2b*, where CREST is required to mediate their expression (Qiu et al., 2008). One key transcription factor that has been shown to link BAF complexes to synapse development is MEF2C. Gene expression profiling from a recent study revealed a significant overlap between neuronal activity-induced genes that are disrupted in the absence of Brg1 and genes that are targets of regulation by MEF2. Knocking out MEF2C was shown to impair the activity-dependent recruitment of Brg1 to gene promoters, and, conversely, knocking out Brg1 impaired the ability of MEF2C overexpression to drive synapse elimination (Zhang et al. 2015). These data suggest that Brg1 functions as a coactivator of the MEF2C-dependent transcriptional program that mediates excitatory synapse elimination. Taken together, these studies suggest that identifying and selectively disrupting specific BAF subunit-transcription factor interactions offers a strong opportunity to dissect the many roles of BAF complexes in synapse development.

1.4.2 CHD4: timing transcriptional repression

Whereas the BAF complexes illustrate how subunit specificity can allow a chromatin remodeler to differentially control distinct stages in the process of synapse formation, recent findings about the CHD family chromatin remodeler CHD4 have provided new insights into regulation of gene expression on distinct timescales during synapse development.

The ATPases of the CHD family are characterized by the presence of a chromodomain in addition to the conserved DEAD/H-related ATPase domain. CHD4 assembles with DNA binding proteins and histone deacetylases into a large protein complex called the nucleosome-remodeling and histone deacetylase (NuRD) complex (Hargreaves and Crabtree 2011). NuRD functions as a transcriptional repressor and has canonically been suggested to play an opposing role to the gene activation mediated by BAF complexes in regulation of gene transcription (Ho and Crabtree,

2010). Although NuRD is well established to play a critical role in the differentiation of embryonic stem cells, far less is known about functions of NuRD in postmitotic tissue. However, a recent study showed that knocking out CHD4 in granule neurons in the cerebellar cortex results in a reduction in the density of synapses and neurotransmission between parallel fibers and Purkinje cell dendrites, suggesting that the NuRD complex promotes synaptogenesis (Yamada et al., 2014). Genomewide chromatin state profiling in the cerebellum of mice lacking CHD4 revealed that in the absence of NuRD a number of gene promoters fail to undergo developmentally regulated, NuRD-dependent repression. Expression of these NuRD target genes, which include *Nhlh1*, *Elavl2*, and *Cplx3*, is highly developmentally regulated in wild-type mice, such that expression peaks at postnatal day 6 and then decreases to very low levels in the adult brain. In the absence of CHD4, expression of the NuRD target genes remains high. Because in vivo RNAi knockdown reveals that many of these genes suppress presynaptic differentiation in the developing cerebellar cortex, these findings suggest that NuRD-dependent gene repression mediates the timing of proper synapse development by releasing the suppression of presynaptic differentiation in granule neurons during neural development (**Fig. 6**).

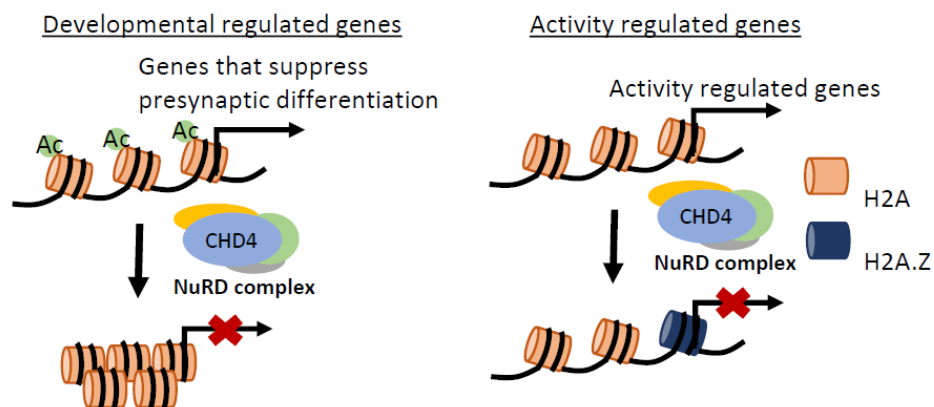


Figure 6: NuRD controls the timing of gene expression by turning genes off both on a developmental timescale and in response to transient neuronal activity. During cerebellar development, NuRD turns off genes that suppress presynaptic differentiation by histone deacetylation and inactivates neuronal activity-dependent gene transcription by replacing H2A with H2A.Z.

Interestingly, in addition to its role in gene repression on a developmental timescale, CHD4-dependent repression has also been found to act much more rapidly to regulate the dynamics of neural activity-dependent gene expression in neurons (Yang et al., 2016). Surprisingly, given its known functions in gene repression, genomewide CHD4 binding and chromatin state profiling revealed that CHD4 occupies the promoters of most actively transcribed genes in the mouse cerebellum including the classic activity-inducible genes *Bdnf*, *Fos*, and *Npas4*. Conditional knockout mice lacking CHD4 in cerebellar granule neurons show a prolonged time course of expression after the induction of activity-regulated genes is triggered, and this gene expression change is associated with defective activity-dependent granule neuron dendrite pruning. A clue to the mechanism of CHD4's action in neuronal activity-regulated gene transcription came when the authors observed that binding of the histone variant H2A.Z at the promoters of activity-regulated genes was reduced in CHD4-knockout granule neurons. In yeast, the homolog of H2A.Z is enriched at the promoters of genes when they are in their inactive state but is rapidly lost from gene promoters when transcription is induced, which suggested that H2A.Z might poise genes in the off state for their rapid activation (Zhang et al., 2005). However, in the absence of CHD4, H2A.Z is depleted from activity-inducible gene promoters, and, rather than affecting induction, knockdown of H2A.Z phenocopies the prolonged time course of activity-induced transcription seen in CHD4-knockout neurons. (Yang et al. 2016) Thus these data suggest a new model in which CHD4-dependent recruitment of H2A.Z to activity-inducible gene promoters in neurons controls the timing of transcriptional inactivation, perhaps by serving to facilitate recruitment of repressors to promoters as has been observed for H2A.Z in embryonic stem cells (Hu et al., 2013). In sum, these data reveal two distinct functions for CHD4 in cerebellar synapse regulation—one of which relies on the classic function of the NuRD complex in developmental gene silencing and the other of which is mediated by interactions between CHD4 and the histone variant H2A.Z to control the inactivation kinetics of stimulus-inducible genes. Future understanding of the CHD4-dependent mechanisms that differentiate its function in

these two processes will enhance our understanding of the timescales of gene transcription that contribute to synapse formation and refinement in the developing CNS.

1.4.3 Epigenome editing by CRISRP-based method

Genome-level sequencing studies have identified DNA regulatory elements controlled by these chromatin regulatory factors and study the role of chromatin state at these DNA regulatory elements in neuronal activity-regulated gene transcription (Cholewa-Waclaw et al., 2016; Gray et al., 2015; Kim et al., 2010; Malik et al., 2014; Su et al., 2017; Sweatt, 2013). While sequencing methods provided information about epigenetic changes following neuronal activity, they can only show correlation between these epigenetic changes and gene transcription. To establish the causative relationship between epigenetic changes and gene transcription, protein engineers have developed several synthetic proteins, which are modified from endogenous DNA binding proteins, to achieve site-specific manipulation. Zinc finger nuclease (ZFN) and transcription activator-like effector nucleases (TALENs) are two of such tools (Boch et al., 2009; Moscou and Bogdanove, 2009; Urnov et al., 2005). While these tools can achieve site-specific manipulation in the genome, the significant financial and technical cost of these tools limits their usages. In recent years, a simpler and cheaper genome editing system, CRISPR/Cas9, has been developed and widely adopted. CRISPR/Cas is a nuclease system from bacteria that recognizes RNA-DNA hybrids (Barrangou et al., 2007). The Cas9 nuclease is recruited to the specific DNA sequence in the genome upon expression of an RNA that complement to the targeting DNA sequence (Cong et al., 2013; Gersbach, 2014; Ran et al., 2015). Because of the RNA-guided mechanism, CRISPR/Cas9 system can easily change the binding site in the genome. Fusing a transcriptional effector or catalytic domain of histone-modifying enzymes to catalytically-dead Cas9, provides an easy and fast way to manipulate chromatin state at any genome region (Gilbert et al., 2013; Hilton and Gersbach, 2015; Maeder et al., 2013; Mali et al., 2013; Perez-Pinera et al., 2013). In Chapter 4, I will apply a CRISPR-based epigenome editing method to examine the role of enhancer histone acetylation in neuronal activity-regulated gene transcription.

2. The transcription factor CaRF limits NMDAR-dependent transcription in the developing brain

2.1 Summary

Neuronal activity sculpts brain development by inducing the transcription of genes such as *Brain-Derived Neurotrophic Factor (Bdnf)* that modulate the function of synapses. Sensory experience is transduced into changes in gene transcription via the activation of calcium signaling pathways downstream of both L-type voltage gated calcium channels (L-VGCCs) and NMDA-type glutamate receptors (NMDARs). These signaling pathways converge on the regulation of transcription factors including Calcium-Response Factor (CaRF). Whereas CaRF is dispensable for the transcriptional induction of *Bdnf* following the activation of L-VGCCs, here we show that loss of CaRF leads to enhanced NMDAR-dependent transcription of *Bdnf* as well as *Arc*. We identify the NMDAR subunit-encoding gene *Grin3a* as a regulatory target of CaRF, and we show that expression of both *Carf* and *Grin3a* is depressed by the elevation of intracellular calcium, linking the function of this transcriptional regulatory pathway to neuronal activity. We find that light-dependent activation of *Bdnf* and *Arc* transcription is enhanced in the visual cortex of young CaRF knockout mice, suggesting a role for CaRF-dependent dampening of NMDAR-dependent transcription in the developing brain. Finally, we demonstrate that enhanced *Bdnf* expression in CaRF-lacking neurons increases inhibitory synapse formation. Taken together these data reveal a novel role for CaRF as an upstream regulator of NMDAR-dependent gene transcription and synapse formation in the developing brain.

2.2 Introduction

In the developing mammalian brain, transient sensory stimuli drive long-lasting changes in synapse development and neuronal function by inducing the transcription of activity-regulated genes (West and Greenberg, 2011). Calcium plays a key role in this signal transduction by initiating intracellular signaling cascades that carry the signal to the nucleus where they activate

multiple transcription factors that bind regulatory elements of activity-regulated genes (Lyons and West, 2011). In addition to ubiquitous immediate early genes (IEGs) such as *Fos* and *Jun*, synaptic activity regulates a functionally important set of neuron-selective genes, which include the neurotrophin BDNF, the intracellular scaffolds Arc and Homer, the glutamate receptor binding protein Narp, and the transcription factor Npas4 (Bloodgood et al., 2013; Gu et al., 2013; Hong et al., 2008; Hu et al., 2010; Leslie and Nedivi, 2011; Wang et al., 2006). Induced expression of these gene products couples synapse development and function with sensory-driven neuronal activity to adapt brain development to the environment.

Glutamate release at synapses drives calcium into neurons by opening both NMDA-type glutamate receptors (NMDARs) and L-type voltage-gated calcium channels (L-VGCCs). Calcium acts locally at these channels to induce the signaling cascades that regulate nuclear transcription factors, and the source of calcium entry can influence the specificity of downstream signaling (Bito et al., 1996; Dolmetsch et al., 2001; Hardingham et al., 2002; Karpova et al., 2013). We and others have used transcription of *Bdnf* as a model to discover the neuronal activity-regulated transcriptional mechanisms that are important for developmental synapse plasticity. BDNF is a key effector of activity-dependent synapse development and plasticity, and it is the precise temporal and spatial control of *Bdnf* transcription that permits this signaling molecule to regulate these dynamic processes (Leslie and Nedivi, 2011; West et al., 2014).

The *Bdnf* gene contains nine alternative promoters, each of which is activity-inducible in neurons and most of which are regulated by multiple activity-dependent transcription factors (West et al., 2014). *Bdnf* exon IV-containing transcripts (*Bdnf* IV) are the most highly expressed and activity-regulated of the *Bdnf* splice variants in developing neurons, and the transcription factors that regulate *Bdnf* promoter IV have been well described. We first identified Calcium Response Factor (CaRF) as a transcription factor based on its ability to bind the L-VGCC-responsive calcium-response element 1 (CaRE1) in *Bdnf* promoter IV (Tao et al., 2002a). Basal expression of *Bdnf* IV is reduced in the cortex of adult CaRF knockout mice, consistent with

CaRF functioning as an activator of *Bdnf* promoter IV (McDowell et al., 2010). However L-VGCC-induced transcription of *Bdnf* IV is unaffected by the loss of CaRF and instead the transcription factor MEF2C mediates the actions of CaRE1 in response to this stimulus (Lyons et al., 2012).

Given our evidence for the stimulus-specific contributions of CaRF to *Bdnf* promoter IV regulation, here we set out to determine the requirement for CaRF in NMDAR-induced transcription of *Bdnf*. Here we report that loss of CaRF leads to enhanced NMDAR-dependent induction of both *Bdnf* IV and the activity-regulated gene *Arc*, and we investigate potential mechanisms as well as biological consequences of this change in transcriptional regulation. These data reveal a novel role for CaRF as an upstream regulator of NMDAR-dependent processes in the developing brain.

2.3 Materials and Methods

2.3.1 Dissociated Neuron Cultures

Neuron-enriched cultures were generated from cortex of male and female E16.5 CD1 mouse embryos (Charles River Laboratories) and cultured as previously described (McDowell et al., 2010; Tao et al., 2002). Withdrawal from tetrodotoxin (TTX WD) was done by treating neurons for 48 hrs with 1 μ M TTX (Tocris) prior either to harvesting cells (for the control condition) or washing out the TTX with Neurobasal medium (Invitrogen). Isotonic membrane depolarization with 55mM extracellular KCl was done as previously described (Lyons *et al.*, 2012). APV (Tocris) was used at a concentration of 100 μ M. Nimodipine (Sigma) was used at a concentration of 5 μ M. EGTA (Sigma) was used at 2.5mM. Actinomycin D (Sigma) was used at 30nM. Pharmacological blockers were added 2 min prior to TTX WD or KCl addition and maintained throughout the period of stimulation. All experiments were conducted in accordance with an animal protocol approved by the Duke University Institutional Animal Care and Use Committee.

2.3.2 Quantitative PCR

RNA was harvested from cultured mouse cortical neurons on DIV7 following 90min or 6hrs of KCl-mediated membrane depolarization or TTX WD as described in the text. RNA was harvested using the Absolutely RNA Miniprep Kit (Agilent) and cDNA was synthesized by Superscript II (Invitrogen). Quantitative SYBR green PCR was performed on an ABI 7300 real-time PCR machine (Applied Biosystems) using intron-spanning primers (IDT) listed in

Appendix A. Data were all normalized to expression of the housekeeping gene *Gapdh* to control for sample size and processing. For CaRF luciferase assay, RNA was harvested from HEK293T cells at 2 days after transfection. cCaRE-Luc plasmid was previously described (Lyons et al., 2012; Pfenning et al., 2010) and TK-renilla luciferase is from Promega. The *firefly luciferase* mRNA levels were normalized for each well to cotransfected *renilla luciferase* mRNA levels.

Primers

2.3.3 RNAi and Lentiviral Infection

Four independent shRNAs were used to knockdown mouse *Carf*, and were paired with a vector-matched control (Ctrl). *Carf* shRNA1 (5'-GAAGACAGCACCAGCAATTAC-3') and Ctrl1(5'-AAACAAGCCCATTCGCGGATT-3), which is a scrambled version of *Carf* shRNA1, were cloned into vector pLLx3.8 (Zhou et al. 2007). *Carf* shRNA2 (TRCN0000086260; 5'-GCAGATGAACATAGCCCTCAA-3'), *Carf* shRNA3 (TRCN0000086262; 5'-GACGATGGTGAGAAGTCAGAA-3'), *Carf* shRNA4 (TRCN0000086261; 5'-CCAGCCAGGATATACATTTAAA-3') were purchased from Thermo Scientific and the empty pLKO.1 vector was used as Ctrl2. *Bdnf* shRNA (TRCN0000065384; 5'-CAAGGCTGTTAGAGAGATAATTGGA-3') were purchased from Thermo Scientific and the empty pLKO.1 vector was used as Ctrl. The rat GluN3A and rat CaRF-myc expression plasmids were constructed by placing the rat *Grin3a* or *Carf-myc* coding sequences under control of the ubiquitin promoter in the lentiviral expression vector pFUIGW (Lois et al., 2002). The C-terminally truncated rat CaRF(1-268) expression plasmid was cloned by PCR from rat brain

cDNA generating a fragment expressing amino acids 1-268, which corresponds to the shortest truncated version of mouse CaRF (AAs 1-251). The construct was placed under control of the ubiquitin promoter in the lentiviral expression vector pFUIGW (Lois et al., 2002). For viral infection of neurons, shRNA or viral expression constructs were packaged as lentiviral particles in HEK 293T cells following standard procedures. Concentrated viruses were titered on mouse cortical neurons which were infected for 6 hrs on day in vitro (DIV) 1 at a multiplicity of infection of 1 in BME medium (Sigma) with 0.4 μ g/mL added polybrene (Sigma).

2.3.4 Immunofluorescence

Embryonic mouse cortical neurons were cultured on PDL/laminin coated glass coverslips (Bellco) and fixed in 4% paraformaldehyde at room temperature for 10mins. Neurons were blocked in 10% normal goat serum and permeabilized in 0.3% Triton X-100 prior to antibody incubation. Coverslips were incubated in primary antibodies overnight at 4°C. Secondary antibodies were incubated at room temperature for 1 hr. Hoechst dye (0.1 μ g/ml, Sigma) was used to label nuclei. Primary antibodies used in this study for immunocytochemistry were mouse anti-MEF2D, 1:1000 (BD Biosciences; #610774). mouse anti-Gephyrin, 1:500 (Synaptic Systems; 147021), rabbit anti-GAD65, 1:500 (Millipore; AB5082), chicken anti-GFP, 1:2000 (Millipore; AB16901).

2.3.5 Western Blotting

Cells were homogenized in homogenization buffer (320 mM Sucrose, 10mM HEPES pH 7.4, 2mM EDTA, 1mM DTT and protease inhibitors). Nuclear pellet was centrifuged out at 1500xg for 15min. Cytosolic and membrane fractions were separated by centrifuging at 200000xg for 20min. Membrane, cytoplasmic, and nuclear extracts were run for SDS-PAGE and transferred to Nitrocellulose for western blotting following standard procedures. Primary antibodies used in this study for western blotting were mouse anti-Actin, 1:5000 (Millipore; MAB1501); rabbit anti-CaRF, 1:500 (#4510, McDowell et al., 2010); rabbit anti-Histone H3,

1:5000 (Millipore; catalog #070-690); rabbit anti-GluN3A, 1:1000 (Millipore; #07-356); mouse anti-Transferrin Receptor, 1:2000 (Invitrogen; #13-6800).

2.3.6 Electrophoretic Mobility Shift Assays (EMSA)

Nuclear extracts from cultured mouse cortical neurons infected on DIV1 with viruses expressing the shRNAs targeting *Carf* or their respective controls were harvested on DIV7 and used for EMSA as previously described (McDowell *et al.*, 2010). Probes were end labeled with ³²P and EMSA images were captured on a Storm phosphorimager (Molecular Dynamics). The high affinity CaRF-binding cCaRE probe, CaRE1 and mCaRE1 have been previously described (Pfenning *et al.* 2010; Lyons *et al.* 2012). The probes of two potential CaRF binding sites near *Grin3a* promoter are listed here (gCaRE1: 5'-TCATTATGAGACAGA, gCaRE2: 5'-TCTCGAGGAGACAGA).

2.3.7 BDNF ELISA

Two-site BDNF ELISA was performed as previously described (Hong *et al.*, 2008; McDowell *et al.*, 2010). Total protein concentration in the lysate was measured by BCA protein assay kit (Pierce) and BDNF protein concentrations were measured by the BDNF Emax ImmunoAssay System (Promega).

2.3.8 Pilocarpine-induced Seizure

Adult (8-12 week old) male C57BL6/J mice (Charles River Labs) were weighed and injected with 1 mg/kg methyl scopolamine nitrate (i.p.). 30 min later mice were injected i.p. with either 337 mg/kg pilocarpine HCl or saline (control mice) and monitored for status epilepticus as previously described (Wijayatunge *et al.*, 2014). 1, 3, or 6 hrs following the onset of status epilepticus, mice were deeply anesthetized with isofluorane and decapitated for brain harvesting. Brains of control mice were harvested 3 hrs after the saline injection. 5-6 mice were used for each time point. The hippocampus was rapidly dissected bilaterally, flash frozen on dry ice/ethanol, and stored at -80°C prior to RNA harvesting, cDNA synthesis, and quantitative PCR as described above.

2.3.9 Dark Adaptation and Light Exposure

Male and female *Carf* wildtype (WT) and knockout (KO) adult mice (McDowell et al., 2010) or pups with their mothers at postnatal day 14 (P14) were transferred from their normal housing room with a 12 hr:12 hr light:dark cycle into a light-tight dark housing room to maintain constant darkness for 7 days. Animals in the unstimulated (dark) condition were killed and their eyes enucleated in the dark prior to bringing the body into the light to dissect the brain. Animals in the stimulated (light-exposed) condition were removed from the dark room and exposed to normal lighting for 6 hrs prior to tissue harvesting. For MK-801 (Sigma) experiments, 6-month-old adult were injected intraperitoneally (i.p.) in the dark with either saline (control) or 1mg/kg MK-801 diluted in 0.9% NaCl 30 min prior to being brought into the light. V1 visual cortex and S1 somatosensory cortex were isolated based on anatomical landmarks and immediately flash frozen. RNA and protein were harvested and measured as described above.

2.3.10 Quantification of inhibitory synapse density

Embryonic mouse cortical neurons were cultured on PDL/laminin coated glass coverslips (Bellco). Neurons were transfected with Ctrl1 or *Carf* shRNA1 by lipofectamine 2000 on DIV 3 and fixed in 4% paraformaldehyde at room temperature for 10mins on either DIV14 or DIV19. Neurons were blocked in 16% normal goat serum and permeabilized in 0.2% Triton X-100 prior to antibody incubation. Coverslips were incubated in primary antibodies overnight at 4°C. Secondary antibodies were incubated at room temperature for 1 hr. Hoechst dye (0.1µg/ml, Sigma) was used to label nuclei. Primary antibodies used in this study were mouse anti-Gephyrin, 1:500 (Synaptic Systems; 147021), rabbit anti-GAD65, 1:500 (Millipore; AB5082), chicken anti-GFP, 1:2000 (Millipore; AB16901). Images were acquired on a Leica SP8 confocal microscope with a 40X objective at 1024X1024 pixel resolution. Images were collected as a z-stack of 10-12 sections at 0.5µm step size, and maximum intensity projections generated from the z-stack were used for analysis. Synapse density was quantified with ImageJ using NeuronJ and SynapCountJ

plugin. For each experiment, approximately 5-10 neurons from at least two different coverslips were analyzed, and between 2-3 experiments were conducted per condition.

2.3.11 Statistical Analyses

Unless otherwise indicated, all data presented are the average of at least three biological replicates from each of at least two independent experiments. Also unless otherwise indicated, data were analyzed by a Student's unpaired t-test, and $p < 0.05$ was considered significant. Bar and line graphs show mean values and all error bars show S.E.M.

2.4 Results

2.4.1 Loss of CaRF results in potentiation of NMDAR-dependent transcription

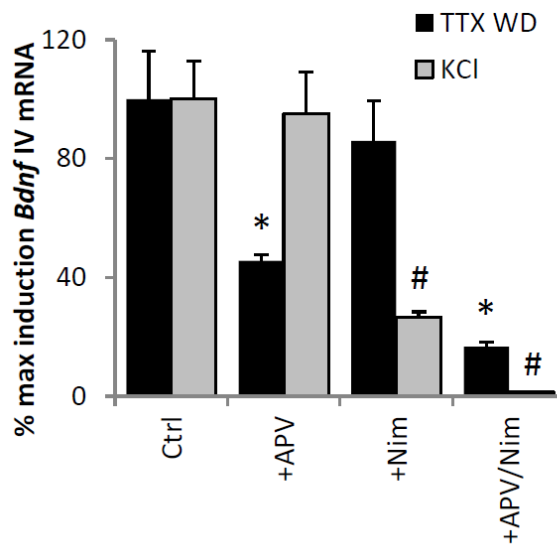


Figure 7: Relative induction *Bdnf* exon IV-containing mRNA in mouse cortical neurons either without stimulation (Basal) or 6 hrs following TTX withdrawal (TTX WD) or 55mM elevated extracellular potassium (KCl) prior to RNA harvesting. Stimulation was done in the presence of the following pharmacological blockers of NMDARs and L-VSCCs: none (Ctrl), +APV, nimodipine (+Nim), or APV + Nim (+APV/Nim). mRNA levels are reported as fold induction relative to Basal. $n=3$. We set the fold induction reached by either TTX WD or KCl in the Ctrl group to 100%. * $p < 0.05$ compared with Ctrl in TTX WD. # $p < 0.05$ compared with Ctrl in KCl.

To assay NMDAR-dependent activation of *Bdnf* transcription, we stimulated dissociated mouse cortical neuron cultures with tetrodotoxin withdrawal (TTX WD). This stimulus has previously been characterized for its ability to induce IEG expression in neurons in an NMDAR-dependent manner (Ghiretti et al., 2014; Rao et al., 2006; Saha et al., 2011), including exon IV-

containing forms of *Bdnf*. We confirmed that pretreatment with the NMDAR antagonist APV significantly attenuated TTX WD-induced *Bdnf* IV expression ($p=0.0285$). Conversely, pretreatment with the L-VGCC antagonist Nimodipine alone had no significant effect on TTX WD-induced *Bdnf* IV expression ($p=0.5372$), though it blocked *Bdnf* IV transcription induced by membrane depolarization with elevated extracellular KCl ($p=0.0047$) (**Fig. 7**). Thus, using these two stimulation paradigms (TTX WD and elevation of extracellular KCl) we can selectively activate gene transcription in an NMDAR- or L-VGCC-dependent manner.

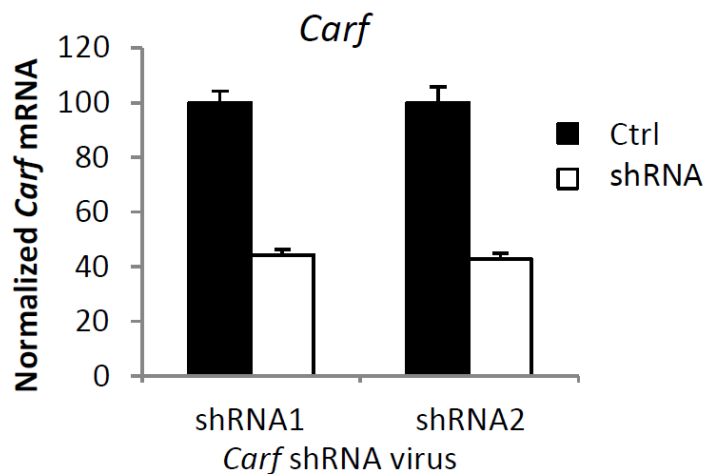


Figure 8: Levels of *Carf* mRNA in mouse cortical neurons infected with lentiviruses encoding shRNAs targeting two independent sequences in *Carf*. *Carf* mRNA levels are shown normalized to expression in cells infected with the paired control viruses. $n=3$.

To test the requirement for CaRF in NMDAR-dependent activation of *Bdnf* IV, we characterized two independent shRNAs in lentiviral vectors that knockdown (KD) expression of CaRF in cultured neurons (**Fig. 8**). We then measured *Bdnf* IV mRNA following TTX WD. To our surprise, given that we have previously characterized CaRF as an activator of *Bdnf* transcription, we found that *Bdnf* IV induction was significantly potentiated upon TTX WD in CaRF KD neurons compared with neurons that were infected with paired control viruses (*Carf* shRNA1: $p=0.0171$; *Carf* shRNA2: $p=0.0269$; **Fig. 9A**). This effect was selective for the activation of *Bdnf* IV transcription by NMDARs because we did not observe any significant difference in *Bdnf* IV induction between CaRF control and KD neurons when we stimulated L-

VGCC-dependent transcription with the elevation of extracellular KCl (*Carf* shRNA1: $p= 0.8989$; *Carf* shRNA2: $p= 0.9814$; **Fig. 9B**). The transcriptional activation of *Bdnf* IV by both TTX WD and KCl leads to increased expression of BDNF protein as measured by ELISA (Fold induction BDNF after KCl: 4.54 ± 0.17 , $n=6$; after TTX WD: 3.06 ± 0.49 , $n=6$). Importantly, the potentiation of NMDAR-dependent *Bdnf* IV transcription we observed in CaRF KD neurons

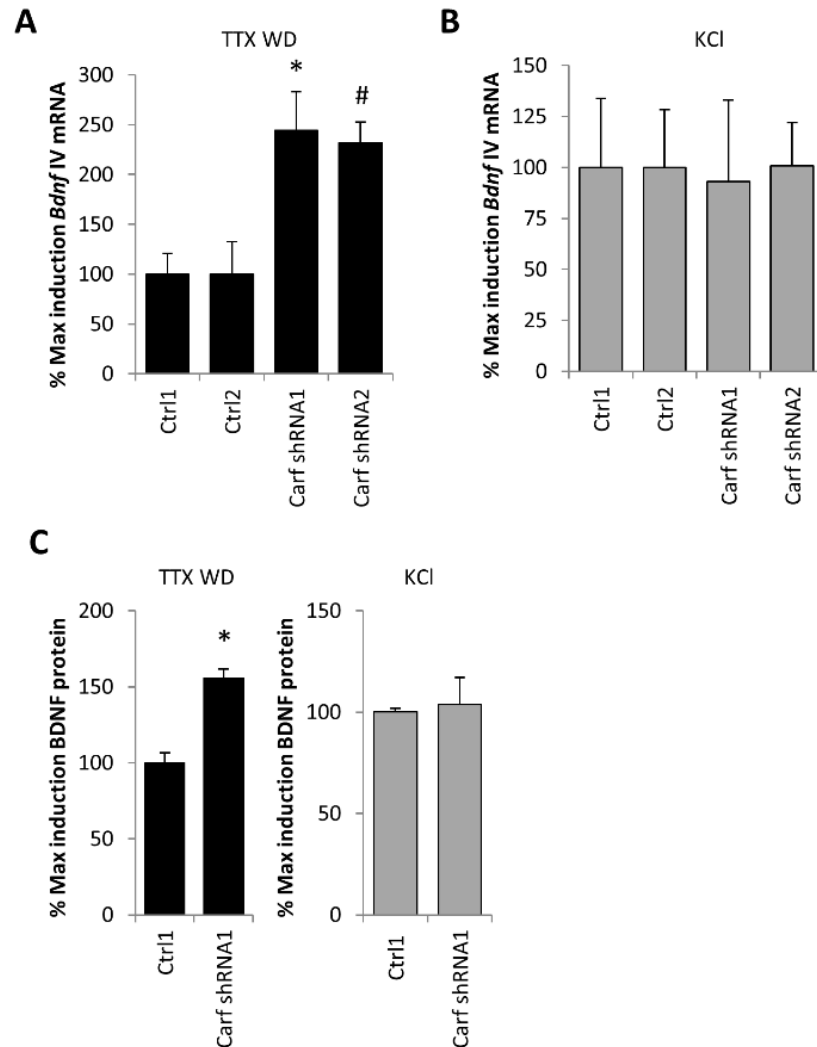


Figure 9: (A) Levels of *Bdnf* exon IV mRNA in cortical neurons infected with the indicated lentiviruses then stimulated with 6hrs TTX WD. Induced mRNA levels for neurons infected with each shRNA targeting *Carf* (shRNA1, shRNA2) are reported as percentages of induction relative to their respective control vectors (Ctrl1 or Ctrl2). $n=3-4$, $*p<0.05$ compared with Ctrl1, $\#p<0.05$ compared with Ctrl2. (B) Levels of *Bdnf* exon IV mRNA in cortical neurons infected with the indicated lentiviruses then stimulated with 55mM extracellular KCl for 6hrs. Induced mRNA levels for neurons infected with each shRNA targeting *Carf* (shRNA1, shRNA2) are reported as percentages of induction relative to their respective control vectors (Ctrl1 or Ctrl2). $n=3-4$ (C) Levels of BDNF protein as measured by ELISA from neurons treated for 6 hrs as in (A) and (B). Protein levels are reported as percentages of induction by TTX WD or KCl relative to control shRNA (Ctrl1) $n=6$, $*p<0.05$ compared with Ctrl1.

resulted in enhanced expression of BDNF protein in CaRF KD compared with control neurons ($p < 0.0001$; **Fig. 9C**). By contrast, KCl-mediated membrane depolarization induced BDNF protein expression to similar levels in both CaRF control and KD neurons ($p = 0.7889$; **Fig. 9C**).

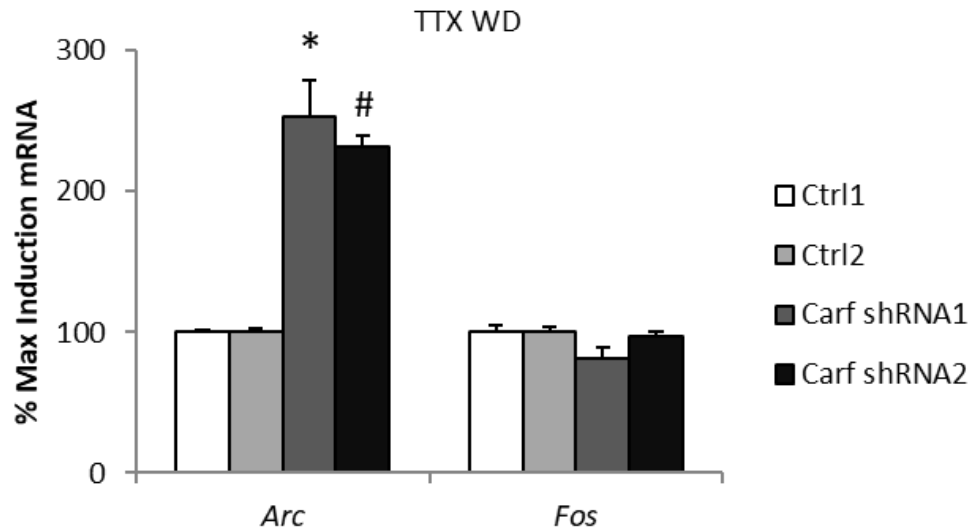


Figure 10: Levels of *Arc* and *Fos* mRNA in cortical neurons infected with the indicated lentiviruses then stimulated with 90min TTX WD. $n=3-4$ * $p < 0.05$ compared with Ctrl1, # $p < 0.05$ compared with Ctrl2.

In addition to *Bdnf*, other IEGs including *Fos* and *Arc* are strongly induced by TTX WD stimulation and the activation of NMDARs (Saha et al., 2011). We found that KD of CaRF did not lead to a nonspecific increase in all NMDAR-activated transcription (**Fig. 10**), because the TTX WD-induced expression of *Fos* was not different between CaRF control and KD neurons (*Carf* shRNA1: $p=0.1926$; *Carf* shRNA2: $p=0.6159$). However, KD of CaRF did lead to a potentiation of TTX WD-induced *Arc* expression compared with that seen in control-infected neurons (*Carf* shRNA1: $p=0.0264$; *Carf* shRNA2: $p < 0.0001$), demonstrating that the effects of CaRF on NMDAR-dependent gene expression extend beyond the regulation of *Bdnf*. These data reveal for the first time that CaRF regulates NMDAR-dependent neuronal plasticity by selectively inhibiting NMDAR-dependent activation of a subset of IEGs, which include not only *Bdnf* IV but also *Arc*.

2.4.2 The NMDAR subunit gene *Grin3a* is a regulatory target of CaRF

CaRF is a DNA binding transcription factor that in neurons is bound to a large number of regulatory elements dispersed across the genome (Pfenning et al., 2010). Because the effects of CaRF KD were selective for NMDAR-dependent transcription, we reasoned that CaRF might confer this specificity via regulation of components of the NMDAR itself. In addition to the obligatory GluN1 subunit encoded by the *Grin1* gene, forebrain neurons most highly express the GluN2A and B subunits encoded by *Grin2a* and *Grin2b* as well as the GluN3A subunit encoded by *Grin3a* (Fig. 11). Of the genes encoding these subunits, only *Grin3a* was among those we

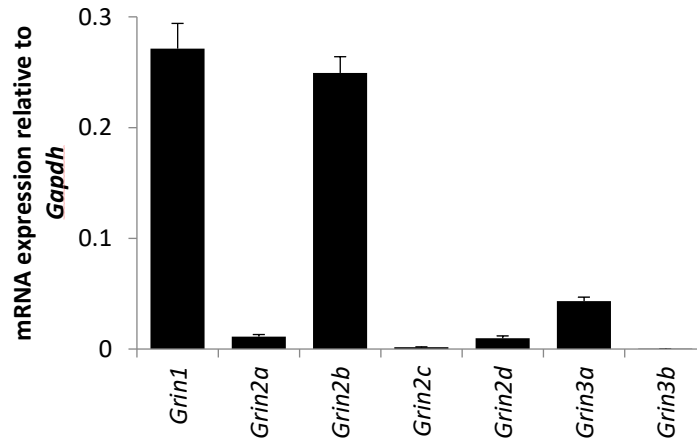


Figure 11: mRNA levels of NMDAR subunits in cultured mouse cortical neurons. Levels of the indicated mRNAs in cultured mouse cortical neurons (DIV 7). mRNA levels are shown relative level to *Gapdh* expression. n=4. found significantly changed in microarray analysis of gene expression in mouse cortical neurons lacking *Carf* (Whitney et al., 2014). Q-PCR confirmed that CaRF knockdown had consistent and

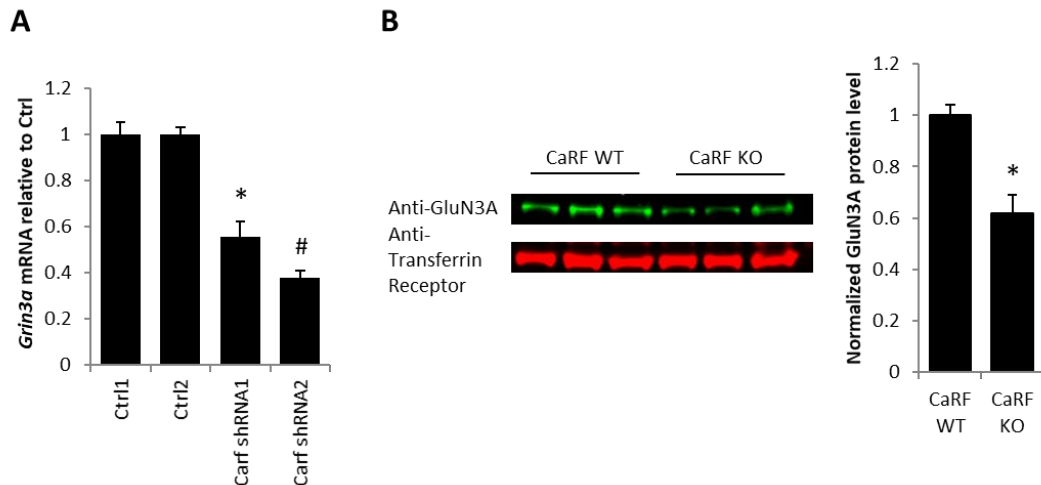


Figure 12: (A) *Grin3a* mRNA levels in mouse cortical neurons infected with the indicated lentiviruses. n=8, * $p < 0.05$ compared with Ctrl1. # $p < 0.05$ compared with Ctrl2. (B) Representative image (left) and quantification (right) of Western blot showing GluN3A level in membrane fractions from the cortex of p21 CaRF WT or CaRF KO mice. Transferrin receptor is shown as a loading control. Band density in each lane was quantified using ImageJ. n= 6WT, 3KO. * $p < 0.05$ compared with CaRF WT.

significant effects expression on the *Grin3a* gene, which was reduced by more than 50% in CaRF KD neurons relative to control (*Carf* shRNA1: $p = 0.0001$; *Carf* shRNA2: $p < 0.0001$; **Fig. 12A**). Furthermore, levels of GluN3A were significantly reduced in membrane fractions taken from the cortex of postnatal day 21 (P21) CaRF knockout (KO) mice as compared with their wildtype (WT) littermates ($p = 0.0013$; **Fig. 12B**).

If *Grin3a* is a regulatory target of CaRF, these gene products should be co-regulated. *Grin3a* is most highly expressed during a transient period in early postnatal forebrain development (Ciabarra et al., 1995; Sucher et al., 1995), and notably, CaRF expression follows a similar pattern of temporal regulation (McDowell et al. 2010). Furthermore, our data show that, in addition to this slow developmental regulation, expression of CaRF is under the more acute control of activity-regulated signaling pathways. Following pilocarpine-induced seizure, which rapidly upregulated expression of *Bdnf* IV and *Fos* in hippocampus (Fold induction *Bdnf* IV 1hr after pilocarpine injection: 9.24 ± 1.53 , n=5-6; Fold induction *Fos* 1hr after pilocarpine injection: 105.73 ± 23.5 , n=5-6), *Carf* expression was significantly reduced ($F_{1,21} = 19.15$, $p < 0.0001$; **Fig. 13A**). *Grin1*, *Grin2a*, and *Grin2b* showed no significant change in their expression over this timecourse (*Grin1*: $F_{1,21} = 0.42$, $p = 0.7342$; *Grin2a*: $F_{1,21} = 0.96$, $p = 0.4296$; *Grin2b*: $F_{1,21} = 0.17$, $p = 0.9148$; **Fig. 13B**), however like *Carf*, *Grin3a* expression was significantly reduced following pilocarpine treatment ($F_{1,21} = 7.26$, $p = 0.002$; **Fig. 13A**). The downregulation of both *Carf* and *Grin3a* was recapitulated by elevation of extracellular KCl in cultured hippocampal neurons, suggesting a role for calcium signaling pathways in this regulation (*Carf*: $p < 0.0001$; *Grin3a*: $p = 0.0001$; **Fig. 13C**). Consistent with this hypothesis, treating cultures with 2.5mM EGTA, which chelates free extracellular calcium, drove a significant increase in both *Carf* and *Grin3a* mRNA

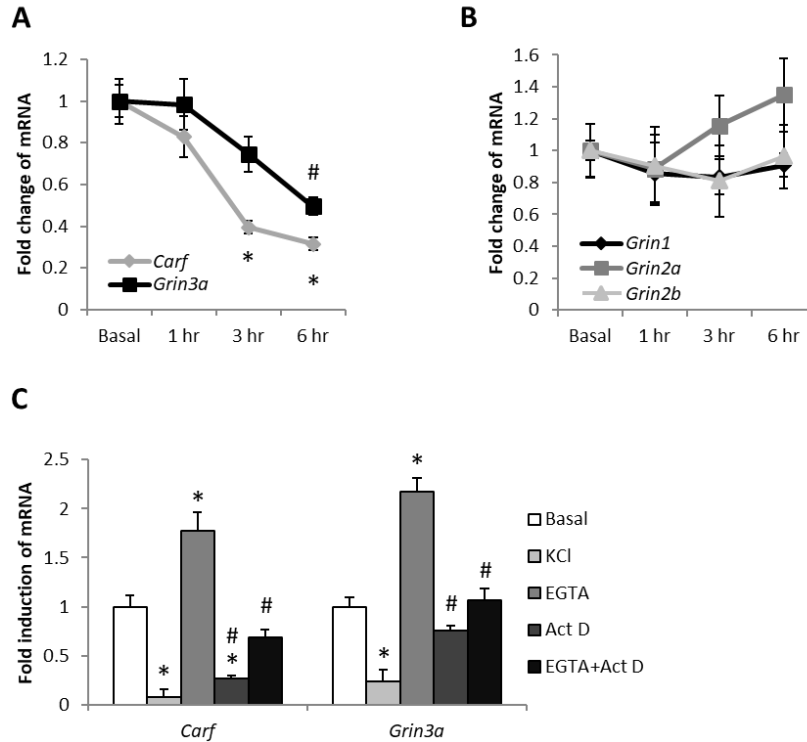


Figure 13: (A) *Carf* and *Grin3a* mRNA levels in the hippocampus of mice injected with either saline (Basal) or pilocarpine for the indicated amounts of time. $n=5-6$, $*p < 0.01$ compared with *Carf* Basal. $\#p < 0.05$ compared with *Grin3a* Basal. (B) Indicated mRNA levels in the hippocampus of mice injected with either saline (Basal) or pilocarpine for the indicated amounts of time. $n=5-6$. (C) *Carf* and *Grin3a* mRNA levels in mouse cortical neurons treated with KCl, EGTA, Actinomycin D or EGTA + Actinomycin D for 6hrs. $n=5-6$, $*p < 0.05$ compared with Basal. $\#p < 0.05$ compared with EGTA. Data from Michelle Lyons.

expression (*Carf*: $p=0.0051$; *Grin3a*: $p=0.0001$; **Fig. 13C**). This induction was transcription-dependent, because the EGTA-dependent increase of *Carf* and *Grin3a* mRNA expression was blocked by pre-treatment with the transcriptional inhibitor Actinomycin D (*Carf*: $p=0.0002$; *Grin3a*: $p < 0.0001$; **Fig. 13C**).

Because CaRF can function as a DNA sequence-specific transcriptional activator (Tao *et al.* 2002), it could regulate the expression of *Grin3a* directly by binding to the *Grin3a* promoter. Although a search of the proximal *Grin3a* promoter revealed two elements with partial homology to the consensus CaRF binding site, electrophoretic mobility shift assays revealed no evidence for CaRF binding at these sites (**Fig. 14**) and furthermore CaRF binding was not detected at the proximal *Grin3a* promoter by ChIP-seq (Pfenning *et al.*, 2010). Thus these data suggest that CaRF does not directly bind the proximal *Grin3a* promoter.

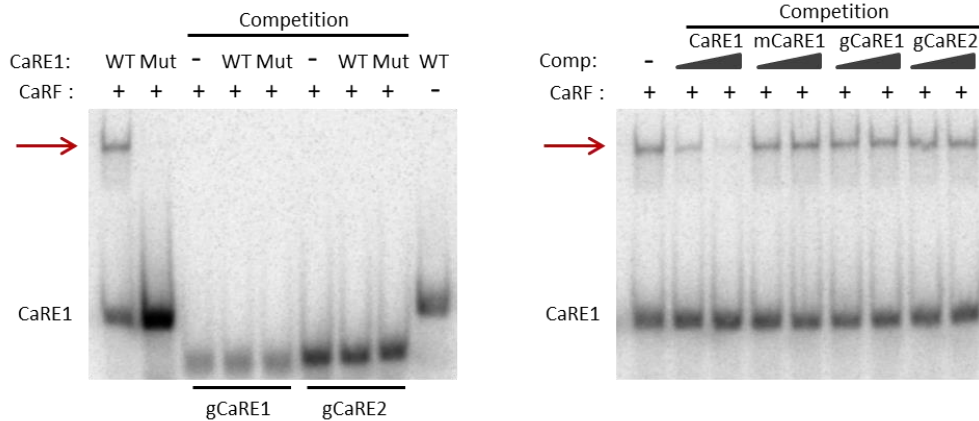


Figure 14: CaRF does not bind to *Grin3a* promoter directly. Electrophoretic mobility shift assays. Left, in vitro transcribed and translated CaRF protein was incubated with either with a radiolabeled CaRF binding sequence (CaRE1) or one of the two sequences with partial homology to the CaRF binding sequence identified in the proximal *Grin3a* promoter (gCaRE1 and gCaRE2). The red arrows indicate nuclear protein-DNA complexes. Specificity of the interaction is shown by competition of the interaction with incubation of an excess of unlabeled WT CaRE1 probe but not an unlabeled mutant probe (MUT) that lacks CaRF binding. Right, CaRF is first bound to the CaRE1 probe and association with the gCaRE sequences is tested by asking if the gCaREs can compete binding. The ramps indicate increasing concentration of unlabeled competitor probe. Competition of labeled CaRE1 binding by unlabeled CaRE1 is shown as a positive control. The red arrows indicate nuclear protein-DNA complexes. Data from Anne West.

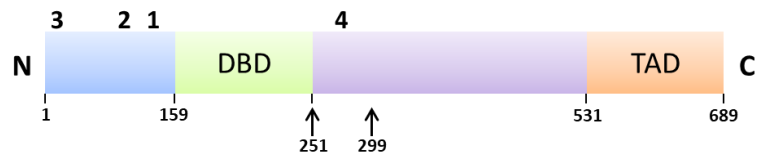


Figure 15: Schematic diagram showing the protein domain organization of CaRF and the targeting sites of *Carf* shRNAs. The numbers above the diagram indicate the target site of *Carf* shRNAs. The numbers below the diagram indicate the protein residues corresponding to mouse CaRF (NP_631889.1). The arrows mark the C-terminal end of truncated forms of CaRF reported previously (Tao et al. 2002). The rCaRF(1-268) construct corresponds to the truncated mouse CaRF terminating at amino acid 251. DBD, DNA binding domain; TAD, transcriptional activation domain.

The *Carf* gene encodes several splice variants, some of which lack the C-terminal activation domain and are predicted to encode truncated CaRF isoforms that function as transcriptional repressors (Fig. 15) (McDowell et al., 2010; Pfenning et al., 2010; Tao et al., 2002b). To determine which forms of CaRF are required for regulation of *Grin3a* we tested the consequences of knocking down CaRF using shRNAs that are either specific to the longer forms or common to sequences contained within all variants. Whereas all shRNAs reduced the expression of CaRF mRNA (Fig. 16A) only the shRNAs that targeted all of the truncated and the full-length CaRF variants resulted in reduced expression of *Grin3a* (*Carf* shRNA2: $p = 0.0018$;

Carf shRNA3: $p < 0.0001$; *Carf* shRNA4: $p = 0.0882$; **Fig. 16B**). Because these data suggested that expression of the shorter truncated version of CaRF might be sufficient to promote expression of

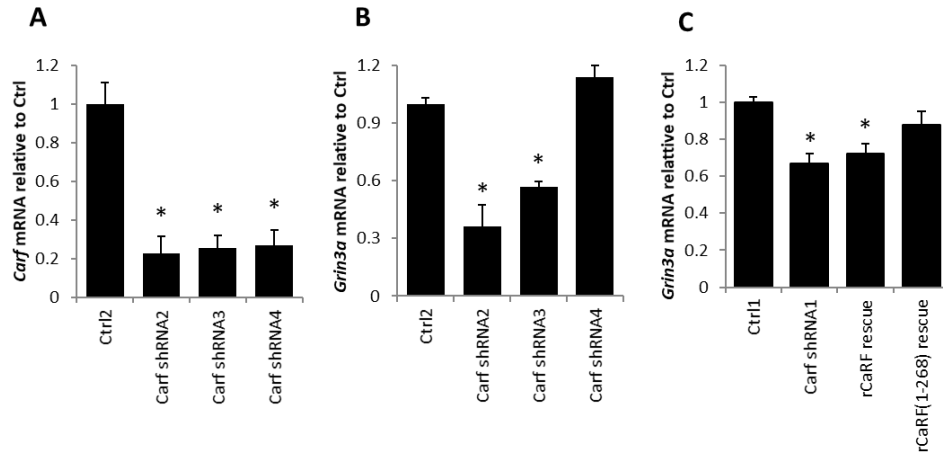


Figure 16: (A) Levels of *Carf* mRNA in mouse cortical neurons infected with lentiviruses encoding shRNAs targeting three independent sequences in *Carf*. *Carf* mRNA levels are shown normalized to expression in cells infected with the paired control virus (Ctrl2). $n = 3$. * $p < 0.05$ compared with Ctrl2. (B) *Grin3a* mRNA levels in mouse cortical neurons infected with the indicated lentiviruses. $n = 3$, * $p < 0.05$ compared with Ctrl2. (C) *Grin3a* mRNA levels in mouse cortical neurons infected with the indicated lentiviruses. $n = 4-10$, * $p < 0.05$ compared with Ctrl1.

Grin3a, we selectively re-expressed rat isoforms of either truncated or full-length CaRF in CaRF KD neurons, which due to sequence variation in the region targeted by *Carf* shRNA1 are resistant to knockdown. Though both rescue constructs were overexpressed relative to endogenous levels of CaRF, only the truncated form of rat CaRF was able to restore *Grin3a* expression in CaRF KD neurons (*Carf* shRNA1: $p < 0.0001$; rCaRF rescue: $p = 0.009$; rCaRF(1-268): $p = 0.1018$; **Fig. 16C**). Since this variant of CaRF lacks the transcriptional activation domain (**Fig. 15**), taken together with the lack of CaRF binding to the *Grin3a* promoter (**Fig. 14**), these data suggest that CaRF functions in an indirect manner to drive *Grin3a* expression.

Regardless of the mechanism by which CaRF regulates expression of *Grin3a*, if the potentiation of NMDAR-dependent transcription in CaRF KD neurons is due to the reduced GluN3A expression we observed, then rescuing the expression of GluN3A in these neurons should be sufficient to restore the regulation of TTX WD-induced *Bdnf* IV expression to control levels. To test this hypothesis, we first asked whether selective re-expression of the truncated form of rat CaRF would restore NMDAR-regulated *Bdnf* IV induction to control levels in CaRF

KD neurons. Consistent with this hypothesis we found that expression of an shRNA-resistant form of CaRF significantly reduced NMDAR-dependent *Bdnf* IV induction in shRNA-expressing

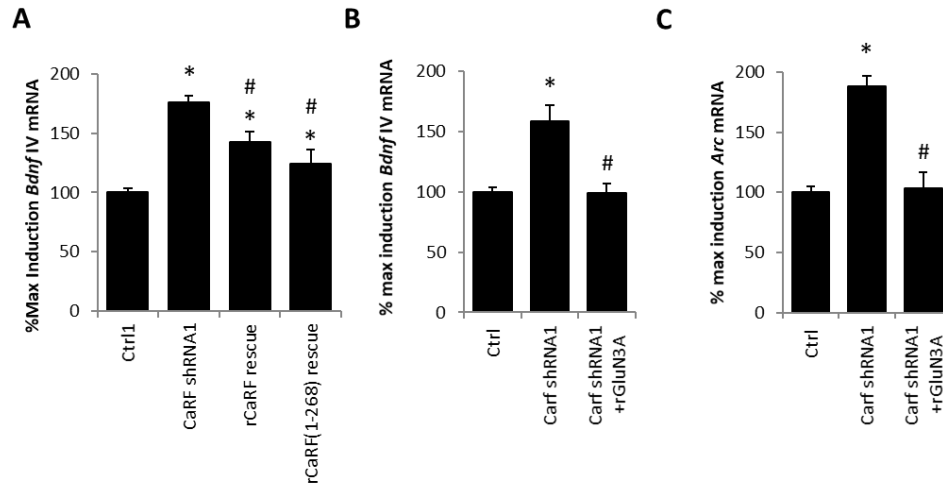


Figure 17: (A) *Bdnf* exon IV mRNA level in cortical neurons infected with the indicated lentiviruses following stimulation with 6hrs TTX WD. n=6-10, * $p < 0.05$ compared with Ctrl1. # $p < 0.05$ compared with *Carf* shRNA1. (B) *Bdnf* exon IV and (C) *Arc* mRNA level in cortical neurons infected with the indicated lentiviruses following stimulation with 6hrs TTX WD. n=5-6, * $p < 0.05$ compared with Ctrl1. # $p < 0.05$ compared with *Carf* shRNA1.

neurons toward control levels (rCaRF(1-268): $p = 0.0005$; **Fig. 17A**). Notably, re-expressing full-length rat CaRF also partially rescued *Bdnf* IV inducibility despite the fact that it did not rescue *Grin3a* expression (rCaRF: $p = 0.0031$; **Fig. 16C and 17A**). Because our previous microarray and chromatin immunoprecipitation experiments have identified a large number of putative CaRF target genes (Pfenning et al. 2010; Whitney et al. 2014), we interpret these latter data to suggest that full length CaRF may regulate gene products other than *Grin3a* that can also impact *Bdnf* inducibility. Thus to more directly determine whether restoration of GluN3A can rescue *Bdnf* inducibility in neurons lacking CaRF, we overexpressed rat GluN3A or GFP as a control in both CaRF KD and control neurons and measured the induction of *Bdnf* IV mRNA upon TTX WD. Whereas CaRF KD neurons expressing GFP showed potentiated induction of *Bdnf* IV and *Arc* relative to control neurons, when we expressed rat GluN3A together with the *Carf* shRNA, the induction of *Bdnf* IV and *Arc* was not significantly different from control (*Bdnf* IV: $p = 0.8960$; *Arc*: $p = 0.8243$; **Fig. 17B and 17C**). Together these data place CaRF as an indirect upstream regulator of *Grin3a*, and *Grin3a* upstream of *Bdnf* IV and *Arc* induction, establishing a

mechanism by which CaRF can selectively modulate NMDAR-dependent processes in the developing brain.

2.4.3 Enhanced sensory experience induced gene transcription in the developing cortex of CaRF knockout mice.

NMDARs and activity-regulated genes like *Bdnf* play an important role in the sensory experience-dependent refinement of cortical organization in the postnatal brain. Given that both CaRF and GluN3A show peak expression during of the first two postnatal weeks of brain development (Ciabarra et al., 1995; McDowell et al., 2010; Sucher et al., 1995), we hypothesized that the CaRF-GluN3A pathway we have elucidated here may be important for regulating NMDAR-dependent gene expression by sensory stimuli in the developing postnatal brain. To test this hypothesis, we assayed light-dependent activation of transcription in the visual cortex of mice that were dark-adapted from postnatal day 14 (P14) to P21.

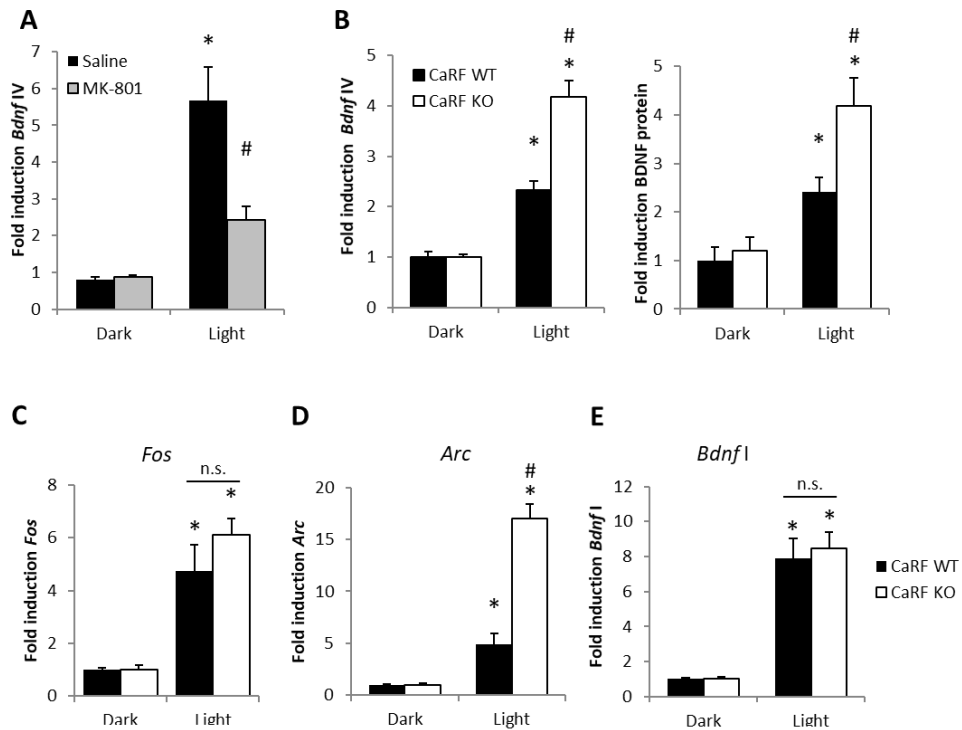


Figure 18: (A) Levels of *Bdnf* exon IV mRNA in the primary visual cortex of adult mice adapted to darkness for 7 days. Mice were injected with either saline or the NMDAR blocker MK-801 in the dark, then 30 min later they were either maintained in darkness (Dark) or exposed to light for 2hrs (Light) prior to tissue harvesting. $n = 3$, $*p < 0.05$, Saline vs MK-801. (B) Levels of *Bdnf* exon IV mRNA and BDNF protein in the primary visual cortex of P21 CaRF WT and KO mice after 7 days of constant darkness (Dark) or following exposure to light for 6hrs (Light) prior to tissue

harvesting. n=8-11 animals per condition, * p <0.05, Dark vs. Light. # p <0.05 WT vs. KO. (C-E) *Fos* (C), *Arc* (D), and *Bdnf* exon I (E) mRNA levels in primary visual cortex of mice from (B). n=8-11 animals per condition, * p <0.05, Dark vs. Light. # p <0.05 WT vs. KO. Data from Michelle Lyons.

Light exposure drives rapid upregulation of *Bdnf* expression in visual cortex (Castrén et al., 1992). This induction is NMDAR-dependent because when we pretreated dark-adapted mice with the NMDAR inhibitor MK-801 prior to light exposure we significantly inhibited the induction of *Bdnf* IV mRNA by light (p = 0.0309; **Fig. 18A**). Because we found that GluN3A expression is reduced in the developing cortex of CaRF KO mice relative to their WT littermates at P21 (**Fig. 12B**) we predicted that light-dependent activation of NMDAR-dependent gene transcription at this time point would be enhanced in the visual cortex of these mice. Indeed we found that light-induced expression of both *Bdnf* IV mRNA and BDNF protein were potentiated in visual cortex of P21 dark-adapted CaRF KO mice compared with their identically treated WT littermate controls (mRNA: p = 0.0003; protein: p =0.0156; **Fig. 18B**). The induction of gene expression was specific to brain regions activated by the light stimulus, because we saw no light-dependent regulation of activity-dependent genes in somatosensory cortex of the same mice (Fold induction *Fos*: 1.21 ± 0.56 ; *Arc*: 0.90 ± 0.32 ; *Bdnf* IV: 0.67 ± 0.12 . **Fig. 19**). The potentiation of

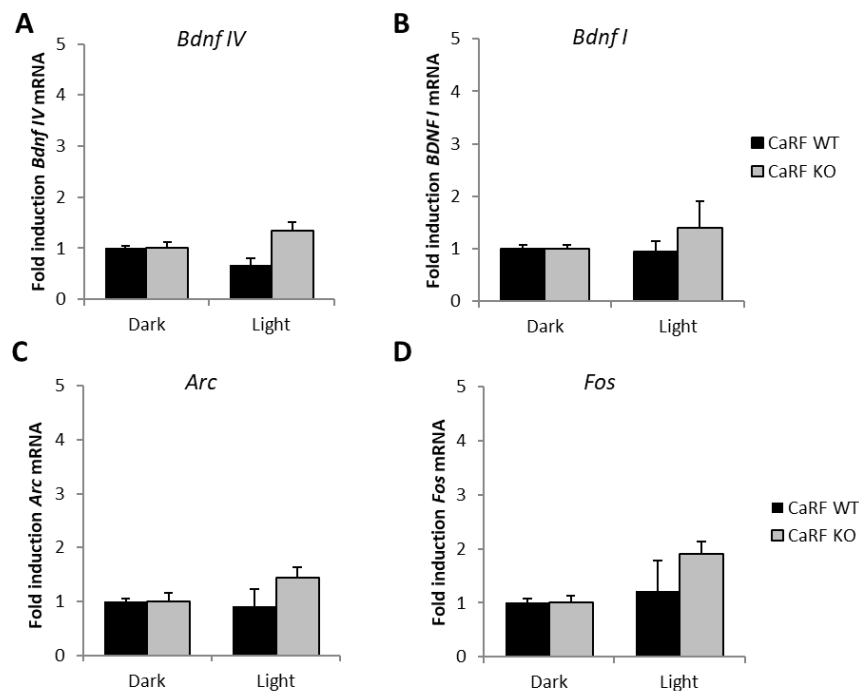


Figure 19: Light exposure does not induce gene transcription in somatosensory cortex. Levels of (A) *Bdnf* exon IV, (B) *Bdnf* exon I, (C) *Arc*, and (D) *Fos* in the primary somatosensory cortex of P21 CaRF WT and KO mice after 7 days of constant darkness (Dark) or following exposure to light for 6hrs (Light) prior to tissue harvesting. $n=9-11$.

Bdnf IV transcription in CaRF KO mice did not reflect a general increase in all NMDAR-dependent transcription because we saw no difference between CaRF WT and KO mice in the light-dependent induction of *Fos* ($p=0.2446$; **Fig. 18C**). However, similar to our results in cultured neurons, the potentiation of NMDAR-dependent transcription in CaRF KO mice did extend to other NMDAR-dependent genes including *Arc* ($p=0.0001$; **Fig. 18D**). Interestingly, although transcriptional regulation of *Bdnf* promoter I is also regulated by NMDARs expression of *Bdnf* exon I does not show potentiation of light-induced expression in the visual cortex of CaRF KO mice ($p=0.7034$; **Fig. 18E**). Taken together these data demonstrate that CaRF plays an important role in limiting sensory stimulus-regulated transcription of NMDAR-dependent genes in the developing postnatal brain.

2.4.4 Enhanced BDNF expression in CaRF-knockdown neurons accelerates inhibitory synapse development

The best characterized function of neuronal activity-dependent BDNF transcription in the developing brain is its role in promoting the formation of GABAergic synapses (Hong et al., 2008). We previously reported that we found increased expression of GABAergic synaptic proteins in the striatum of adult *Carf* KO mice (McDowell et al., 2010). To determine whether the enhanced NMDAR-dependent BDNF expression we detected in the CaRF KO and KD neurons could contribute to increases in GABAergic synapse formation, we assayed the development of GABAergic synapses by co-localization of pre- and post-synaptic markers in cultured control and *Carf* KD neurons. The density of GABAergic synapses increased between Day 14 in culture (DIV14) and DIV19 (Ctrl1: $p<0.0001$; **Fig. 20**). This developmental increase in GABAergic synapses was attenuated by transfection of an shRNA that knocks down expression of *Bdnf*, demonstrating the importance of BDNF as a modulator of GABAergic synapse number (DIV19,

Ctrl1+Bdnf shRNA: $p=0.0417$). This increase was significantly greater in CaRF KD neurons compared with control (DIV19, *Carf* shRNA1: $p=0.0425$) indicating that CaRF functions to limit

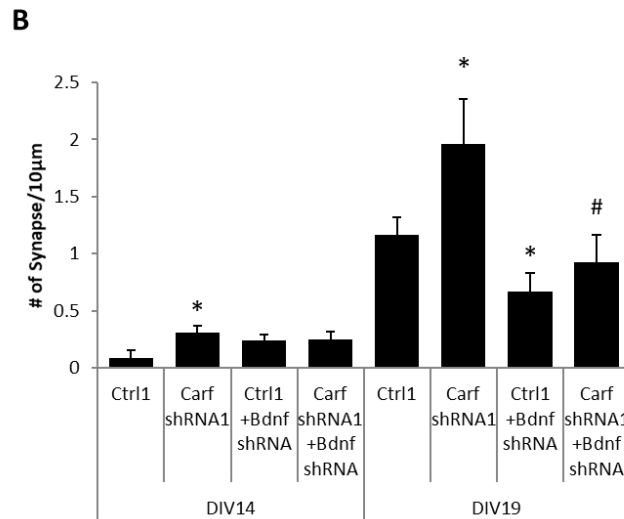
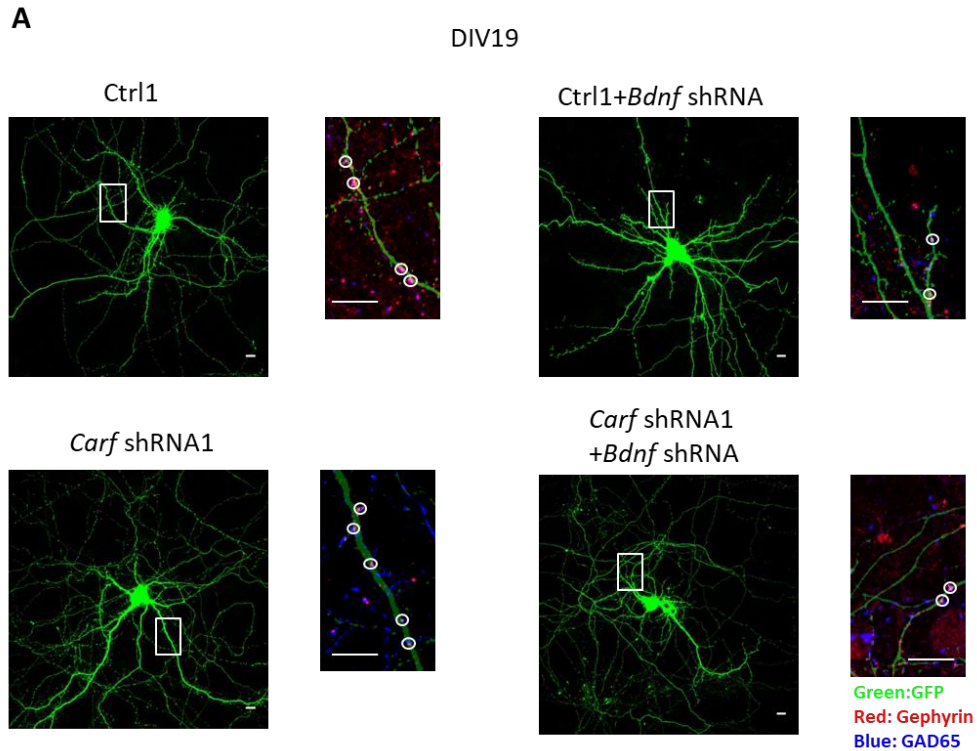


Figure 20: (A) Representative low and high magnification images of shRNA transfected mouse cortical neurons immunostained with indicated antibodies. The smaller images are the enlargement of the boxed area in low magnification images shows details of dendrites. Scale bar, 10 μ m. (B) Quantification of the average density of GAD65/Gephyrin coclusters along the dendrites of mouse cortical neurons transfected with indicated shRNA. 10-15 cells per condition, * $p < 0.05$ compared with Ctrl. # $p < 0.05$ compared with *Carf* shRNA1.

GABAergic synapse formation during development. The effect of losing CaRF on GABAergic synapse number was BDNF-dependent because knocking down BDNF in CaRF KD neurons

blocked the increase of GABAergic synapses compared to control on DIV19 (DIV19, *Carf* shRNA1+ *Bdnf* shRNA: p=0.0473; **Fig. 20**). Together these data demonstrate that CaRF-dependent modulation of BDNF transcription is important for regulating GABAergic synapse formation during development.

2.5 Discussion

NMDA-type glutamate receptors couple sensory experience with synapse maturation and neuronal survival in the developing brain (Cull-Candy and Leszkiewicz, 2004; Scheetz and Constantine-Paton, 1994). NMDARs exert long-lasting effects on brain development at least in part via their ability to activate calcium-regulated gene transcription (Bading, 2013). Our studies provide a new angle on the molecular mechanisms of this experience-dependent brain development by showing for the first time that the transcription factor CaRF regulates NMDAR-dependent gene transcription. Specifically, we find that neurons lacking CaRF have enhanced NMDAR-dependent activation of *Bdnf* and *Arc*, transcription of which mediates experience-dependent synaptic plasticity in the developing cortex (Leslie and Nedivi, 2011). Interestingly our data further suggest that CaRF acts upstream of NMDARs to limit synaptic activity-dependent gene transcription in the developing brain by regulating NMDAR subunit composition.

2.5.1 Permissive and instructive actions of CaRF on activity-regulated genes

It is well established that the promoters and enhancers of activity-regulated genes including *Bdnf* and *Arc* are bound by multiple activity-responsive transcription factors (e.g. CREB, MEF2, SRF) (Lyons and West, 2011). Under basal conditions these activity-dependent transcription factors are either inactive or they actively repress their target genes. In response to synaptic activity, calcium signaling pathways rapidly convert these factors into potent transcriptional activators. CaRF is also bound to the promoters of many activity-regulated genes including *Bdnf* (Tao et al., 2002; Pfenning et al., 2010). However, unlike CREB and MEF2, full-length CaRF is competent to mediate transcription even in the absence of synaptic activity and it

undergoes a comparatively small increase in its ability to promote transcription following membrane depolarization (Tao et al., 2002; West, 2011). CaRF can likely also act as a basal repressor, because among the set of genes that have CaRF bound at their promoters, equal numbers are up- versus down-regulated in CaRF knockout neurons compared with control (Pfenning et al., 2010). Although the mechanisms that allow CaRF to both activate and repress genes are not fully understood, the *Carf* gene does encode short variants that contains the DNA binding domain but lack the transcriptional activation domain (Tao et al., 2002) and our evidence that selective re-expression of the truncated form of CaRF in CaRF KD neurons is sufficient to rescue both *Grin3a* expression and NMDAR-dependent *Bdnf* IV induction (**Fig. 16C and 17A**) suggests that the repressor forms contribute to neuronal gene regulation. Taken together, we interpret these data to suggest that CaRF primarily acts at activity-regulated gene promoters not as a calcium-inducible activator, but rather as a basal activator or repressor.

Stimuli that increase synaptic activity decrease CaRF expression (**Fig. 13A**). Thus, we propose that it is the loss of the basal activator or repressor activity at CaRF-regulated promoters following synaptic activity that permits transcription of these genes to rise or fall. This model helps to explain our previous microarray analysis of L-VGCC regulated transcription in CaRF knockout and knockdown neurons (Whitney et al., 2014). In those experiments we discovered a set of genes that increase or decrease their expression following membrane depolarization in CaRF wildtype neurons, but which show either basally increased or decreased expression, respectively, in neurons that lack CaRF. Furthermore, these genes show no change in their expression following membrane depolarization in neurons lacking CaRF. The occlusion of L-VGCC-dependent regulation in CaRF-lacking neurons suggests that the activity-induced loss of CaRF expression mediates the transcriptional regulation of these target genes. Conversely, since CaRF expression is elevated by pharmacological inhibition of intracellular calcium (**Fig. 13C**) our model also predicts that CaRF may play an instructive role in activating or repressing gene transcription following the inhibition of synaptic activity. This is interesting because although

increases in transcription are required to mediate homeostatic synaptic scaling following inhibition of neuronal firing (Ibata et al., 2008), very few transcription factors have been described that show increases in their transcriptional activity under conditions of reduced neuronal activity. Other than CaRF the only known transcription factor that may show inactivity-induced increases in its transcriptional activity is CCAT, which is derived from an alternative promoter in an intron of the gene encoding the L-VGCC subunit *Cacna1c* and which translocates to the nucleus of neurons under conditions of low intracellular calcium (Gomez-Ospina et al., 2006, 2013). Whether CaRF or CCAT is required for inactivity-dependent glutamatergic synaptic scaling remains to be determined.

2.5.2 Modulation of NMDAR-dependent transcription

In addition to regulating a subset of activity-responsive genes directly, our data suggest that CaRF also impacts NMDAR-dependent transcription by promoting the expression of the *Grin3a* gene, which encodes the NMDAR subunit GluN3A. NMDARs are comprised of an obligatory GluN1 subunit together with variable GluN2(A-D) and GluN3(A-B) subunits (Köhr, 2006). Expression of GluN3A is strongly developmentally regulated in the mouse forebrain, with highest levels of expression occurring during the first two postnatal weeks of life (Al-Hallaq et al., 2002; Sasaki et al., 2002; Wong et al., 2002). Transient expression of GluN3A in this time period is required for the proper temporal regulation of excitatory synapse maturation (Henson et al., 2012; Kehoe et al., 2014; Roberts et al., 2009). Our data are the first to suggest that GluN3A may contribute to activity-dependent synapse development by modulating NMDAR-dependent changes in gene transcription. Specifically our observation that rescuing the expression of GluN3A in CaRF knockdown neurons is sufficient to restore the induction of *Bdnf* and *Arc* to control levels (**Fig. 17B,C**), places the actions of GluN3A downstream of CaRF and upstream of NMDAR-dependent *Bdnf* and *Arc* inducibility.

The presence of GluN3A could impact NMDAR-dependent transcription either by altering the biophysical or the biochemical signaling properties of NMDARs. NMDARs

containing GluN3A have reduced calcium permeability (Kehoe et al., 2013), and because calcium is a key mediator of NMDAR-induced gene transcription (Lyons and West, 2011) it is possible that GluN3A inhibits the induction of activity-dependent genes by limiting the synaptic activity-induced elevation of postsynaptic calcium. However this model fails to explain why only a subset of activity regulated genes (e.g. *Bdnf* IV and *Arc*, but not *Fos* and *Bdnf* I) appear to be sensitive to GluN3A expression. An alternative possibility, in analogy to the differential ability of GluN2A versus GluN2B containing NMDARs to activate CREB (Martel et al., 2012), is that GluN3A-containing and GluN3A-lacking NMDARs differ in their abilities to activate specific downstream transcription factors. This could explain the specificity of gene regulation because different activity-regulated genes are induced by distinct complements of transcription factors (Lyons and West, 2011). The long intracellular C-terminal tail of GluN3A, which is distinct from that of other NMDAR subunits, provides docking sites for an assortment of intracellular signaling molecules (Henson et al., 2010). If GluN3A-mediated recruitment of one or more of these signaling molecules to NMDARs were to change the ability of NMDARs to signal to specific transcription factors in the nucleus, this could impact the transcriptional outcome of NMDAR activation. Identifying whether specific stimulus-regulated transcription factors are differentially activated in the presence or absence of GluN3A will help advance understanding of the mechanisms by which subunit composition can affect the specificity of NMDAR-dependent transcriptional regulation.

2.5.3 Activity-dependent transcription in the developing brain

Our evidence that young CaRF knockout mice show enhanced light-dependent induction of *Bdnf* and *Arc* in the visual cortex (**Fig. 18B and 18D**) suggests that CaRF-dependent modulation of NMDAR-dependent transcription may contribute to the fidelity of experience-dependent synapse maturation in the developing brain. Consistent with this model we find that CaRF knockdown neurons show enhanced GABAergic synapse development in culture that is BDNF-dependent (**Fig. 20**). The expression of both *Bdnf* and *Arc* is under tight spatial and

temporal control in the developing cortex and even subtle disruption of this regulation can have a substantial impact on cortical development. Activity-dependent transcription of *Bdnf* mediated by CREB activation is required for proper development of inhibitory GABAergic synapses in the developing brain (Hong et al., 2008). Inhibition has been tightly linked to timing the critical period for plasticity in visual cortex (Hensch, 2005), and indeed transgene expression of BDNF early in postnatal development both accelerates maturation of GABAergic synapses and leads to premature closure of the critical period for ocular dominance plasticity (Huang et al., 1999). Arc functions in excitatory synapse maturation and the loss of Arc in the postnatal brain is associated with impaired sensory-dependent synapse plasticity in the visual cortex (McCurry et al., 2010; Wang et al., 2006). Given that expression of CaRF is highly developmentally regulated, with peak expression in the early postnatal brain (McDowell et al., 2010), we propose that CaRF may act to refine the fidelity of sensory- and NMDAR-dependent gene transcription in the developing cortex in ways that optimize the timing of critical period plasticity. Adult CaRF knockout mice have enhanced expression and synaptic localization of GABAergic synapse proteins (McDowell et al., 2010) and display aberrant learning in Morris Water Maze, novel object, and interval timing tasks (Agostino et al., 2013; McDowell et al., 2010). Determining whether these defects arise from impaired postnatal expression of CaRF will enhance our understanding of the importance of tuning activity-dependent gene regulation in this critical period of brain development.

3. The NMDA receptor subunit GluN3A inhibits synaptic activity-induced and MEF2C-dependent transcription

3.1 Summary

Neuronal activity induces gene transcription via calcium dependent signaling pathway. Two main calcium sources in neurons are NMDA-type glutamate receptors (NMDARs) and L-type calcium channel. NMDARs drive the activation of multiple transcription factors to induce long-lasting effects on brain development and synapse plasticity. NMDAR subunit composition can impact the nature of this transcriptional response, but the role of the developmentally regulated GluN3A subunit in NMDAR-induced transcription was not known. We demonstrated that neurons lacking GluN3A showed selective enhancement of NMDAR-induced transcription. This enhancement was mediated by the accumulation of activated p38 kinase in the nucleus which leads to activation of the transcription factor MEF2C. These data demonstrate that GluN3A negatively regulates NMDAR-dependent activation of gene transcription and they reveal a novel mechanism that confers stimulus-specificity on the transcription of activity-regulated genes.

3.2 Introduction

NMDA-type glutamate receptors (NMDARs) are essential for coupling sensory experience with brain development. NMDARs activate intracellular signaling cascades, which subsequently impact synapse formation, maturation, and function. NMDARs are heterotetrameric receptors comprised of GluN1, GluN2, and GluN3 subunits, and the subunit composition of these receptors determines the specificity of the downstream signaling cascades initiated following receptor activation (Lau and Zukin, 2007; Sasaki et al., 2002). For example GluN2A- and GluN2B-containing NMDARs have opposing effects on phosphorylation of the transcription factor CREB (Martel et al., 2012). Interestingly, neurons in the developing postnatal brain also transiently express high levels of the GluN3A subunit, which is incorporated into functional

GluN1-GluN2-GluN3 glutamate-activated NMDARs (Al-Hallaq et al., 2002; Ciabarra et al., 1995; Pilli and Kumar, 2012; Sucher et al., 1995). Genetic deletion of GluN3A is associated with dysregulation of the plasticity of glutamatergic synapses in the developing brain, implicating the expression of this subunit in NMDAR-dependent aspects of brain development (Das et al., 1998; Larsen et al., 2011). Functionally, excitatory synapses show evidence of premature maturation in GluN3A knockout mice (Das et al., 1998; Henson et al., 2012), whereas prolonging expression of GluN3A into adulthood causes excitatory synapses to persist in a juvenile state (Roberts et al., 2009). Although these data indicate that GluN3A is a negative regulator of synapse development, the mechanism of its action is poorly understood. Furthermore, although it is well-established that NMDAR-dependent induction of genes such as *Bdnf* and *Arc* make an important contribution to synapse maturation and refinement in the developing brain (Hong et al., 2008; McCurry et al., 2010), the role of GluN3A in this program of inducible gene transcription has been unknown.

Here to address this, we knock down GluN3A in primary rat hippocampal neurons to examine the role of GluN3A in NMDAR dependent transcription and identify the downstream signaling pathways that regulated by GluN3A. we discovered that the GluN3A subunit of the NMDAR inhibits the activation of a subset of activity-regulated genes including *Bdnf*. GluN3A impacts downstream gene transcription by inhibiting the nuclear translocation of the p38 mitogen-activated protein kinase (MAPK), which limits the activation of genes that depend on the transcription factor MEF2C. The net effect of this pathway is the NMDAR-selective inhibition of a subset of synaptic activity-regulated genes. These data bring new understanding of the mechanisms by which NMDARs regulate activity-dependent brain development.

3.3 Materials and Methods

3.3.1 Plasmids

Two independent shRNAs were used to knockdown rat *Grin3a* and each was paired with a vector-matched control. *Grin3a* shRNA1 (TRCN0000100220; 5'-GCTCCATGACAAGTGGTACAA-3') was purchased from Thermo Scientific and the empty pLKO.1 vector was used as Ctrl1. *Grin3a* shRNA2 (5'-GTATCCGGCAGATATTTGAAA-3') was cloned into the pLLx3.8 vector and a scrambled version of the shRNA2 sequence (5'-GCCTGCAGTATGACTCAGTAA-3') in pLLx3.8 was used as Ctrl2. The shRNA-resistant GluN3A expression plasmid was constructed by using PCR to introduce silent mutations (GCTaCATGACAAGTtGTACAA) into the region of rat *Grin3a* targeted by *Grin3a* shRNA1, and then placing the *Grin3a* coding sequence under control of the ubiquitin promoter in the lentiviral expression vector pFUIGW (Lois et al., 2002). Gal4 DNA binding domain fusions with human MEF2C α 1 β and MEF2C α 1 β γ have been previously described (Zhu and Gulick, 2004) and were kindly provided by Dr. Gulick (Burnham Institute, Orlando, FL). The TT293/300AA and S387A mutations of Gal4-MEF2C α 1 β were generated by PCR. The viral expression plasmid for the rescue of MEF2 expression in neurons infected with the shRNA targeting rat *Mef2c* was generated by cloning the full coding sequence of human MEF2C α 1 β , which is not targeted by the rat *Mef2c* shRNA used, into the vector pFUIGW. The CRE luciferase reporter plasmid was purchased from Agilent and TK-renilla luciferase plasmid from Promega. The following plasmids were reported previously: MRE luciferase reporter plasmid (Flavell et al., 2006), the UAS luciferase reporter plasmid (Tao et al., 2002a), and shRNAs targeting rat *Mef2a*, *Mef2c*, and *Mef2d* in the vector pLKO.1 (TRCN0000095959, TRCN0000012068, and TRCN0000085268 respectively, Thermo Scientific) (Lyons et al., 2012).

3.3.2 Dissociated Neuron Cultures

Neuron-enriched cultures were generated from cortex of male and female E16.5 CD1 mouse embryos (Charles River Laboratories) or from hippocampus of male and female E18.5 CD

IGS rat embryos (Charles River Laboratories) and cultured as previously described (McDowell et al., 2010; Tao et al., 2002a). Withdrawal from tetrodotoxin (TTX WD) was done by treating neurons for 48 hrs with 1 μ M TTX (Tocris) prior either to harvesting cells (for the control condition) or washing out the TTX with Neurobasal medium (Invitrogen). Isotonic membrane depolarization with 55mM extracellular KCl was done as previously described (Lyons et al., 2012). Pharmacological blockers were added 2 min prior to TTX WD or KCl addition and maintained throughout the period of stimulation. All experiments were conducted in accordance with an animal protocol approved by the Duke University Institutional Animal Care and Use Committee.

3.3.3 Lentiviral Infection

For viral infection of neurons, shRNA or viral expression constructs were packaged as lentiviral particles in HEK 293T cells following standard procedures. Concentrated viruses were titered on cultured neurons and mouse cortical neurons or rat hippocampal neurons were infected for 6 hrs on day in vitro (DIV) 1 at a multiplicity of infection of 1 in BME medium (Sigma) with 0.4 μ g/mL added polybrene (Sigma).

3.3.4 Neuronal Transfection for Luciferase Assays

Neuron cultures were transfected with calcium phosphate on DIV3-5 as described previously (Tao et al., 2002a). Cotransfection of pTK-renilla luciferase (Promega) was used to control for transfection efficiency and sample handling. For the MRE-luc and CRE-luc reporters, luciferase reporters plasmid were transfected into cultured embryonic rat hippocampal neurons that had been infected with either *Grin3a* shRNA1 or Ctrl1 lentiviruses. Lysates were harvested on DIV9-10 after 0, 4, 6, 8, 14, or 22 hrs of TTX WD. For the UAS-luc reporter, luciferase reporter was cotransfected with either *Grin3a* shRNA1 or control (Ctrl1) plasmid. Lysates were harvested on DIV7 \pm 6 hrs TTX WD as described above. Luciferase activity was determined using the Dual-Luciferase® Reporter Assay System (Promega).

3.3.5 Western Blotting

Cells were homogenized in homogenization buffer (320 mM Sucrose, 10mM HEPES pH 7.4, 2mM EDTA, 1mM DTT and protease inhibitors). Nuclear pellet was centrifuged out at 1500xg for 15min. Cytosolic and membrane fractions were separated by centrifuging at 200000xg for 20min. Membrane, cytoplasmic, and nuclear extracts were run for SDS-PAGE and transferred to Nitrocellulose for western blotting following standard procedures. Bands were visualized with fluorescent secondary antibodies (Biotium) using the Odyssey imaging system (LI-COR Bioscience) and quantified using ImageJ. Actin was used as a loading control.

3.3.6 Immunofluorescence

Embryonic mouse cortical neurons or rat hippocampal neurons were cultured on PDL/laminin coated glass coverslips (Bellco; #1943-10015) and fixed in 4% paraformaldehyde at room temperature for 10mins. Neurons were blocked in 10% normal goat serum and permeabilized in 0.3% Triton X-100 prior to antibody incubation. Coverslips were incubated in primary antibodies overnight at 4°C. Secondary antibodies were incubated at room temperature for 1 hr. Hoechst dye (0.1µg/ml, Sigma) was used to label nuclei. Images were captured on a Leica SP8 confocal microscope with 1µm thickness optical section. Nuclear and cytoplasmic total pixel intensities were quantified by ImageJ macro: Intensity Ratio Nuclei Cytoplasm Tool. ~300 cells in 15 images per treatment group were quantified.

3.3.7 Antibodies

Primary antibodies used in this study for western blotting were mouse anti-Actin, 1:5000 (Millipore; MAB1501); mouse anti-phospho-S133 cAMP response element binding protein (CREB), 1:1000 (Millipore, #05-667); rabbit anti-GluN3A, 1:1000 (Millipore; #07-356); mouse anti-GluN1, 1:1000 (Affinity Bioreagents; #OMA1-04010); mouse anti-Transferrin Receptor, 1:2000 (Invitrogen; #13-6800); rabbit anti-phospho-Thr180/Tyr182 p38 MAPK, 1:1000 (Cell Signaling; #4511); rabbit anti-phospho-Ser387 MEF2C, 1:200 (Santa Cruz; #sc-13920). Primary antibodies used in this study for immunocytochemistry were mouse anti-MEF2D, 1:1000 (BD Biosciences; #610774); mouse anti-phospho-Tyr182 p38 MAPK, 1:50 (Santa Cruz; #sc-7973).

3.3.8 Quantitative PCR

RNA was harvested on DIV7 following 90min or 6hrs of KCl-mediated membrane depolarization or TTX WD as described in the text. RNA was harvested using the Absolutely RNA Miniprep Kit (Agilent) and cDNA was synthesized by Superscript II (Invitrogen). Quantitative SYBR green PCR was performed on an ABI 7300 real-time PCR machine (Applied Biosystems) using intron-spanning primers (IDT) listed in **Appendix A**. Data were all normalized to expression of the housekeeping gene *Gapdh* to control for sample size and processing. In most cases as described in the text we reported mRNA levels as relative expression in neurons infected with any single independent shRNA compared with its paired control shRNA (Ctrl1 or Ctrl2).

3.3.9 Statistical Analyses

Unless otherwise indicated, all data presented are the average of at least three biological replicates from each of at least two independent experiments. Also unless otherwise indicated, data were analyzed by a Student's unpaired t-test, and $p < 0.05$ was considered significant. Time courses were analyzed by one-way analysis of variance (ANOVA) using SPSS v11.0 statistical software (SPSS, Chicago, IL). Bar and line graphs show mean values and all error bars show S.E.M.

3.4 Results

3.4.1 The NMDAR subunit GluN3A inhibits NMDAR-induced MEF2 transcriptional program

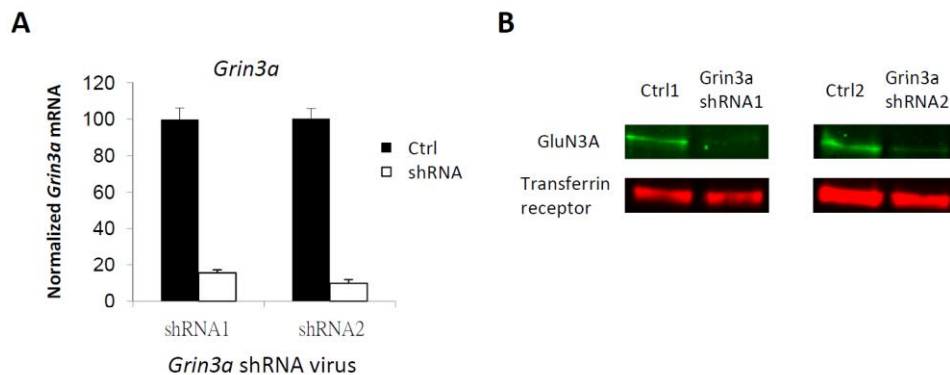


Figure 21: (A) Levels of *Grin3a* mRNA in rat hippocampal neurons infected with lentiviruses encoding shRNAs targeting two independent sequences in *Grin3a*. *Grin3a* mRNA level are shown normalized to levels in cells infected with the paired control viruses. $n=4-20$. (B) Membrane fractions from cultured neurons infected with the

indicated lentiviruses were analyzed by Western blot using an antibody that detects the GluN3A protein. Transferrin receptor is shown as a loading control.

To directly test the functions of GluN3A in NMDAR-inducible transcription, we characterized two independent shRNAs in lentiviral vectors to knockdown the expression of GluN3A in cultured rat hippocampal neurons (**Fig. 21**). Similar to our observations in CaRF KD neurons in chapter 2, we found that knockdown of GluN3A resulted in potentiation of both *Bdnf* IV mRNA transcription and BDNF protein expression upon TTX WD compared with control infected neurons (**Fig. 22A**). This potentiation was selective for transcription induced by NMDARs, because there were no significant differences in the levels of *Bdnf* IV mRNA or BDNF protein induced in GluN3A KD and control neurons following KCl-mediated membrane depolarization (**Fig. 22B, C**). The potentiation of NMDAR-dependent transcription was limited to

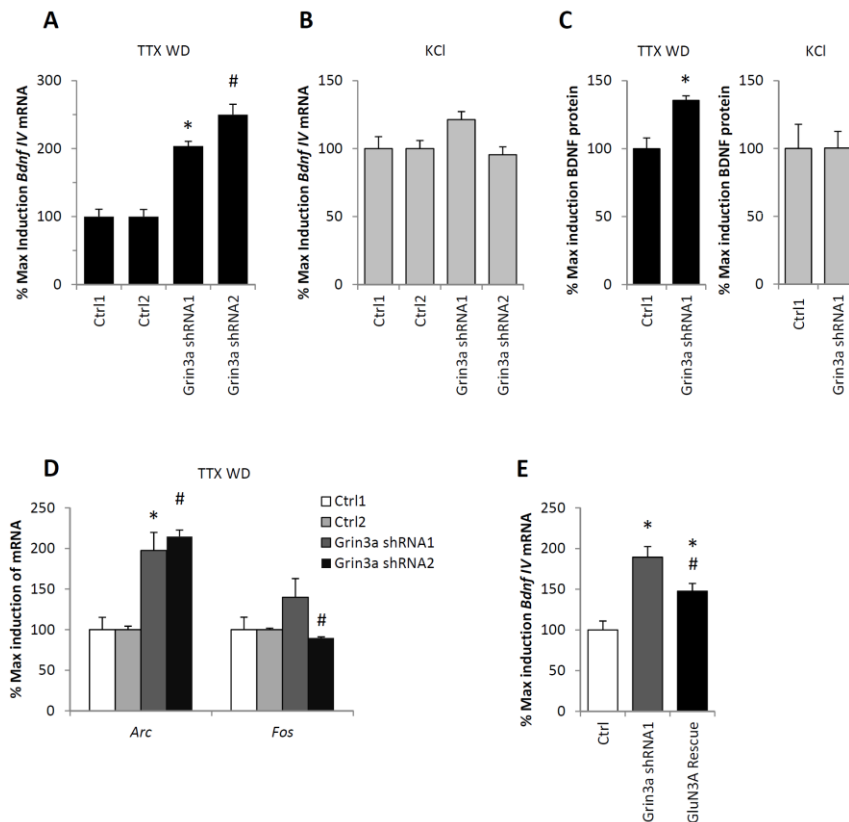


Figure 22: (A) Levels of *Bdnf* exon IV mRNA in hippocampal neurons infected with the indicated lentiviruses then stimulated with 6hrs TTX WD. Induced mRNA levels for neurons infected with each shRNA targeting *Grin3a* (shRNA1, shRNA2) are reported as percentages of induction relative to their respective control vectors (Ctrl1 or Ctrl2). n=5-6, * $p < 0.05$ compared with Ctrl1, # $p < 0.05$ compared with Ctrl2. (B) Levels of *Bdnf* exon IV in hippocampal neurons infected with the indicated lentiviruses then stimulated with 55 mM KCl for 6 hrs. n=2-4. (C) Levels of BDNF protein measured by ELISA from neurons stimulated as in (A) and (B). Induced protein levels are reported as percentages of induction relative to control shRNA (Ctrl1) n=6, * $p < 0.05$ compared with Ctrl1. (D) Levels

of *Arc*, and *Fos* mRNA in hippocampal neurons infected with the indicated lentiviruses then stimulated with 30min TTX WD. Induced mRNA levels for neurons infected with each shRNA targeting *Grin3a* (shRNA1, shRNA2) are reported as percentages of induction relative to their respective control vectors (Ctrl1 or Ctrl2). n=3-4, * $p < 0.05$ compared with Ctrl1, # $p < 0.05$ compared with Ctrl2. (E) Levels of *Bdnf* exon IV mRNA in hippocampal neurons infected with the indicated lentiviruses. Neurons were infected by shRNA virus at DIV1 and rescue virus at DIV5 then stimulated with 6hrs TTX WD and harvested at DIV8. Induced mRNA levels are shown relative to the control condition (Ctrl). n=6, * $p < 0.05$ compared with Ctrl. # $p < 0.05$ compared with *Grin3a* shRNA1.

a subset of NMDAR-inducible gene targets, because TTX WD-induced *Fos* expression did not differ between GluN3A KD and control neurons. However, similar to our observations with CaRF, the TTX WD induced expression of *Arc* was also potentiated in the GluN3A KD neurons compared with control (Fig. 22D). Finally, to determine whether the enhanced activation of *Bdnf* IV and *Arc* transcription in GluN3A KD neurons is a direct result of the absence of GluN3A, as opposed to a secondary effect of the lack of GluN3A on excitatory synapse development, we performed an acute rescue of GluN3A expression in GluN3A KD neurons (Fig. 23). Whereas GluN3A KD led to potentiation of *Bdnf* IV induction by TTX WD relative to control, re-

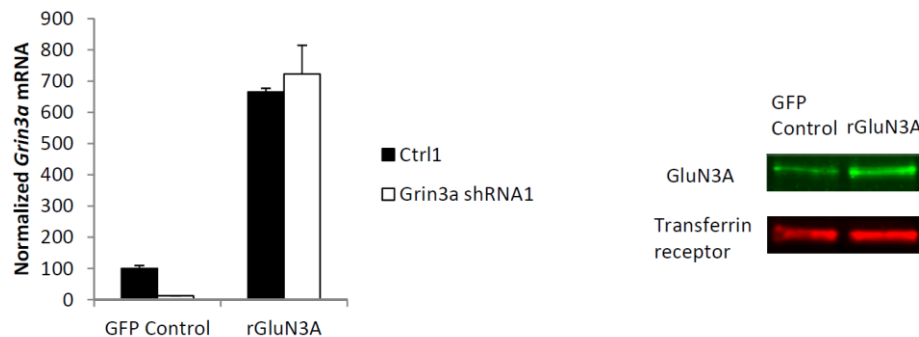


Figure 23: Left, levels of *Grin3a* mRNA in the hippocampal neurons infected with the indicated lentiviruses. n=3. Right, membrane extracts from cultured neurons infected with the indicated lentiviruses were analyzed by Western blot using an antibody that detects the GluN3A protein. Transferrin receptor is shown as a loading control.

expression of GluN3A in KD neurons was sufficient to significantly reduce *Bdnf* IV potentiation (Fig. 22E). Thus these data demonstrate for the first time that GluN3A inhibits NMDAR-dependent transcription. Specifically GluN3A selectively limits the ability of NMDARs but not LVGCCS to induce a set of neuronal-selective, synaptic activity-regulated genes including *Bdnf* IV and *Arc*.

3.4.2 GluN3A inhibits NMDAR-dependent gene transcription via a p38MAPK-MEF2C pathway

The neuronal activity-dependent transcription of *Bdnf*, *Fos*, *Arc* and other IEGs is mediated by the activation of transcription factors bound to regulatory elements in the proximal promoters and distal enhancers of these genes (Lyons and West, 2011). We hypothesized that the potentiation of *Bdnf* IV and *Arc* transcription reflected a change in the activation of a subset of these transcription factors. We focused on NMDAR-dependent activation of CREB and MEF2, two of the transcription factors that mediate activity-dependent expression of both *Bdnf* IV and *Arc* (Kawashima et al., 2009; Lyons et al., 2012; Tao et al., 2002a). To monitor the activity of these transcription factor families, we transfected GluN3A KD or control infected neurons with luciferase reporter plasmids in which the expression of luciferase is under the control of binding sites for either the CREB (CREB response elements; CRE) or MEF2 (MEF2 response elements; MRE) families of transcription factors. In control infected neurons TTX WD induced a significant increase in luciferase expression from both the CRE and MRE reporters (**Fig. 24A**), demonstrating NMDAR-dependent activation of CREB and MEF2 family transcription factors

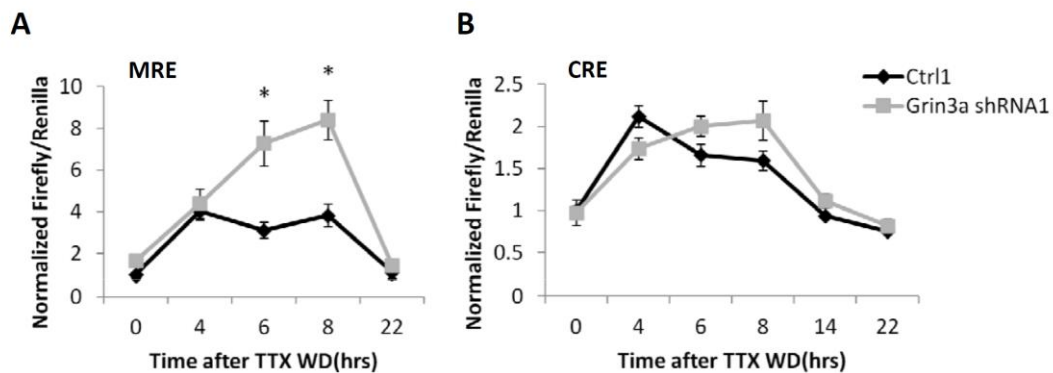


Figure 24: (A) Luciferase expression in hippocampal neurons transfected with MRE-Luc plasmid and infected with either *Grin3a* shRNA1-containing or control (Ctrl) lentiviruses. Neurons were stimulated with TTX WD for the indicated amounts of time prior to lysis. Data expressed as fold induction over untreated (Basal) condition. n=6-9, *p<0.05 Ctrl1 vs. *Grin3a* shRNA1. (B) Luciferase expression in hippocampal neurons transfected with CRE-Luc plasmid and infected with either *Grin3a* shRNA1-containing or control (Ctrl) lentiviruses. Neurons were stimulated as described in (A). n=3-6/time point. Data from Michelle Lyons.

(MRE, $F_{1,36}=20.2$, $p<0.0001$; CRE, $F_{1,17}=22.9$, $p<0.0001$). However, in GluN3A KD neurons, we detected significantly more luciferase expression from the MRE reporter after 6hr

(cntr1=3.11±0.38, *Grin3a* shRNA1=7.28±1.08, n=7, p=0.003) and 8hr (cntr1=3.82±0.54, *Grin3a* shRNA1=8.41±0.94, n=7, p=0.001) of TTX WD compared with the expression in control infected neurons. By contrast CRE reporter activity was not different in GluN3A KD neurons as compared with controls at any time point (**Fig. 24B**). These data suggest that the potentiation of NMDAR-dependent transcription in GluN3A KD neurons arises from enhanced activation of MEF2 transcription factors.

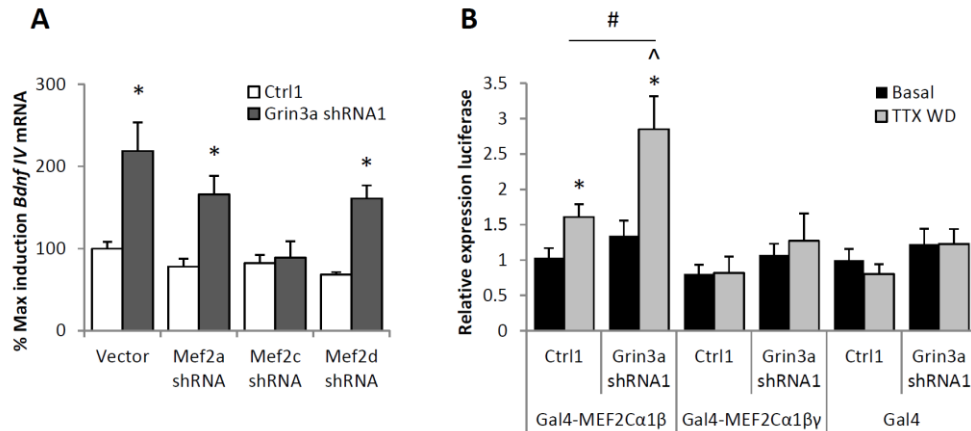


Figure 25: (A) Levels of *Bdnf* exon IV in hippocampal neurons infected both with lentiviruses containing *Grin3a* shRNA1 or its paired control and lentiviruses expressing shRNAs targeting individual MEF2 family members. Neurons were stimulated with TTX WD for 6 hrs. Induced mRNA levels are shown as percentages of induction relative to control condition (Ctrl1/Vector). n=5-6, **p*<0.05 compared with Ctrl1/Vector. (B) Luciferase expression in hippocampal neurons cotransfected with the pUAS-Luc plasmid, plasmids expressing Gal4 fusions of the indicated MEF2C splice variants, and either *Grin3a* shRNA1 or its paired Ctrl1 vector. Neurons were stimulated with TTX WD for 6 hrs prior to lysis. Data are shown as relative expression level compared to control condition (Ctrl1/Basal). n=4-8, **p*<0.05 compared with Ctrl1/Basal. #*p*<0.05 Ctrl1/TTX WD vs. *Grin3a* shRNA1/TTX WD. ^*p*<0.05 compared with *Grin3a* shRNA1/Basal.

To determine whether MEF2 family transcription factors are required for the potentiation of NMDAR-induced gene transcription in GluN3A KD neurons, we used lentiviral shRNAs to knockdown expression of MEF2A, MEF2C, and MEF2D, the three major MEF2 family members expressed in cultured hippocampal neurons (Lyons et al., 2012). Previously we showed that knockdown of MEF2C but not MEF2A or MEF2D impairs the LVGCC-dependent induction of *Bdnf* exon IV (Lyons et al., 2012). Here we found that while knocking down any of the three MEF2 family members did not affect TTX WD-induced *Bdnf* IV expression in control neurons, knockdown of MEF2C, but not MEF2A or MEF2D, eliminated the potentiation of *Bdnf* IV expression in GluN3A KD neurons (**Fig. 25A**).

To test whether knockdown of GluN3A potentiates the transcriptional activity of MEF2C, we cotransfected neurons with plasmids encoding a Gal4-MEF2C fusion protein and a UAS-luciferase reporter along with either the GluN3A shRNA or the paired control vector. Neuronal MEF2C is comprised of two major splice variants: both isoforms contain exons encoding the α 1 and β domains, but the alternatively spliced exon encoding the γ domain is present in only about 50% of *Mef2c* mRNA transcripts in hippocampus and cortex (Lyons et al., 2012; Zhu and Gulick, 2004). MEF2C splice variants lacking the γ -domain (MEF2C γ -) are the most highly activated of the MEF2C isoforms following LVGCC activation (Lyons et al., 2012) and here we found that only Gal4-MEF2C fusion proteins that lack the γ -domain are activated upon TTX WD (**Fig. 25B**). Furthermore, only the γ - isoform of MEF2C (MEF2C α 1 β) showed potentiation upon TTX WD in GluN3A KD neurons compared with control neurons (**Fig. 25B**). Importantly, because these studies were done with co-transfection of the knockdown and the Gal4 reporter plasmids, which leads to expression of both constructs in only about ~1% of the neurons in our cultures, these experiments demonstrate that the effects of GluN3A knockdown on the activation of MEF2C are cell autonomous.

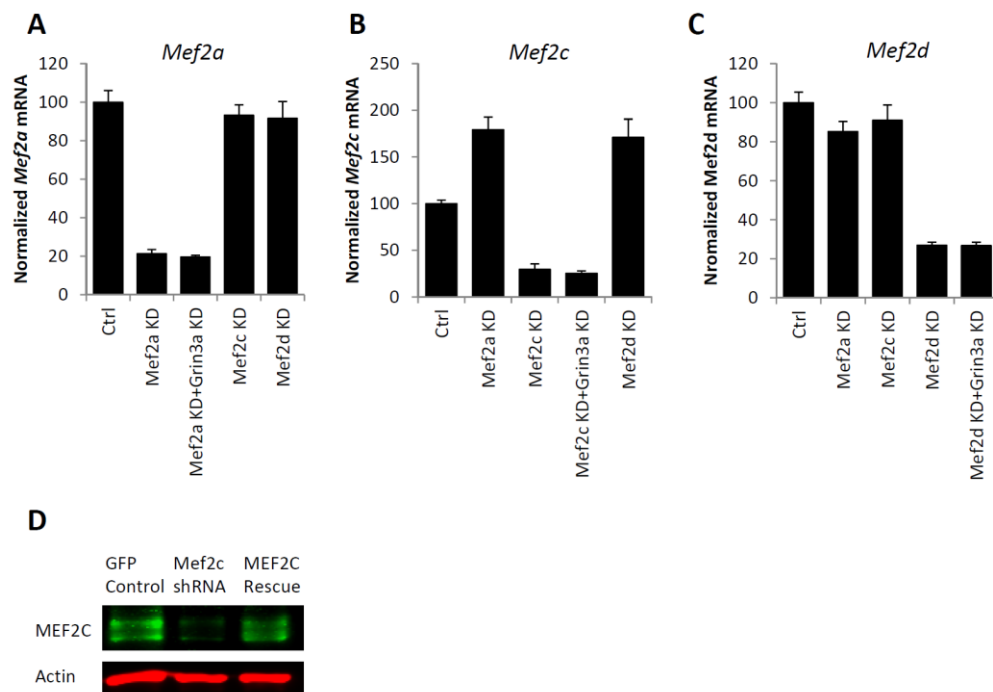


Figure 26: Levels of (A) *Mef2a* (B) *Mef2c* and (C) *Mef2d* mRNA in hippocampal neurons infected with the indicated shRNA lentiviruses. mRNA levels are shown normalized to levels in cells infected with the control pLKO.1 virus. n=5-6. (D) N1 Nuclear fractions from cultured neurons infected with the indicated lentiviruses were analyzed by Western blot using an antibody that detects the MEF2C protein. Actin is shown as a loading control.

To confirm that expression of the MEF2C γ - isoform is sufficient to drive NMDAR-dependent *Bdnf* IV transcription, we overexpressed human MEF2C γ -, which is resistant to the rat *Mef2c* shRNA, in GluN3A and MEF2C double knockdown neurons (**Fig. 26**). Whereas the knockdown of MEF2C eliminated the potentiation of both *Bdnf* IV and *Arc* transcription in GluN3A KD neurons, replacement of human MEF2C γ - in GluN3A and MEF2C double KD neurons was sufficient to restore induction of expression to the levels seen in GluN3A KD neurons (**Fig. 27**).

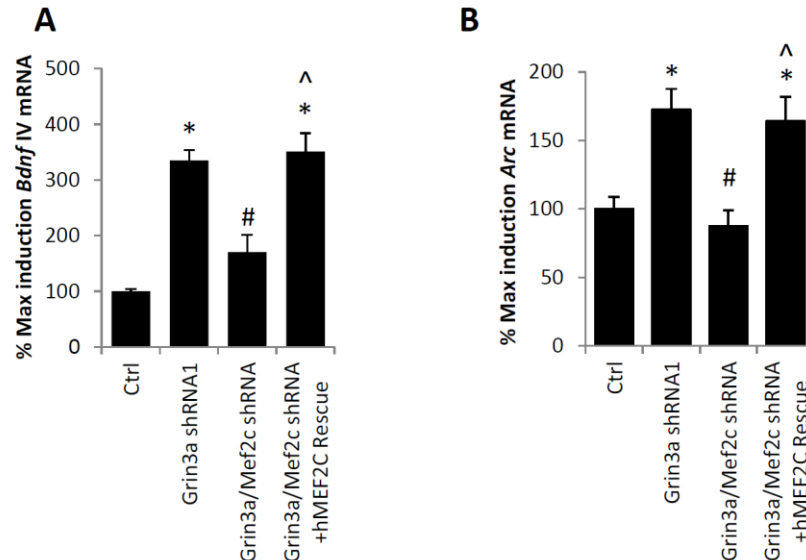


Figure 27: Levels of (A) *Bdnf* exon IV or (B) *Arc* mRNA in hippocampal neurons infected with the indicated lentiviruses then stimulated for 6hrs with TTX WD. Induced mRNA levels are shown as percentage of induction relative to control condition (Ctrl). n=6, * $p < 0.05$ compared with Ctrl. # $p < 0.05$ compared with *Grin3a* shRNA. ^ $p < 0.05$ compared with *Grin3a/Mef2c* shRNA.

To identify the signaling mechanisms underlying the potentiation of NMDAR-induced transcription in GluN3A KD neurons, we first asked whether pharmacological blockade of known MEF2 regulatory pathways (McKinsey et al., 2002) would inhibit the potentiation of Gal4-MEF2C activity upon TTX WD. Although calcineurin-dependent dephosphorylation of MEF2s is required for the membrane depolarization-dependent activation of MEF2-dependent transcription in cultured hippocampal neurons (Flavell et al., 2006), we found that inhibition of calcineurin

with CSA and FK506 had no effect on Gal4-MEF2C activation following TTX WD in either control or GluN3A KD neurons. By contrast pretreatment of neurons with the p38 MAPK inhibitor SB203580 inhibited the induction of Gal4-MEF2C activity only in GluN3A KD neurons (**Fig. 28A**). Interestingly, p38 MAPK blockade had no significant effect on TTX WD-induced Gal4-MEF2C activity in control infected neurons indicating a selective requirement for the p38 pathway in MEF2C activation in GluN3A KD neurons (**Fig. 28A**).

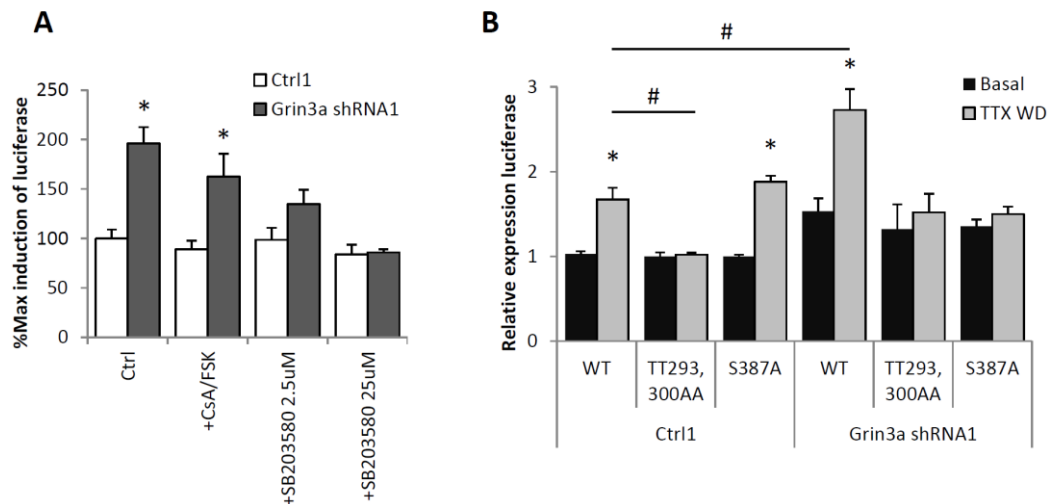


Figure 28: (A) Luciferase expression in hippocampal neurons cotransfected with the UAS-Luc plasmid, a Gal4-MEF2C α 1 β expression plasmid and either the *Grin3a* shRNA1 plasmid or its paired control. Hippocampal neurons were stimulated for 6 hrs with TTX WD in the absence or presence of Cyclosporin A +FK 506(CsA/FK; CsA) or SB203580 at the doses indicated. Induced luciferase levels are shown as percentages of induction relative to the control condition (Ctrl/Ctrl1). n=6, * p <0.05 *Grin3a* shRNA1 vs. Ctrl1. (B) Luciferase expression in hippocampal neurons cotransfected with the pUAS-Luc plasmid, expression plasmids encoding the indicated Gal4-MEF2C α 1 β constructs, and either the *Grin3a* shRNA1 plasmid or its paired control. Gal4-MEF2C constructs were either wildtype (WT) or bearing Ser (S) or Thr (T) to Ala (A) mutations at key phosphorylation sites. Data are shown as fold change in luciferase levels compared to the control condition (Ctrl1/WT/Basal). n=4-8, * p <0.05 Basal vs. TTX WD. # p <0.05 *Grin3a* shRNA1 vs. Ctrl1.

p38 MAPK activates MEF2C by inducing its phosphorylation at three sites: Thr293, Thr300, and Ser387, with the numbering referring to amino acid positions in human MEF2C α 1 β + γ - (Han et al., 1997). To test the functional importance of these phosphorylation sites in neurons, we mutated each of these residues to Ala in the context of the Gal4-MEF2C γ - fusion protein and assessed the effects on TTX WD-induced luciferase expression in neurons cotransfected with the GluN3A KD shRNA plasmid or its paired control. Whereas mutating MEF2C at both Thr293 and Thr300 rendered the Gal4 fusion protein unresponsive to TTX WD in both control and GluN3A

knockdown neurons, MEF2C bearing the Ser387 to Ala mutation showed impairment of TTX WD-induced activation only in neurons lacking GluN3A (**Fig. 28B**). These data suggest that p38 MAPK-dependent phosphorylation of MEF2C at Ser387 is selectively required for the activation of MEF2C in GluN3A knockdown neurons.

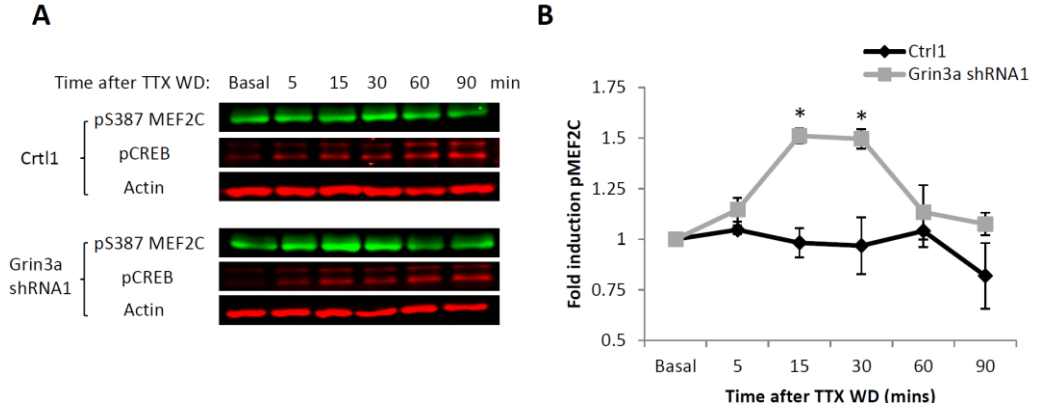


Figure 29: (A) Phosphorylated CREB-S133 (pCREB) and phosphorylated MEF2C-S387 (pMEF2C) levels in nuclear extracts from hippocampal neurons infected with the indicated shRNA virus then stimulated with TTX WD for the indicated amounts of time prior to lysis. Actin is shown as a loading control. (B) Quantification of three independent experiments as described in (A). Band density in each lane was quantified using ImageJ. Expression was normalized to actin for each sample. pMEF2C levels are reported as fold induction relative to unstimulated (Basal) condition. * $p < 0.05$ *Grin3a* shRNA1 vs. Ctrl1.

To determine whether endogenous MEF2C is phosphorylated at Ser387 in response to TTX WD in hippocampal neurons, we ran western blots using a phosphoSer387-MEF2C specific antibody on nuclear extracts from GluN3A KD and control neurons. We found that TTX WD did not induce phospho-Ser387 MEF2C in control neurons (**Fig. 29**). By contrast in GluN3A KD neurons, phospho-Ser387 MEF2C was significantly induced, reaching a peak around 30mins after stimulation with TTX WD (**Fig 29**).

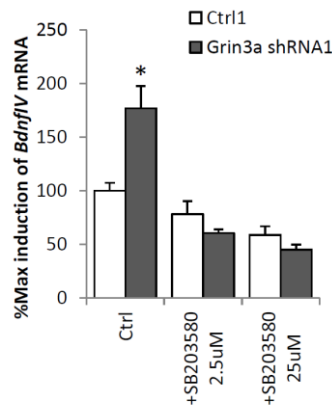


Figure 30: Levels of *Bdnf* exon IV mRNA in hippocampal neurons infected with the indicated lentiviruses then stimulated for 6hrs with TTX WD. During TTX WD neurons were either left untreated (Ctrl) or SB203580 (2.5 μ M) or SB203580 (25 μ M) was added. mRNA levels are reported as percentage of induction relative to control condition (Ctrl/Ctrl1). n=3-4, * p <0.05 compared with Ctrl1.

Finally, if p38 MAPK-dependent phosphorylation of MEF2C is selectively mediating the potentiation of NMDAR-dependent transcription in GluN3A KD neurons, then pharmacological inhibition of the p38 MAPK pathway in GluN3A KD neurons should restore transcriptional activation following TTX WD to the levels observed in control neurons. Indeed, pretreatment of neurons with the p38 MAPK inhibitor SB203580 had no effect on the magnitude of TTX WD-induced *Bdnf* IV expression in control neurons, but it abolished the potentiation of *Bdnf* IV induction in GluN3A KD neurons (**Fig. 30**). Taken together, these data suggest that GluN3A inhibits NMDAR-dependent transcription by opposing the p38 MAPK-dependent phosphorylation and activation of MEF2C.

3.4.3 Enhanced NMDAR-dependent nuclear activation of p38 MAPK in GluN3A knockdown neurons

To determine whether the differential p38 MAPK-dependent phosphorylation of MEF2C we observed in GluN3A KD neurons reflects differential NMDAR-dependent activation of the p38 MAPK pathway, we subjected GluN3A KD or paired control neurons to TTX WD and measured the activation of p38 MAPK by western blotting with an antibody selective for the MKK3/6 phosphorylation sites on p38 at Thr180/Tyr18. When we assayed cytoplasmic fractions from our neuronal cultures, we found that p38 MAPK was phosphorylated within five minutes after TTX WD in both control and GluN3A KD neurons, and we saw that the magnitude and time course of activation of p38 MAPK did not differ between these cultures (**Fig. 31A,B**). Thus GluN3A does not inhibit the activation of cytoplasmic p38 MAPK. However many signaling proteins, including those in the p38 MAPK pathway, must undergo rapid nuclear translocation to induce gene transcription following extracellular stimulation (Plotnikov et al., 2011; Zehorai and Seger, 2014). To determine whether the nuclear activation of p38 MAPK is affected by the presence of GluN3A in NMDARs, we harvested nuclei from GluN3A KD and control neurons

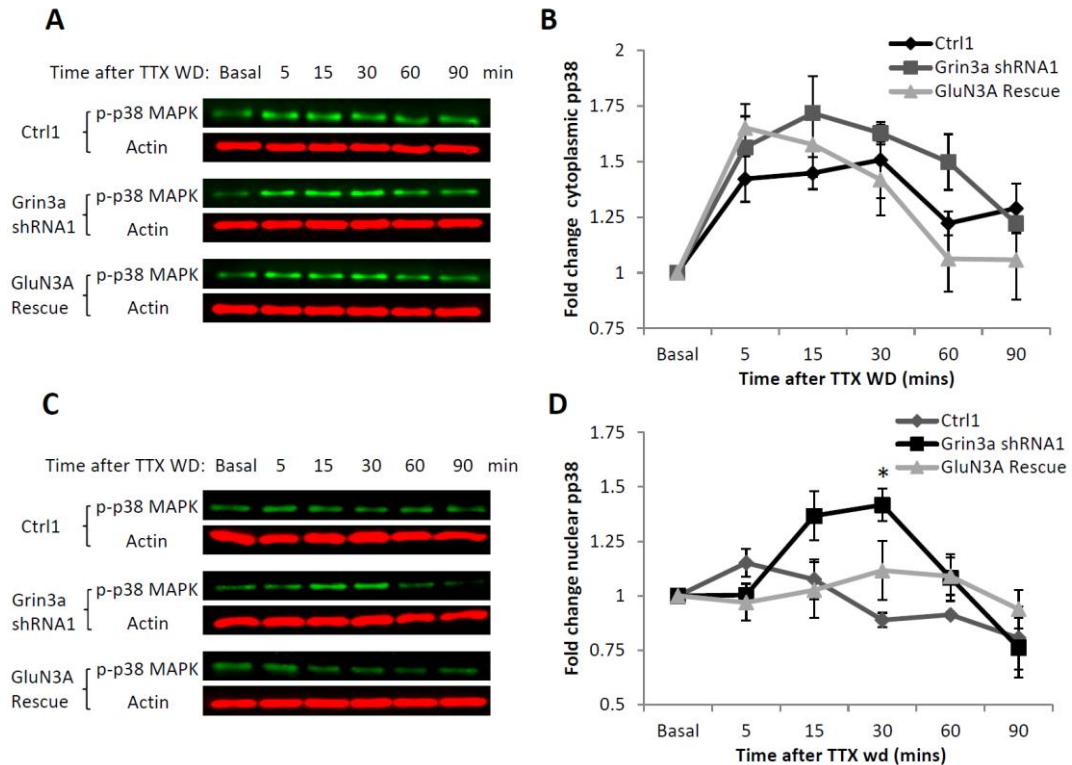


Figure 31: (A) Phosphorylated p38/MAPK (p-p38) in the cytoplasm of hippocampal neurons infected with the indicated shRNA virus or paired control virus then stimulated with TTX WD for the indicated amounts of time prior to lysis. (B) Quantification of two independent experiments as described in (A). Band density in each lane was quantified using ImageJ. Expression was normalized to actin for each sample. p-p38 levels are reported as fold induction relative to unstimulated (Basal) condition. (C) Phosphorylated p38/MAPK (p-p38) in the nucleus of hippocampal neurons as shown in (A). (D) Quantification of three independent experiments described in (C). * $p < 0.05$ *Grin3a* shRNA1 vs. Ctrl.

and ran them for western analysis. In contrast to the activation of p38 MAPK in the cytoplasm, we saw TTX WD-induced phosphorylation of p38 MAPK only in the nuclei of GluN3A KD neurons, with no significant increase in phosphorylation in the control-infected neurons (**Fig. 31C,D**). To confirm the differential localization of phospho-p38 MAPK after TTX WD in GluN3A KD and control neurons, we used immunostaining with the phospho-p38 MAPK antibody to localize the activated kinase in dissociated hippocampal neurons (**Fig. 32A**). Confocal images through control-infected cells show a robust TTX WD-induced signal in the cytoplasm that is absent from the nucleus. By contrast in GluN3A KD neurons the phospho-p38 MAPK signal fills the cell including the nucleus. Quantification of the relative distributions of phospho-p38 MAPK in these two compartments demonstrates that there is a significant increase in the

nuclear:cytoplasmic ratio of phospho-p38 MAPK immunostaining signal in neurons lacking GluN3A (**Fig. 32B**). This difference in the localization of activated p38 MAPK in the GluN3A

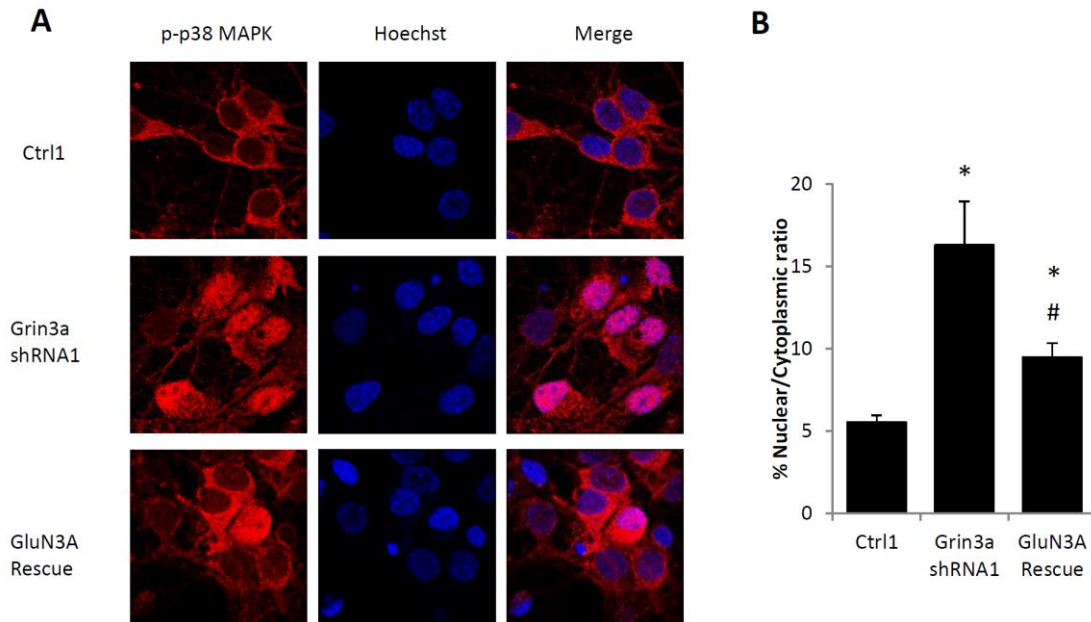


Figure 32: (A) Representative images of hippocampal neurons (DIV7) immunostained with antibodies against p-p38 (red) and Hoechst nuclear dye (blue). Neurons were infected with the indicated lentiviruses then stimulated with TTX WD for 30mins. (B) Quantification of nuclear-to-cytoplasmic ratio of p-p38 in (E). n=15, * $p < 0.05$ compared with Ctrl1. # $p < 0.05$ compared with *Grin3a* shRNA1.

neurons is due to the lack of GluN3A because we were able to restore the control distribution by re-expressing shRNA resistant GluN3A in the GluN3A KD neurons (**Fig. 31 and 32**). Taken together, these data suggest that GluN3A inhibits NMDAR-dependent transcription by blocking the activation of nuclear p38 MAPK.

3.5 Discussion

Our data describe a novel mechanism that regulates NMDAR-dependent gene expression in the developing brain. We show for the first time that the NMDAR subunit GluN3A inhibits the ability of NMDARs to induce activity-dependent gene transcription. Because GluN3A is directly incorporated into NMDARs, it provides a means to selectively inhibit the ability of NMDARs to induce activity-regulated genes, while leaving LVGCC-induced transcription intact. This is important because many activity-regulated neuronal genes have pleiotropic functions that are differentially coupled to the activation of distinct upstream calcium signals. For example, though

Bdnf is induced by both LVGCCs and NMDARs, LVGGC-induced BDNF expression is strongly linked to neuronal survival pathways (Ghosh et al., 1994), where NMDAR-induced BDNF is implicated in GABAergic synapse maturation (Huang et al., 1999). It is likely that the consequences of BDNF expression are defined by the context in which it is induced. Thus by inhibiting the coupling of activity-regulated genes to NMDAR activation, GluN3A has the ability to limit NMDAR-dependent effects on synapse development without impairing the activation of these genes by stimuli such as spontaneous action potentials that promote neuronal survival and neurite outgrowth (West and Greenberg, 2011).

GluN3A is highly expressed only during a brief period of early postnatal forebrain development (Al-Hallaq et al., 2002; Sasaki et al., 2002; Wong et al., 2002) and downregulation of GluN3A prior to the onset of the critical period for sensory-driven cortical plasticity is required for the maturation of excitatory synapse development (Roberts et al., 2009). However, the mechanisms that allow GluN3A to exert this inhibitory effect on cortical plasticity have been unknown. Our evidence that GluN3A limits NMDAR dependent *Bdnf* and *Arc* transcription suggest that the GluN3A dependent inhibition of NMDAR-dependent gene transcription inhibits premature synaptic maturation by restricting the activation of plasticity-inducing gene products. In the visual cortex, *Arc* is required for the experience-dependent establishment of normal ocular dominance (McCurry et al., 2010; Wang et al., 2006) and BDNF promotes the maturation of GABAergic inhibition in the developing cortex, which drives closure of the critical period (Huang et al., 1999). The developmental downregulation of GluN3A would permit the robust induction of this transcriptional program, promoting the onset of the later stages of critical period plasticity.

Although NMDARs pass current and contribute to synaptic potentials, it is primarily the ability of these channels to function as synaptic activity-regulated signaling receptors that underlies their unique roles in brain development and synaptic plasticity. All functional glutamate-sensing NMDARs are comprised of both GluN1 and GluN2 subunits, and the

biophysical and biochemical properties of specific subtypes of these receptors vary based on their subunit composition. GluN2A and GluN2B-containing NMDARs have been particularly highly studied given the evidence linking these two subtypes of receptors to distinct biological functions (Wyllie et al., 2013). The distinct signaling consequences of activating these two classes of NMDARs has been shown to depend on the ability of their intracellular C-terminal tails to differentially recruit signaling complexes to the NMDAR (Martel et al., 2012). Similar to the GluN2s, the long C-tail of GluN3A provides unique NMDAR docking sites for intracellular signaling proteins that can influence the functional impact of NMDAR activation. For example, GluN3A-dependent association with the endocytic protein Pacsin1 (Syndapin1) enhances the membrane trafficking of NMDARs (Pérez-Otaño et al., 2006), and the association of GluN3A with the phosphatase PP2A promotes dephosphorylation of the GluN1 subunit at Ser897 (Chan and Sucher, 2001). In addition to effects on the NMDAR itself, protein associations with the GluN3A C-terminal tail regulate local synaptic signaling in dendritic spines (Fiuza et al., 2013). Our data now further indicate that incorporation of GluN3A can modulate the ability of NMDARs to signal to the nucleus. Interestingly whereas GluN2A and GluN2B differentially regulate NMDAR-dependent activation of the transcription factor CREB, we find that GluN3A selectively inhibits the activation of MEF2 transcription factors. Thus in addition to controlling the likelihood of transcriptional activation, differential use of NMDAR subunits can confer specificity on the set of downstream transcription factors that are activated by synaptic stimulation.

Although activation of any single activity-regulated transcription factor is sufficient to induce transcription of a reporter gene (e.g. **Fig. 28B**) the regulation of most neuronal IEGs is under the control of multiple activity-regulated transcription factors (Lyons and West, 2011). We have proposed that the presence of multiple transcription factor binding sites in the promoters and enhancers of neuronal activity-dependent genes may allow for specificity in the coupling of subsets of activity-responsive genes to distinct sources of upstream activation (West et al., 2002).

Consistent with this prediction we find that GluN3A selectively inhibits the component of NMDAR-induced transcription of *Bdnf* and *Arc* that depends on MEF2C while leaving LVGCC and CREB-dependent transcription of these genes intact. However we also find that the selective regulation of these pathways results in the activation of these genes being driven to two different levels – either high levels of transcription through the coordinate activation of MEF2C and CREB, or a lower level of activation, mediated by CREB in the absence of MEF2C. Importantly, substantial data support the hypothesis that the levels to which these IEGs are induced is important for their function in the brain. The spatial and temporal induction of BDNF is particularly tightly regulated in the brain, and even mild increases or decreases in BDNF levels are associated with developmental and functional neuronal abnormalities (Chen et al., 2006; Genoud et al., 2004; Korte et al., 1995; McDowell et al., 2010). Increases in *Arc* expression due to impaired ubiquitination in mice bearing mutations of the Angelman Syndrome protein Ube3A leads to a decrease in the number of synaptic AMPA receptors and impaired synaptic transmission (Greer et al., 2010).

One of the most interesting questions raised by this study is how incorporation of GluN3A into NMDARs at the cell surface leads to the regulation of gene transcription in the nucleus. Our data indicate that a key step in this process is the ability of GluN3A to inhibit the activation of nuclear p38 MAPK. The p38 MAPK is rapidly activated by glutamate-induced calcium influx through NMDARs in neurons (Kawasaki et al., 1997), and in this context p38 has attracted interest for its involvement in the recycling of AMPA-type glutamate receptors that underlies activity-dependent changes in synaptic strength (Zhu et al., 2005). NMDARs activate p38 MAPK via the regulation of the small GTPases Ras, Rac1, and/or Rap1, and the differential association of GTPase exchange factors (GEFs) and GTPase activating proteins (GAPs) with NMDARs that have distinct GluN2 subunit composition has been suggested to contribute to the ability of NMDARs to induce LTP versus LTD (Zhu et al., 2005). Like the GluN2 subunits, GluN3A regulates the NMDAR-dependent activation of small GTPases by binding directly to the

small GTPase Rheb and indirectly inhibiting the activation of Rac1 (Fiuza et al., 2013; Sucher et al., 2010). However our data indicate that GluN3A has no effect on the time course or magnitude of p38 MAPK activation; instead the primary consequence of GluN3A is to restrict the subcellular distribution of activated p38 MAPK to the cytoplasm, whereas NMDARs lacking GluN3A can also drive the appearance of activated p38 MAPK in neuronal nuclei.

Nuclear translocation of p38 requires the phosphorylation-dependent association of p38 with β -like importins in the cytoplasm followed by active transport through the nuclear pore that is mediated by the small GTPase Ran (Zehorai and Seger, 2014). The nuclear export of p38 MAPK is also regulated, either as a consequence of dephosphorylation in the nucleus (Gong et al., 2010) or via the physical association of p38 MAPK with a downstream substrate bearing a nuclear export signal (Ben-Levy et al., 1998). One mechanism that controls the localization of phospho-p38 MAPK is the mechanism of its upstream activation. In addition to phosphorylation by the canonical upstream MAPK kinases MKK3/6, p38 MAPK can be activated by autophosphorylation in complex with the TAB-1 scaffold protein (Ge et al., 2002). In cardiomyocytes, when TAB-1 binds to and induces the autophosphorylation of p38 it prevents the nuclear translocation of the activated kinase and antagonizes the activation of gene transcription driven by MKK-dependent p38 activation (Lu et al., 2006). Future investigation of the mechanisms of NMDAR-induced p38 MAPK activation in neurons may expand our understanding of the regulatory processes that control this important kinase signaling cascade.

4. Histone acetylation at enhancers prolongs the activation of neuronal activity-inducible gene transcription

4.1 Summary

Neuronal activity induces gene transcription and drives acetylation of histones at promoters and enhancers of activity-inducible genes. However, whether histone acetylation plays a causative role in regulating activity-inducible gene transcription has remained unknown. We applied CRISPR-mediated epigenome editing, single-cell transcriptional analysis, and mathematical modeling to identify the role of histone acetylation at enhancers of activity-induced *Fos* transcription in primary mouse hippocampal neurons. Locally-induced enhancer histone acetylation was sufficient to increase *Fos* mRNA expression both under basal conditions and following membrane depolarization, via a mechanism that involves enhancer recruitment of Brd4, increased transcriptional elongation by the release of paused polymerase, and prolonged activation of *Fos* promoters. The increase in *Fos* mRNA was translated into increased Fos protein expression and associated with elevation of resting membrane potential. These data causally demonstrate that enhancer histone acetylation can increase the transcription of activity-regulated genes in a manner that is sufficient to alter neuronal function.

4.2 Introduction

Sensory-driven neural activity shapes the processes of brain development and plasticity in ways that both permit and instruct adaptive cognition. Transient sensory experiences are transduced into long-lasting changes in synaptic connectivity and neuronal function at least in part through the activity-dependent regulation of new gene transcription (West and Greenberg, 2011). Synaptic activity, via subsequent membrane depolarization of the postsynaptic neuron, regulates gene transcription by activating intracellular calcium-dependent signaling cascades that modify the function and/or expression of activity-dependent DNA-binding transcription factors and chromatin regulatory proteins (Greer and Greenberg, 2008). The targets of these activity-

regulated transcriptional signaling pathways in neurons include both immediate-early gene transcription factors (*Fos*, *Fosb*, *Npas4*), which induce cell-type specific secondary gene transcription programs to effect cellular adaptations to environmental change, as well as neural-specific programs of gene expression (*Bdnf*, *Narp*, *Arc*), which directly alter aspects of neuronal and synapse structure and function (Leslie and Nedivi, 2011). In this manner, stimulus-induced transcription provides a compelling mechanism of activity-dependent neuronal plasticity.

Genome-level sequencing studies have revealed important roles for chromatin state and structure in the control of gene transcription. In addition to gene promoters, which lie in close proximity to the transcription start site of genes, distal enhancers also contribute to the activation of gene transcription. Enhancers are characterized by their accessibility to transcription factor binding as well as their enrichment for methylation and acetylation on specific histone H3 residues (H3K4me1, H3K27ac), and are thought to regulate target genes by virtue of conformational loops that bring them in close physical proximity to gene promoters (Heintzman et al., 2009). Enhancers have been best studied for their role in controlling cell-type specific programs of gene expression, in which the differential recruitment of the histone acetyltransferases p300/CBP and the presence of H3K27ac are strong predictors of regulatory elements that are sufficient to drive cell-type specific gene transcription (Blow et al., 2010; Nord et al., 2013; Visel et al., 2013).

Yet despite widespread correlations between histone modifications and enhancer function, whether these modifications themselves play causative roles in enhancer activity has been controversial. For example, although H3K4me1 is a canonical mark of enhancers, mutant versions of the histone methyltransferases Mll3/Mll4 that impair H3K4me1 levels at enhancers are nonetheless sufficient to support enhancer-dependent transcription of some genes through non-enzymatic mechanisms (Dorigi et al., 2017). CRISPR-based methods have emerged as a powerful tool in this context because the site specificity of Cas9 binding together with its ability to be fused to enzymatic domains permits the isolated experimental manipulation of histone and

DNA modifications at specific sites across the genome (Thakore et al., 2016). Using this methodology, local CRISPR-mediated recruitment to enhancers of a nuclease-dead Cas9 (dCas9) fused to the active catalytic domain of p300 was shown to be sufficient to induce expression of several cell-type specific genes including *MYOD* in HEK293T cells (Hilton et al., 2015). Thus these data suggest that, at least for this class of enhancers, histone acetylation may play a causative role in the ability of enhancer elements to promote transcription.

Compared with the regulation of cell-type specific gene expression, far less is known about enhancer function in general, and the role of histone modifications in particular, in the context of neuronal activity-inducible transcription. Membrane depolarization of embryonic mouse cortical neurons has been shown to induce CBP binding and H3K27ac at a subset of putative enhancers near activity-regulated genes, and regulatory elements that show activity-dependent increases in H3K27ac are highly likely to be sufficient to drive activity-dependent transcription of a reporter gene (Kim et al., 2010; Malik et al., 2014). These observations are interesting in the context of neuronal plasticity because drugs that block histone deacetylases (HDACs), and thus globally increase histone acetylation, both enhance the activity-dependent expression of stimulus-inducible genes and correlate with enhanced neuronal plasticity during reconsolidation in a memory task (Graff et al., 2014). It is intriguing to speculate that epigenetic priming of the genome, via the activity-dependent deposition of histone acetylation, could regulate behavioral responses to the environment by modulating activity-dependent transcription (Gräff and Tsai, 2013). However pharmacological inhibition of HDACs leads to genome-wide increases in histone acetylation and likely alters acetylation of non-histone proteins as well, raising questions of mechanistic specificity. Furthermore although biochemical studies have provided snapshots showing increased H3K27ac and gene transcription at steady-state time points following neuronal activation, the temporal ordering of these events has not yet been established. Thus the causal link between histone acetylation at activity-regulated enhancers and transcriptional regulation of neuronal gene expression and function remains unknown.

Here, to test whether enhancer histone acetylation plays a causative role in the induction of neuronal activity-regulated gene transcription, we used CRISPR-based dCas9 epigenome editing to locally induce histone acetylation at well-established enhancers of the *Fos* gene. We applied quantitative single-molecule fluorescence in situ hybridization (smFISH) to measure neuronal activity-induced gene transcription at the single neuron level, taking advantage of the intrinsic stochasticity of transcription to quantify the effects of enhancer regulation on the dynamics of promoter state transitions, and we quantified the electrophysiological consequences of enhancer-driven Fos expression in hippocampal neurons. Taken together these data provide direct evidence for a causal role of enhancer histone acetylation in promoting activity-dependent gene transcription and functional neuronal adaptations.

4.3 Materials and Methods

4.3.1 Plasmids

pcDNA-dCas9-p300 Core (Addgene, 61357) and pcDNA-dCas9-p300 Core (D1399Y) (Addgene, 61358) were generous gifts from Charles Gersbach (Duke University). The CRISPR web interface from the Zhang lab at MIT (<http://crispr.mit.edu>) was used to design CRISPR guide RNA (gRNA) followed by a PAM site (NGG) that have minimal off-target matches. gRNA oligos were clone into a FUGW-based U6 chimeric gRNA expression vector co-expressing GFP (Hilton et al., 2015). gRNA sequences are listed in **Appendix B**. 3xAP1pGL3 (3xAP-1 in pGL3-basic) was obtained from Addgene (40342) (Vasanwala et al., 2002). pRL-TK Renilla Luciferase Control Reporter Vector was purchased from Promega.

4.3.2 Dissociated Neuron Cultures

Neuron-enriched cultures were generated from cortex or hippocampus of male and female E16.5 CD1 mouse embryos (Charles River Laboratories) and cultured as previously described (Lyons et al., 2016). Transfections were performed with Lipofectamine 2000 (Life Technologies) at DIV3-4. Cell were treated with 1 μ M Tetrodotoxin (TTX) (Tocris, 1069) 24 hours before membrane depolarization. Isotonic membrane depolarization with 55mM

extracellular KCl was done as previously described (Lyons et al., 2016). Inhibitors were added 20 hours prior to fixation. Trichostatin A (TSA) (Sigma, T8552) was used at a concentration of 30nM. All experiments were conducted in accordance with an animal protocol approved by the Duke University Institutional Animal Care and Use Committee.

4.3.3 Cell Culture

Neuro2a (N2A) cells (ATCC #CCL-131) were grown in DMEM with 10% FBS (Hyclone) and 100 units/ml penicillin/streptomycin. Transfections were performed with Lipofectamine 3000 (Life Technologies) using protocols recommended by the manufacturer. Cells were harvested for analysis 2 day after transfection.

4.3.4 Immunofluorescence

Embryonic mouse hippocampal neurons were cultured on PDL/laminin coated glass coverslips (neuVtro, GG-12-laminin) and fixed in 4% paraformaldehyde at room temperature for 10 min. Neurons were blocked in 10% normal goat serum and permeabilized in 0.3% Triton X-100 prior to antibody incubation. Coverslips were incubated in primary antibodies overnight at 4°C. Secondary antibodies were incubated at room temperature for 1 hr. Hoechst dye (0.1µg/ml, Sigma) was used to label nuclei. Primary antibodies used in this study for immunocytochemistry were mouse anti-Fos (EnCor, MCA-2H2, 1:800), mouse anti-GAD65 (Millipore, AB5082, 1:500), and chicken anti-MAP2 (Millipore, AB5543, 1:2000).

4.3.5 Immunofluorescence image acquisition and analysis

Images were captured on wide-field microscope (DMI4000, Leica) equipped with a CCD camera (DFC365 FX, Leica) and controlled by MetaMorph (Molecular Devices). For quantification of Fos protein level, images were captured at the best z-plane identified in Hoechst channel and analyzed by Fiji. Transfected neurons were selected based on their GFP signals and then Fos fluorescence intensities were measured in these neurons.

4.3.6 Reverse transcription and quantitative PCR

RNA was harvested using the Absolutely RNA Miniprep Kit (Agilent, 400800) and cDNA was synthesized by Superscript II (Invitrogen, 18064). Quantitative SYBR green PCR was

performed on an ABI 7300 real-time PCR machine (Applied Biosystems) using intron-spanning primers (IDT) listed in **Appendix A**.

4.3.7 Chromatin Immunoprecipitation-Qpcr

Chromatin immunoprecipitation was performed following the protocol of EZ-ChIP (Millipore, 17-371). Briefly, cells were lysed by SDS Lysis Buffer and sonicated for 2 hrs (Diagenode Bioruptor) at 4°C on the high setting with 30 seconds on/off interval. 20 µl Dynabeads Protein G (ThermoFisher, 10003D) was pre-incubated with 2 µg antibodies in ChIP Dilution buffer for 1 hour at 4°C. Cell lysates were then incubated overnight with antibody-bead complexes at 4°C. Subsequently, the beads were washed with Low Salt Immune Complex Wash Buffer, High Salt Immune Complex Wash Buffer, LiCl Immune Complex Wash Buffer and TE Buffer. Bound protein/DNA complexes were eluted by ChIP elution buffer and then reversed the crosslinks. Samples were treated with RNase A and Proteinase K for post-immunoprecipitation and then the DNA was purified using QIAquick PCR Purification Kit (Qiagen, 28104). H3K27Ac (Abcam, ab4729), Brd4 (Bethyl, A301-985A), Pol II Ser-2P (Abcam, ab5095) antibodies were used. Primers used for qPCR are listed in **Appendix A**.

4.3.8 Single molecule fluorescence in situ hybridization

Neurons were hybridized with Stellaris RNA FISH Probe sets labeled with Quasar 570 or Quasar 670 (Biosearch Technologies, Inc.), following the manufacturer's instructions available online at www.biosearchtech.com/stellarisprotocols. Briefly, embryonic mouse hippocampal neurons were cultured on PDL/laminin coated glass coverslips (neuVITRO) and fixed in 4% paraformaldehyde at room temperature for 10mins. Neurons were then permeabilized overnight by 70% (vol./vol.) ethanol at 4°C. Coverslips were hybridized with 500 nM probes in hybridization buffer (10% Formamide, 10% 20x SSC, 10% Dextran sulfate, 1mg/mL Escherichia coli tRNA, 2mM Vanadyl ribonucleoside complex and 20ug/mL BSA) at 37 degree for 4 hours followed by washing and Hoechst staining. Custom Stellaris FISH Probe sets were designed against mouse *Fos* exon, mouse *Fos* intron and mouse *Naps4* exon by utilizing the Stellaris®

RNA FISH Probe Designer (Biosearch Technologies, Inc.) available online at www.biosearchtech.com/stellarisdesigner . Probe sequences are available upon request.

4.3.9 smFISH image acquisition and analysis

Z-stack images were captured on either wide-field microscope (DMI4000, Leica) or confocal microscope (TCS SP8, Leica). Wide-field microscope (DMI4000, Leica) equipped with a CCD camera (DFC365 FX, Leica) and controlled by MetaMorph (Molecular Devices). Objective with NA 1.4 and 63X magnification yielded an xy pixel-size of 146 nm. 35-45 Z-slices were recorded with a 200 nm step-size and 1 second exposure time. Confocal microscope (TCS SP8, Leica) equipped with HyD hybrid detectors (Leica). Objective with NA 1.4 and 100X magnification. The detection field was set at 1024 x 1024 and yielded xy pixel-size of 116 nm. The scan rate was set at 600 Hz and the argon laser was set at 30% intensity. 35-45 Z-slices were recorded with a 200 nm step-size. *Fos* and *Npas4* transcript numbers and active TSs were estimated with FISH-quant (Mueller et al., 2013). Cell body of neurons were segmented manually and active TSs were detected with an intensity threshold (around 1.5 fold of average intensity of single transcript). The average number of transcript per cell in the images obtained from wide-field microscope were equivalent to the number in the images obtained from confocal microscope.

4.3.10 Mathematical modeling

We developed and estimated parameters for multiple gene regulation models from our smFISH data using the BayFish pipeline (Gómez-Schiavon et al., 2017). In all cases, the mRNA degradation rate was 0.0469 min^{-1} , as previously measured (Shyu et al., 1989). For each model, the posterior probability of the model parameters was estimated by running three replicas of BayFish for 100000 iterations with different initial parameters. The proposals for new parameters in the Metropolis Random Walk (MRW) were drawn from a normal distribution with mean zero and covariance diagonal matrix with 10^{-5} for the K_{ON} , k_{OFF} , and μ_0 entries, and 10^{-3} for the μ entry. A limit for the maximum mRNA number of 300 was imposed. To avoid overfitting, we used diverse information criteria metrics (Bayesian (BIC), Akaike (AIC) and Deviance (DIC)

Information Criterion) to select the final mathematical model that best fits the data and minimizes the number of free parameters.

4.3.11 Calcium Imaging

Primary cultured hippocampal neurons plated on glass coverslips were loaded with 2 μ M Fura-2 AM (Invitrogen) and 0.04% Pluronic F-127 (Invitrogen) in HANKS buffer (Sigma) at room temperature for 30 min. Cells were imaged every 5 second with an inverted microscope (Nikon) at 340 nm and 380 nm at room temperature. Movies were analyzed with Nikon Elements software: background was subtracted, regions of interest for neurons selected, and the 340/380 ratio calculated.

4.3.12 Electrophysiology and analysis

Electrophysiology recordings of hippocampal neurons Whole-cell patch-clamp recordings were performed 5 days post-transfection at room temperature using an EPC10 amplifier and Patchmaster software (HEKA Elektronik, Lambrecht, Germany). Data were sampled at 10 kHz and filtered at 2.9 kHz. Borosilicate glass pipettes (1.5 OD, 0.85 ID; Sutter Instrument Company, Novato, CA) had a resistance of 3–6.5 M Ω when filled with pipette buffer solution (120 mM potassium gluconate, 10 mM KCl, 5 mM MgCl₂, 0.6 mM EGTA, 5 mM HEPES, 6 μ M CaCl₂, 10 mM phosphocreatine disodium, 2 mM Mg-ATP, 0.2 mM GTP, pH=7.2 adjusted with KOH). Basic external solution contained 126 mM NaCl, 3 mM KCl, 20 mM HEPES, 2 mM CaCl₂, 1mM MgCl₂, 30 mM glucose, and synaptic blockers 20 μ M 2-amino-5-phosphonovaleric acid (APV) and 20 μ M 6-cyano-7-dinitroquinoxaline-2,3-dione (CNQX), pH=7.3 adjusted with NaOH. Resting membrane potential was recorded over a 3 s period of zero current injection. Analysis was performed with Igor Pro 6.22A (WaveMetrics, Lake Oswego, OR).

4.3.13 Statistical Analyses

Unless otherwise indicated, all data presented are the average of at least two biological replicates from each of at least two independent experiments. Also unless otherwise indicated,

data were analyzed by a Student's unpaired t-test, and $p < 0.05$ was considered significant. Bar and line graphs show mean values and all error bars show S.E.M.

4.4 Results

4.4.1 Local induction of H3K27ac at Fos enhancers is sufficient to drive transcription via Brd4 recruitment and activation of transcriptional elongation

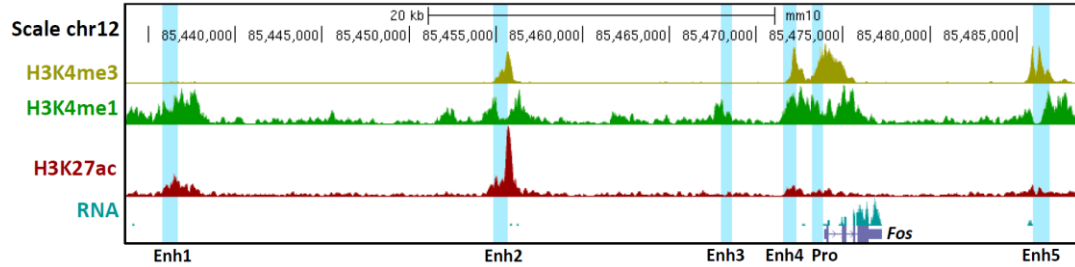


Figure 33: The epigenetic landscape of the *Fos* genomic locus in embryonic 16.5 day mouse forebrain. Blue vertical bars indicate the locations of the *Fos* enhancers and promoter. The ENCODE data GSE82453, GSE82464, GSE82690 and GSE78323 are shown.

To determine whether the accumulation of H3K27ac at distal enhancers plays a causative role in regulating neuronal activity-dependent gene transcription we used CRISPR-based methods to locally recruit a dCas-p300 fusion protein (Hilton et al., 2015) to either the *Fos* promoter or each of five putative activity-regulated enhancers of the *Fos* gene (Kim et al., 2010) (**Fig. 33**). We

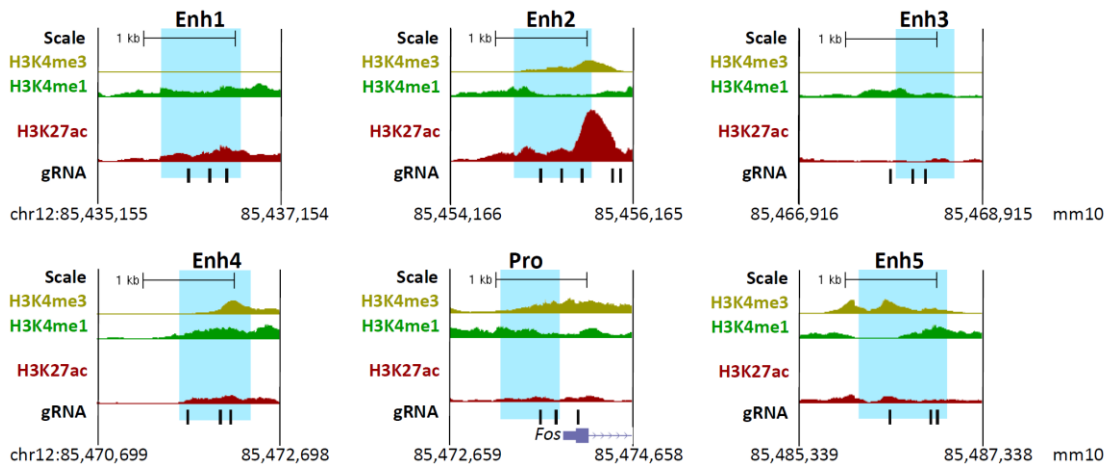


Figure 34: Locations of gRNAs used in this study. Blue vertical bars indicate the locations of the *Fos* enhancers and promoter.

observed a significant increase of *Fos* mRNA in dCas9-p300 transfected N2A cells co-transfected with gRNAs targeting the *Fos* promoter compared with control gRNA and dCas9-p300 co-

transfected cells (**Fig. 35A**, Ctrl n=6, Pro p=0.01 n=4). We also observed a significant increase of *Fos* mRNA expression over control in cells transfected with dCas9-p300 and gRNAs targeting *Fos* enhancers (Enh) 1, 2, 4 or 5, but not Enh3 (**Fig. 35A**, Enh1 p<0.01 n=3, Enh2 p<0.01 n=7, Enh3 p=0.07 n=7, Enh4 p<0.01 n=6, Enh5 p<0.01 n=7). The induction of *Fos* is specifically due

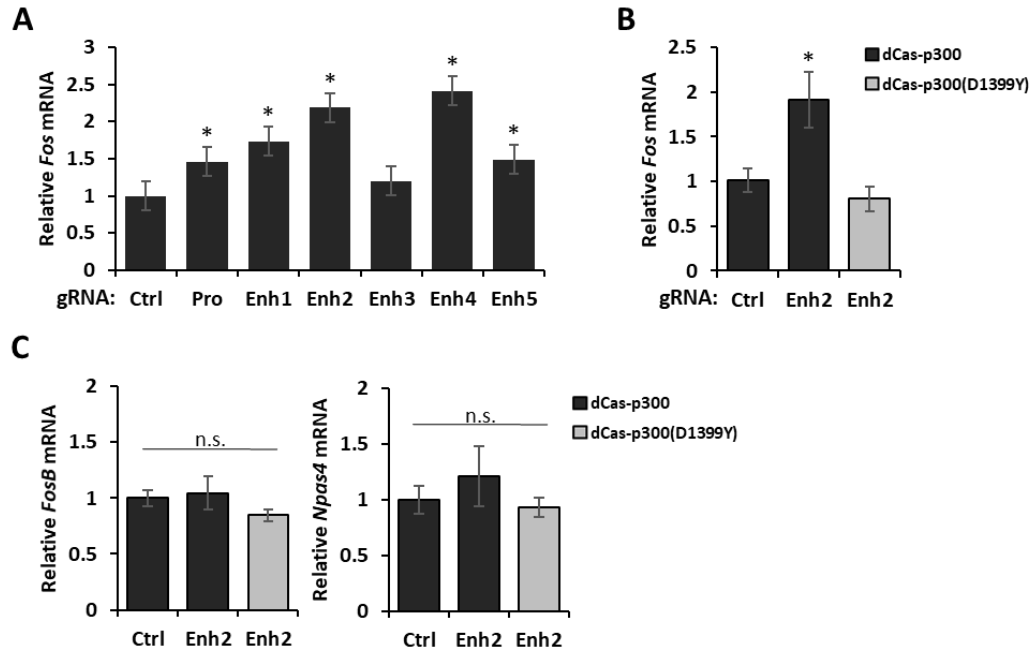


Figure 35: (A) Level of *Fos* mRNA in N2A cells co-transfected with dCas-p300 and gRNAs targeting the *Fos* promoter or the indicated putative distal *Fos* enhancers. Ctrl: n=6, Pro: n=4, Enh1: n=3, Enh2: n=7, Enh3: n=7, Enh4: n=6, Enh5: n=7. (B) *Fos* mRNA levels in N2A cells co-transfected with either the dCas-p300 or an acetyltransferase dead (D1933Y) version of dCas-p300 along with either a control gRNA plasmid or a pool of gRNAs targeted to *Fos* Enh2. n=4/condition. (C) *Fosb* and *Npas4* mRNA levels in N2A cells cotransfected with either the dCas-p300 or an acetyltransferase dead (D1933Y) version of dCas-p300 along with either a control gRNA plasmid or a pool of gRNAs targeted to *Fos* Enh2. n=4/condition.

to dCas9-p300 recruitment to *Fos* enhancers, and is not a non-specific effect on N2A cell physiology, because expression of another *Fos* family member, *Fosb*, and the immediate early gene *Npas4* were unaffected in cells co-transfected with dCas9-p300 and *Fos* Enh2 gRNAs compared to control (**Fig. 35C**, *Fosb*: p=0.80, *Npas4*: p=0.52, control vs. dCas9-p300 at Enh2, n=4/condition). Thus of the five putative enhancers near *Fos* that were initially identified by their inducible CBP binding and H3K27ac accumulation following neuronal membrane depolarization (Kim et al., 2010; Malik et al., 2014), only four are either necessary (Joo et al., 2016) or sufficient (**Fig. 35A**) for *Fos* transcriptional regulation.

To uncover the mechanisms by which the dCas9-p300 fusion protein promotes *Fos* transcription we focused on acetylation of Enh2. We chose Enh2 because each of the four verified *Fos* enhancers shows specificity for activation by different upstream stimuli, and Enh2 is the most responsive to membrane depolarization (Joo et al., 2016), which is the stimulus we use to drive activity-inducible *Fos* transcription in neurons. To test if histone acetyltransferase (HAT) activity of the dCas9-p300 fusion protein is required for Enh2-mediated *Fos* transcription, we utilized a mutant dCas9-p300 fusion protein bearing a single amino acid mutation (D1399Y; dCas9-p300DY) in the enzymatic domain of p300 that eliminates its HAT activity (Hilton et al., 2015). Whereas cells co-transfected with the HAT-active dCas9 fusion protein and the gRNA targeting Enh2 induce *Fos* expression, cells co-transfected with the HAT mutant dCas9 fusion protein failed to induce *Fos* expression (**Fig. 35B**, $p=0.04$ control vs dCas9-p300 at Enh2, $p=0.32$ control vs. dCas9-p300DY at Enh2, $n=4$ /condition). Chromatin immunoprecipitation (ChIP) using an antibody against a FLAG epitope on the dCas9 fusions proteins showed that both dCas9-p300 and dCas9-p300DY were recruited to *Fos* Enh2 by the Enh2 gRNA (**Fig. 36A**, $p=0.02$ control vs. dCas9-p300 at Enh2; $p<0.01$ control vs. dCas9-p300DY at Enh2, $n=3$ /condition). This

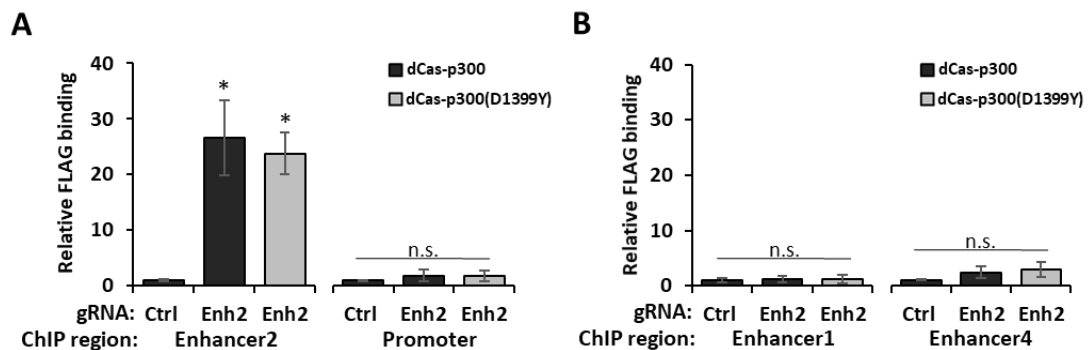


Figure 36: (A) FLAG binding level at *Fos* promoter and enhancer 2 and (B) at *Fos* enhancer 1 and enhancer 4 in N2A cells co-transfected with either a control gRNA plasmid or a pool of gRNAs targeted to *Fos* Enh2 and the indicated FLAG fusion dCas9 variants. $n=3$ /condition.

binding was specific to enhancer 2 because there was no significant interaction of either dCas9 fusion protein at the *Fos* promoter or other *Fos* enhancers (**Fig. 36**, Promoter: $p=0.51$ control vs. dCas9-p300 at Enh2, $p=0.47$ control vs. dCas9-p300DY at Enh2, Enhancer 1: $p=0.82$ control vs.

dCas9-p300 at Enh2, $p=0.76$ control vs. dCas9-p300DY at Enh2, Enhancer 4: $p=0.28$ control vs. dCas9-p300 at Enh2, $p=0.25$ control vs. dCas9-p300DY at Enh2, $n=3$ /condition). To confirm that

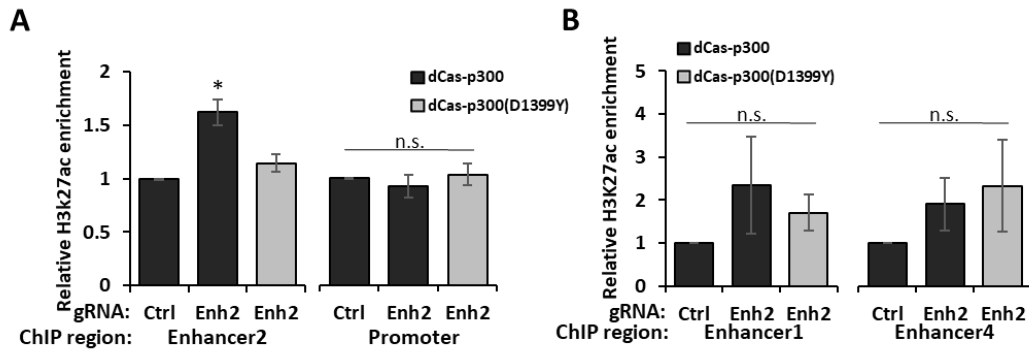


Figure 37: (A) H3K27ac ChIP-qPCR enrichment at *Fos* promoter and enhancer 2 and (B) at enhancer 1 and enhancer 4 in N2A cells co-transfected with either a control gRNA plasmid or a pool of gRNAs targeted to *Fos* Enh2 and the indicated dCas-p300 proteins. $n=5$ /condition.

CRISPR-targeted dCas9-p300 locally increases H3K27ac at targeted enhancers, we performed ChIP to measure H3K27ac at the *Fos* promoter and enhancers in transfected cells. Compared with control, we observed significantly higher H3K27ac at *Fos* Enh2 in cells co-transfected with dCas9-p300 and Enh2 gRNAs, whereas co-transfection of Enh2 gRNAs with the HAT-dead dCas9-p300DY construct did not increase H3K27ac over control levels (**Fig. 37A**, $p<0.01$ control vs. dCas9-p300 at Enh2; $p=0.11$ control vs. dCas9-p300DY at Enh2, $n=5$ /condition). Importantly, this increase in H3K27ac was local to the enhancer where the dCas9-p300 fusion protein was recruited, and we saw no increase of H3K27ac at the *Fos* promoter and other enhancers (**Fig. 37**, Promoter: $p=0.48$ control vs. dCas9-p300 at Enh2, $p=0.78$ control vs. dCas9-p300DY at Enh2, Enhancer 1: $p=0.27$ control vs. dCas9-p300 at Enh2, $p=0.13$ control vs. dCas9-p300DY at Enh2, Enhancer 4: $p=0.18$ control vs. dCas9-p300 at Enh2, $p=0.25$ control vs. dCas9-p300DY at Enh2, $n=5$ /condition).

Fos is one of a large set of neuronal activity-regulated genes whose promoters are occupied under basal conditions by RNA PolIII complexes that are initiated but stably paused (Saha et al., 2011). In response to neural activity or other stimuli, recruitment of the P-TEFb complex triggers PolIII phosphorylation and promotes highly rapid and productive transcriptional

elongation of paused genes (Jonkers and Lis, 2015). Interestingly the acetyl-lysine binding domain protein Brd4 promotes recruitment of P-TEFb and acts as a master regulator of transcriptional elongation (Winter et al., 2017). Brd4 has been shown to mediate stimulus-dependent activation of transcriptional elongation when recruited to enhancers (Zippo et al., 2009) and its function in neuronal activity-inducible gene expression is beginning to be explored (Korb et al., 2015). Thus we considered the possibility that enhancer histone acetylation might activate *Fos* transcription by recruiting Brd4 and promoting transcriptional elongation. Consistent with a role for Brd4 in enhancer acetylation-dependent activation of *Fos*, we observed significantly more Brd4 binding by ChIP at *Fos* Enh2 when dCas9-p300 was recruited to this enhancer compared with control (**Fig. 38A**, $p=0.02$ $n=5$ /condition). This recruitment was dependent on the local induction by dCas9-p300 of H3K27ac at Enh2 (**Fig. 37**), because we saw no significant increase in Brd4 binding at the *Fos* promoter in the same cells (**Fig. 38A**, $p=0.46$ $n=5$ /condition).

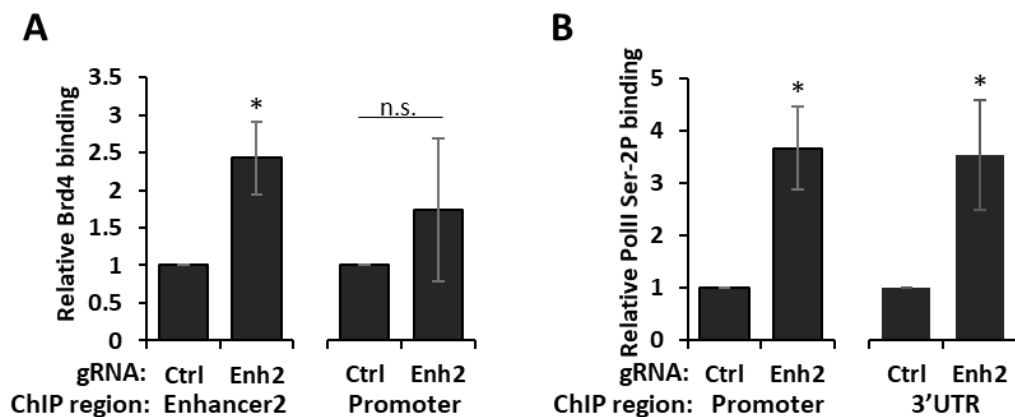


Figure 38: (A) Brd4 ChIP-qPCR enrichment at *Fos* promoter and enhancer 2 in N2A cells co-transfected with dCas-p300 and either a control gRNA plasmid or a pool of gRNAs targeted to *Fos* Enh2. $n=5$ /condition (B) RNAPII phosphorylated at Ser2 (Ser-2P) ChIP-qPCR enrichment at *Fos* promoter and 3'UTR in N2A cells co-transfected with dCas-p300 and either control gRNA plasmid or a pool of gRNAs targeted to *Fos* Enh2. $n=6$ /condition. Data are represented as mean \pm SEM; Two-tailed Student's t test, $*p<0.05$ compared with Ctrl. n.s., not significant.

The increase in Brd4 binding at Enh2 was associated with increased *Fos* elongation, because the level of Ser2 phosphorylated RNA PolII (pSer2-PolII) was significantly elevated on the *Fos* gene in cells co-transfected with dCas9-p300 and Enh2 gRNAs compared to control. pSer2-PolII was elevated at both the 5' and 3' ends of the *Fos* gene in these cells, indicating that acetylation of

Enh2 was sufficient to induce productive increases in RNA PolIII elongation across the length of the *Fos* gene (**Fig. 38B**, 5' end p=0.01 control vs. dCas9-p300 at Enh2, 3' end p=0.04 control vs. dCas9-p300 at Enh2, n=6/condition). Thus these data demonstrate that histone acetylation at *Fos* enhancers mediated by local recruitment of dCas9-p300 is sufficient to drive *Fos* expression by promoting transcriptional elongation.

4.4.2 Transient membrane depolarization drives dynamic H3K27 acetylation at *Fos* regulatory elements that matches the time course of *Fos* transcription

Activity-regulated gene transcription is a dynamic process comprised of multiple steps that include transcriptional initiation, elongation, and termination. Thus to test possible causative roles for histone acetylation in this process, we first needed to establish a stimulus protocol in neurons that would allow us to accurately assess the temporal order in which both histone acetylation and *Fos* transcription occur. Membrane depolarization mediated by the elevation of extracellular potassium chloride levels is a robust stimulus for the induction of neuronal activity-regulated genes that acts via well-established mechanisms (Bito et al., 1997). Membrane depolarization induces gene transcription by opening L-type voltage gated calcium channels, activating intracellular calcium-regulated kinases (CaMKIV, Erk MAP kinase), and promoting the phosphorylation of nuclear transcription factors like CREB and MEF2 that are pre-bound to promoters and enhancers of activity-inducible genes (Lyons and West, 2011). It has been demonstrated that the steps that comprise this process, including intracellular calcium elevation, cytoplasm to nuclear translocation of kinase activity, CREB phosphorylation, and *Fos* induction occur over the time course of minutes (Bito et al., 1996; Dolmetsch et al., 2001; Zhai et al., 2013). On the contrary, prior studies of membrane depolarization-inducible histone acetylation have used hours long stimuli, thus whether the deposition of these histone modifications either precedes or follows the onset of gene transcription is not known (Kim et al., 2010; Malik et al., 2014).

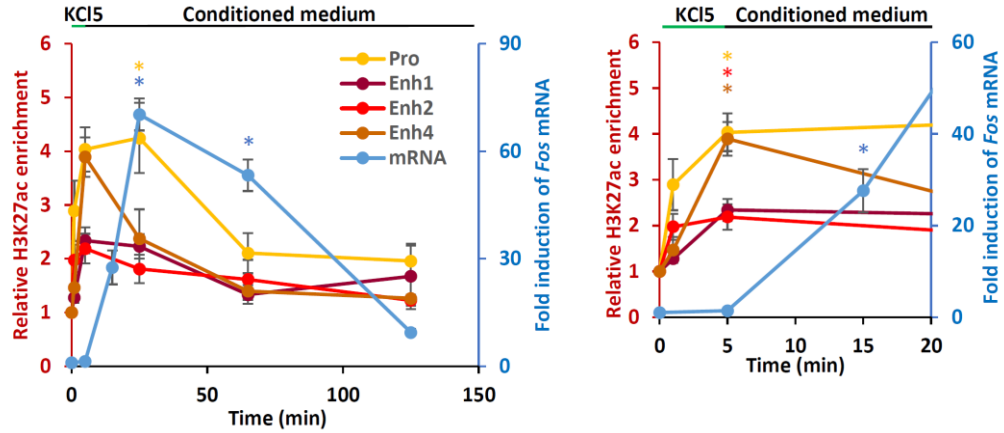


Figure 39: H3K27ac ChIP-qPCR at the *Fos* promoter (yellow) and three distal enhancers (dark red: Enh1, red: Enh2 and brown: Enh4) following 5 min membrane depolarization of primary mouse cortical neurons. Time course of *Fos* mRNA expression is shown in blue. The first 20 min is shown to the right. n for ChIP-qPCR 0 min=6, 1 min=4, 5 min=6, 25 min=6, 65 min=5, 125 min=5. n for mRNA=4/time point. Data are represented as mean \pm SEM. One way ANOVA with Bonferroni post hoc tests, *p<0.05 compared with time 0.

In order to determine whether H3K27ac is induced at *Fos* enhancers on the same time scale as transcription, we stimulated cultured cortical neurons with a 5 min pulse of membrane depolarization by elevating extracellular potassium to 55mM (Lyons et al., 2016) and measured levels of *Fos* mRNA and H3K27ac at regulatory elements of the *Fos* gene as a function of time (**Fig. 39**). We found that 5 min of membrane depolarization is sufficient to drive stimulus-dependent increases in both *Fos* mRNA and H3K27ac at the *Fos* promoter and distal enhancers (**Fig. 39** left, mRNA: $F(5,18)=81.18$, $p<0.01$; H3K27ac: Pro $F(5,26)=5.98$ $p<0.01$, Enh1 $F(5,26)=2.54$ $p=0.05$, Enh2 $F(5,26)=3.48$ $p=0.02$, Enh4 $F(5,26)=5.90$ $p<0.01$). Induction of *Fos* mRNA as well as H3K27ac in response to this stimulus is both rapid and transient, significantly increasing within 10 min following stimulus induction and falling rapidly following cessation of the stimulus (**Fig. 39** right, H3K27ac at 5 min: Pro $p=0.04$, Enh2 $p=0.02$, Enh4 $p<0.01$; mRNA at 15 min: $p<0.01$).

Finally, to establish whether constitutive elevation of histone acetylation can be correlated with increased *Fos* expression in our cultured primary mouse neurons as has been shown in other systems, we treated our neuronal cultures with the histone deacetylase inhibitor TSA overnight and measured both H3K27ac at *Fos* regulatory elements and *Fos* mRNA

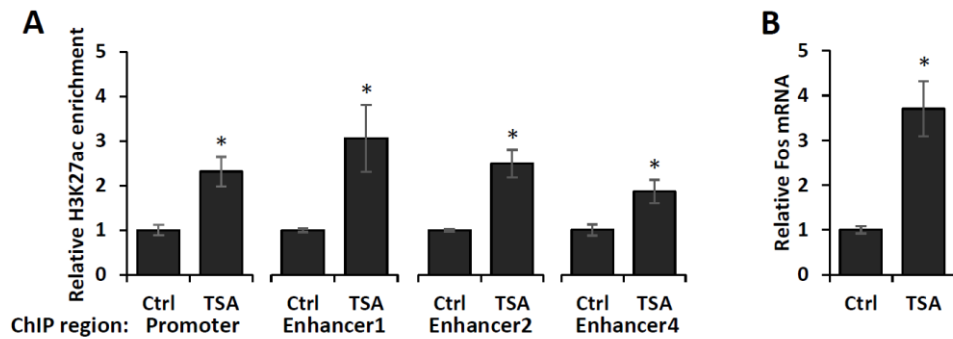


Figure 40: (A) Level of *Fos* mRNA in cultured mouse primary cortical neurons with (TSA) or without (Ctrl) 30 nM TSA treatment for 20 hour before harvesting. n=5/condition. (B) H3K27ac ChIP-qPCR enrichment at *Fos* promoter and enhancers in cultured mouse primary cortical neurons with (TSA) or without (Ctrl) 30 nM TSA treatment for 20 hour before harvesting. n=4/condition. Data are represented as mean \pm SEM. Two-tailed Student's t test, *p<0.05 compared with Ctrl.

expression. Consistent with previous studies using HDAC inhibitors in vivo (Graff et al., 2014), TSA in our system was sufficient to both induce H3K27ac at the *Fos* promoter and distal enhancers and to induce *Fos* mRNA expression (Fig. 40, H3K27ac: Pro p=0.01, Enh1 p=0.03, Enh2 p<0.01, Enh4 p=0.02, n=4/condition; mRNA: p<0.01, n=5/condition).

These data show that we have established a system in which we can study the full time course of stimulus-inducible *Fos* transcription to assess the functional impact of H3K27ac at enhancers. Furthermore by establishing the coincident induction of H3K27ac at *Fos* regulatory elements with the activation of *Fos* transcription, these data provide fundamental support for a possible causative role of histone acetylation in transcriptional regulation.

4.4.3 Single neuron analysis of gene expression reveals gene-local, probabilistic regulation of neuronal activity-dependent transcription

There are only two alleles for any given gene in the nucleus of a post-mitotic neuron. Transcription of any gene in a cell is an inherently stochastic process governed by the probabilities and kinetics of promoter transitions between on and off states in its two alleles (Symmons and Raj, 2016). This stochasticity can be useful because one can measure the probabilistic variance in gene transcription between single cells within a population and infer

quantitative properties of the transcriptional process (Vera et al., 2016). To extract such data from our primary neuronal culture model, we examined stimulus-inducible *Fos* transcription at the

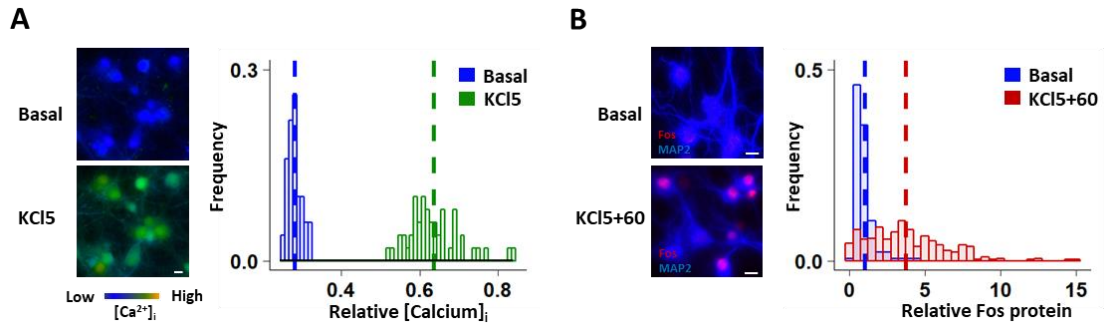


Figure 41: (A) Intracellular calcium concentration in single primary mouse hippocampal neurons measured by Fura-2, 1 min before (Basal, blue) and 1 min after (KCl5, green) 5 min exposure to 55 mM KCl. Dashed lines show average for each group. n=50 neurons per time point from 2 biological replicates. scale bar= 5 μ m. (B) Fos protein levels in single primary mouse hippocampal neurons, before (Basal, red) and 60 mins after (KCl5+60, red) 5min 55mM KCl. Dashed lines show average for each group. Basal n=172 and KCl5+60 n= 345 neurons from 2 biological replicates. scale bar= 5 μ m.

single neuron level. As expected, we observed that 5 min of membrane depolarization was sufficient to drive a robust increase in intracellular calcium concentration that had a unimodal distribution across the sampled population (**Fig. 41A**, Basal vs. KCl5 p<0.01 n=50 neurons/condition). However when we compared the levels of Fos protein induced by membrane depolarization across individual neurons in the population we found a much wider variation (**Fig. 41B**). These data show that although this stimulus has the potential to induce calcium-dependent transcription in each individual neuron, that the efficacy with which this stimulus is coupled to Fos induction varies widely across the population.

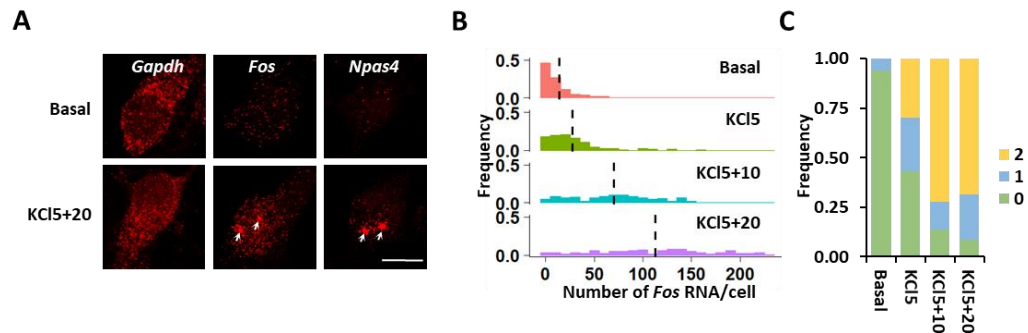


Figure 42: (A) Representative smFISH images for the indicated mRNAs in primary mouse hippocampal neurons before and 20 min after a 5 min exposure to 55mM KCl. White arrows show the two alleles in the nucleus. Scale bar= 5 μ m. Observed distributions of *Fos* (B) RNA and (C) active transcription sites (TSs) per single cell by smFISH. Dashed lines show average RNA number for each group. Basal n=173, KCl5 n=174, KCl5+10 n=122, KCl5+20 n=115 neurons from 3 biological replicates.

To determine the contribution of variation at the transcriptional level to the variation in stimulus-inducible Fos protein expression, we measured gene transcription at the single neuron level using directly labeled fluorescent DNA probe sets to count single molecules of RNA in fixed primary neurons in situ (smFISH, **Fig. 42A**) (Raj et al., 2008). We quantified RNA expression in single primary mouse hippocampal neurons in culture both under basal conditions and over time following 5 min of membrane depolarization (**Fig. 42B**). The time course and magnitude of the average transcriptional activity detected by smFISH across all cells in the

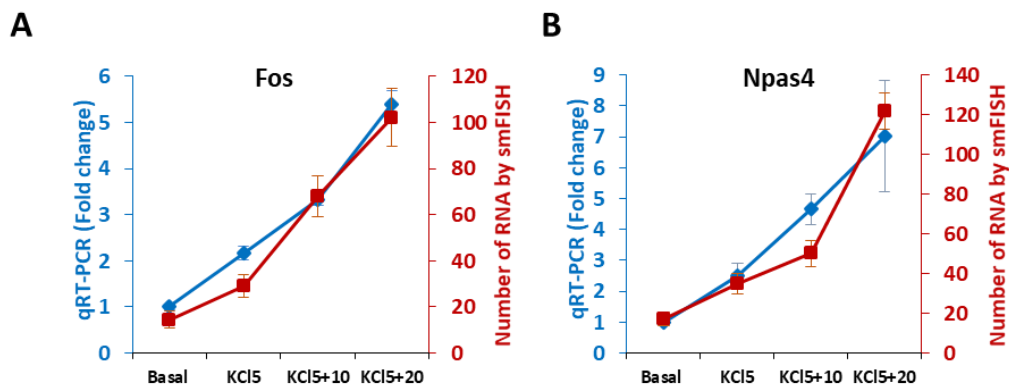


Figure 43: Average (A) *Fos* and (B) *Npas4* RNA levels at different time points before (Basal) and after a 5min pulse of KCl by smFISH (red line) and qRT-PCR (blue line). Error bars are 95% CI for smFISH and SEM for qRT-PCR. n=3 biological replicates/condition.

population precisely paralleled the values we observed for the same stimulus and time course using quantitative PCR, validating the measure (**Fig. 43**). Additionally, because nascent RNA from inducibly transcribed genes like *Fos* accumulates near the transcription site (TS) in the nucleus prior to splicing and export (Bhatt et al., 2012; Senecal et al., 2014), smFISH reveals the number of active alleles of each gene (0, 1, or 2) that are being transcribed in each cell at any given time point, providing a key additional measure of promoter state (**Fig. 42C**). Colocalization of smFISH signal for *Fos* introns with the nuclear *Fos* exon signal confirmed that these nuclear clusters are composed of nascent RNA (**Fig. S3A**).

Similar to our observations for Fos protein (**Fig. 41A**), although we found that *Fos* mRNA rose above basal levels in the great majority of neurons in the culture, we again observed a substantial variation in the quantity of *Fos* mRNA induced per cell comparing individual

neurons in the population (**Fig. 42B**). This variation could not be explained by the presence of excitatory and

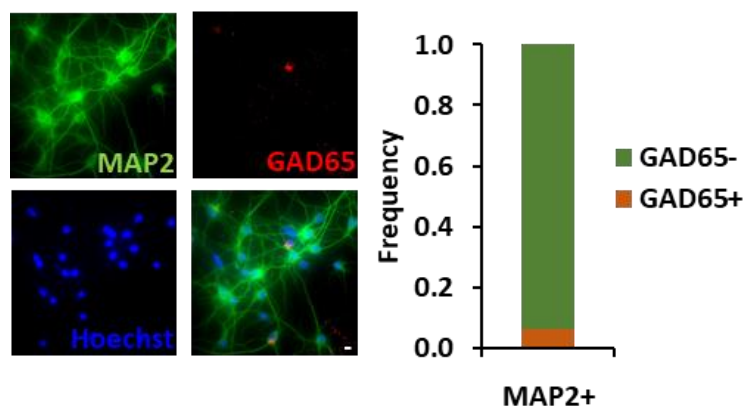


Figure 44: Fraction of excitatory (GAD65-) and inhibitory (GAD65+) neurons (MAP2+) in primary cultured hippocampal neurons. n=1531 neurons from 2 biological replicates. Scale bar= 10 μ m.

inhibitory neurons in our cultures because the vast majority of our MAP2+ neurons were excitatory and did not express the inhibitory neuron marker Gad65 (**Fig. 44**). The proportion of neurons showing both *Fos* alleles active in the nucleus increased following membrane depolarization and reached a peak at 10 min following cessation of the stimulus (**Fig. 42C**). However, at all time points, we still observed a fraction of the neurons that had only one *Fos* allele active (**Fig. 42C**), consistent with the probabilistic regulation of each promoter.

The variation in *Fos* mRNA expression between neurons could arise due to differences in the capacity of individual neurons in the culture to propagate calcium-dependent signaling events to the nucleus in addition to the effects of the probabilistic activation of single gene promoters. If there is substantial cell-to-cell variation in the activation of calcium-dependent transcriptional signaling pathways between neurons in our population, we predicted that we would see concordant degrees of activation of all activity-inducible genes in any single neuron.

Alternatively if the variability we observe for any single gene is predominantly arising from probabilistic activation local to the gene promoter, we predicted that different activity-inducible genes would be regulated independently in single neurons, as evidenced by discordant induction of any two genes in a single neuron. To disambiguate the contribution of these two factors, we

simultaneously quantified mRNA for two neuronal activity regulated genes, *Fos* and *Npas4*, in single hippocampal neurons by two color smFISH (**Fig. 45A**).

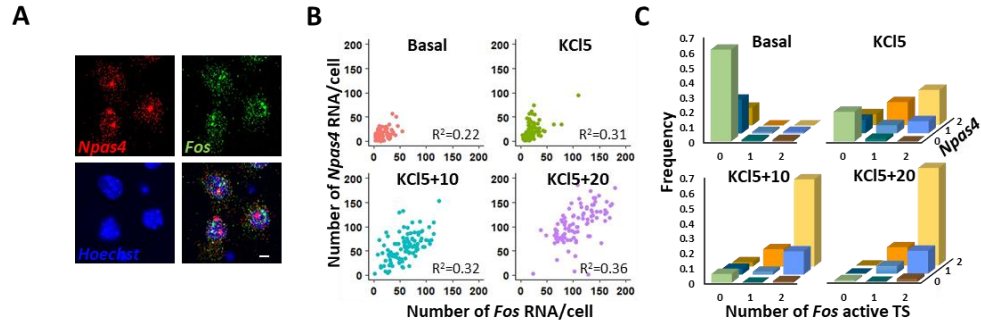


Figure 45: (A) Representative dual color smFISH images for *Fos* and *Npas4* in single neurons at 20 min following 5min 55mM KCl. Scale bar= 5µm. Scatter plot of (B) RNA and distribution of (C) active TSs in single neurons at different time point by dual-color smFISH, Basal n=93, KCl5 n=100, KCl5+10 n=104, KCl5+20 n=99 neurons from 2 biological replicates.

Even though *Fos* and *Npas4* have similar kinetics and magnitude of induction at the population level (**Fig. 43**), we found only a weak correlation between the depolarization-induced levels of these two mRNAs in single neurons (**Fig. 45B**). These data suggest that the interneuronal variability in gene induction arises at least in part because of intraneuronal variability in the probability of promoter activation at each allele. Consistent with this possibility, our data also reveal variability in the transcriptional activation of each of the two *Fos* and *Npas4* alleles within

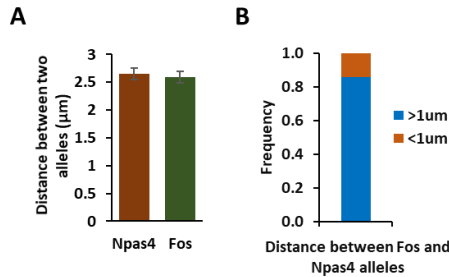


Figure 46: (A) Average distance between two active TSs of indicated genes at 20 min following 5min 55mM KCl. *Npas4* n=132, *Fos* n=154 neurons from 2 biological replicates. (B) Distribution of distance between *Npas4* and *Fos* active alleles in neurons at 20 min following 5min 55mM KCl. n=709 *Fos* and *Npas4* active alleles from 2 biological replicates.

a single cell. Although, on average, the neurons in our population transitioned from having both alleles of *Fos* and *Npas4* off (0,0) to having both alleles on (2,2) following membrane depolarization, at each time point we also found neurons in which a single allele of one gene was

active in various combinations with active alleles of the other gene (0,1; 1,0; 1,1; 2,1; 1,2; 2,0; 0,2) (**Fig. 45C**). Taken together with the substantial physical distances between the four individual alleles of *Fos* and *Npas4* in any given cell (**Fig. 46**), these data indicate that regulatory events local to each allele of any specific gene play a role in modulating the probability of activity regulated gene transcription.

4.4.4 Local induction of H3K27ac at *Fos* enhancers alters the dynamics of *Fos* promoter state transitions, increasing *Fos* protein expression and driving functional neuronal adaptations

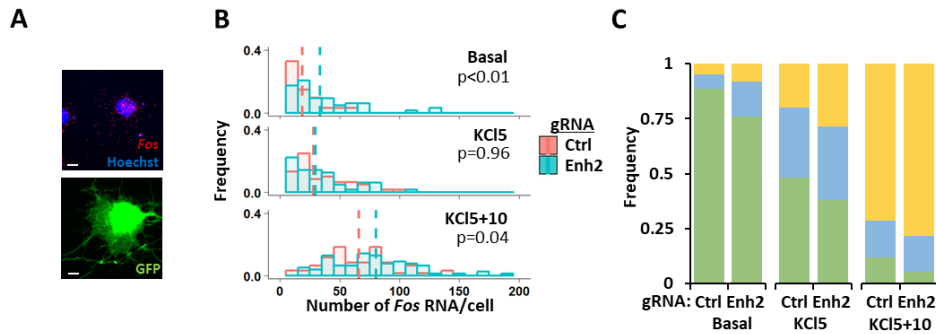


Figure 47: (A) Representative smFISH image of hippocampal neurons transfected with dCas-p300 and gRNAs at 10 min after a 5min exposure to 55mM KCl. GFP expressed from gRNA plasmids. Observed distributions of *Fos* (B) RNA and (C) active TSs measured by smFISH in single neurons at different time points before (Basal), after a 5 min pulse of KCl(KCl5), and 10 minutes after the pulse(KCl5+10). Cultured mouse hippocampal neurons were co-transfected with dCas-p300 and indicated gRNAs. Dashed lines show average RNA number for each group. Data were analyzed by Kolmogorov–Smirnov test. Basal: Ctrl n=62, Enh2 n=63, KCl5: Ctrl n=60, Enh2 n=63, KCl5+10: Ctrl n=60, Enh2 n=78 neurons per group from 3 biological replicates.

To determine how induction of H3K27ac at *Fos* enhancers changes activity-inducible *Fos* transcription in neurons, we co-transfected primary mouse hippocampal neurons with dCas9-p300 and either a control gRNA or a pool of gRNAs targeting Enh2 and quantified the number of *Fos* mRNA per cell and the number of active TSs by smFISH before and at time points after 5 min period of membrane depolarization (**Fig. 47A**). Recruitment of dCas9-p300 to *Fos* Enh2 significantly increased *Fos* mRNA expression in neurons both under basal conditions and following membrane depolarization (**Fig. 47B** $p<0.01$ basal, $p=0.96$ KCl5, $p=0.04$ KCl5+10). We also observed an increase in the average number of active TSs when comparing neurons in which dCas9-p300 had been targeted to *Fos* Enh2 compared with control transfected neurons (**Fig. 47C**)

These data show that recruitment of histone acetylation at *Fos* enhancer 2 is sufficient to increase transcription of *Fos* in neurons even following a robust stimulus like membrane depolarization.

Changes in *Fos* mRNA expression could arise from increased probability of promoter activation, a prolonged time of activation, an increased synthesis rate during activation, or a decreased rate of degradation. We have developed a computational pipeline (BayFish) that uses Bayesian inference to estimate the kinetic parameters of promoter state transitions for any given gene from smFISH data gathered over a time course after cellular stimulation (Gómez-Schiavon et al., 2017). Our method uses the likelihood and posterior probability of a set of kinetic parameters, given the observed experimental data, to evaluate the validity of different gene regulation models. To discover the potential transcriptional mechanisms by which histone

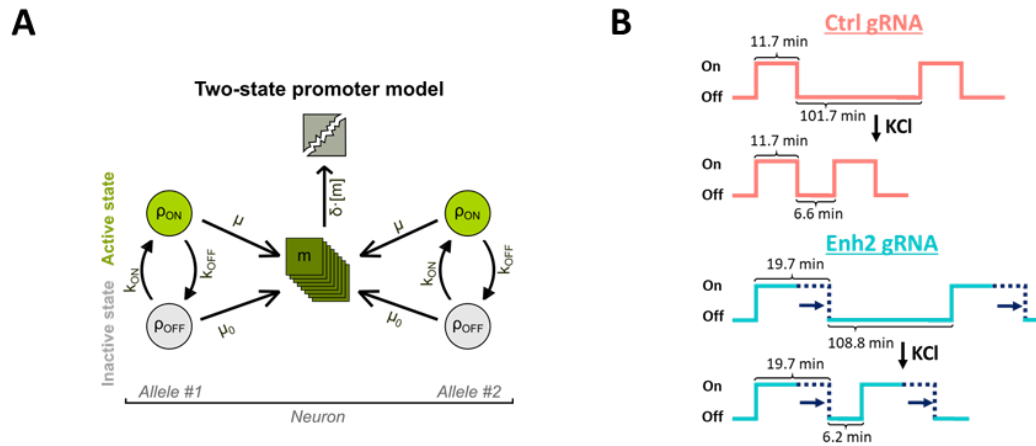


Figure 48: (A) Diagram of the two-state promoter model. The promoter of each allele can be either in an active (P_{ON}) or inactive (P_{OFF}) state. Each allele synthesizes mRNA molecules (m) with rate μ or μ_0 if the promoter is active or inactive, respectively. Transitions between promoter states occur with a promoter activation rate k_{ON} and a promoter deactivation rate k_{OFF} . Finally, each mRNA is degraded with rate δ . The stimulus increases gene expression by changing one or more parameters and we evaluated several different models of stimulation by fitting them to smFISH data. (B) The best fit residence time of the *Fos* promoter in the active (ON) state was obtained by BayFISH for data in Figure 47. Data from Mariana Gómez-Schiavon and Nicolas Buchler.

acetylation at *Fos* Enh2 promotes activity-inducible *Fos* transcription, we applied this pipeline to our single neuron smFISH data. We evaluated a two-state promoter model of gene transcription, in which the promoter of each *Fos* allele can be either active (ON) or inactive (OFF; **Fig. 48A**). This represents the simplest model that can recapitulate the variability of TS activation we observed in our neurons (**Fig. 42C, 45C and 47C**) and is consistent with the widely applied

bursting model of gene regulation that has been previously used to evaluate *Fos* regulation in non-neuronal cells (Senecal et al., 2014). Our two-state promoter model estimates four kinetic parameters – the rate at which each promoter turns on (k_{ON}), the rate at which each promoter turns off (k_{OFF}), the RNA synthesis rate for each ON promoter (μ) and for each OFF promoter (μ_0). The rate of RNA degradation (δ) was previously measured and those data used here (Shyu et al., 1989). We compared and fit different versions of this model in which we allowed membrane depolarization to change one or more parameters. We countered overfitting by using different metrics to penalize models with larger numbers of parameters. For the considered metrics, increasing only the promoter activation rate (k_{ON}) following membrane depolarization showed consistently the best and most parsimonious fit to the *Fos* smFISH data from both groups of neurons (control and Enh2 transfected) (**Fig. 48B**). Varying additional parameters together with k_{ON} had a minimal improvement on the fit, suggesting that membrane depolarization acts to increase *Fos* mRNA primarily by increasing the probability that each *Fos* promoter transitions to the ON state. This outcome of the model is the same as we observed when we analyzed smFISH data for *Npas4* induced by membrane depolarization in neurons (Gomez-Schiavon et al., 2017) and is highly consistent with the well-established activity-dependent molecular mechanisms that regulate the induction of *Fos* transcription in neurons (Lyons and West, 2011).

	Ctrl		Enh2		Units	
	Mean	Std	Mean	Std		
$k_{ON(U)}$	0.0101	0.0015	0.0094	0.0014	1/min	- Activation rate in uninduced conditions
$k_{ON(S)}$	0.1544	0.0169	0.1630	0.0153	1/min	- Activation rate after stimulus
k_{OFF}	0.0880	0.0161	0.0521	0.0084	1/min	- Deactivation rate
μ_0	0.0181	0.0091	0.0302	0.0123	mRNA/min	- Basal synthesis rate
μ	4.6803	0.2642	4.6790	0.2195	mRNA/min	- Synthesis rate
δ	0.0462	-	0.0462	-	1/min	- Degradation rate
τ_{ON}	11.7	2.1285	19.7	3.2293	min	- Burst duration
a	23.2	6.8008	55.6	13.4574	mRNA	- Burst amplitud
$f_{ON(U)}$	0.10	0.0138	0.15	0.0177	promoters	- Fraction of active promoters in uninduced conditions
$\tau_{OFF(U)}$	101.7	15.5328	108.8	15.8083	min	- OFF duration in uninduced conditions
$f_{ON(S)}$	0.64	0.0352	0.76	0.0282	promoters	- Fraction of active promoters after stimulus
$\tau_{OFF(S)}$	6.6	0.7198	6.2	0.5830	min	- OFF duration after stimulus

Table1: The best fit parameters in k_{ON} -sensitive two-state promoter model.

By contrast when we compared the best fit parameters between the two groups of transfected neurons our data from the neurons co-transfected with the Enh2 gRNAs had a smaller promoter inactivation rate (k_{OFF}) compared with the control transfected neurons (**Fig. 48B and Table 1**). The effect of decreasing k_{OFF} is to prolong the time that the promoter stays in the active state after it turns on. This prediction of the model is consistent with our evidence for increased mRNA expression in the presence of persistent enhancer H3K27ac under both basal and stimulus induced conditions. Furthermore the prolonged kinetics of *Fos* promoter activation in the Enh2 transfected cells is consistent with our evidence that enhancer histone acetylation increases the release of paused PolII at the *Fos* gene (**Fig. 38**), because pausing has been found to inhibit multiple rounds of transcription under conditions when upstream stimuli drive synchronous transcriptional activation (Shao and Zeitlinger, 2017). We discuss the mechanistic implications of these data in more detail in the Discussion section below.

Finally, to determine whether enhancer acetylation-dependent promotion of *Fos* transcription has relevance for plasticity of neuronal function, we asked whether the induction of *Fos* transcription we observed in neurons in which dCas9-p300 was targeted to Enh2 was sufficient to drive changes in Fos protein expression and function. We observed a significant increase of Fos protein levels in neurons transfected with *Fos* Enh2 gRNAs compared with control gRNA-transfected neurons, indicating that the increased *Fos* mRNA we observed in these

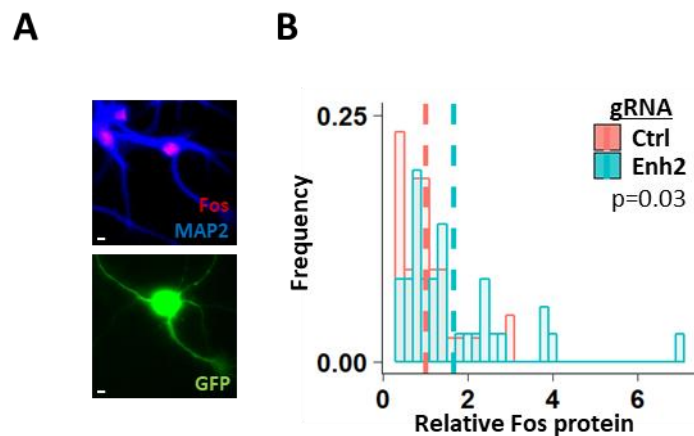


Figure 49: (F) Representative IHC image of hippocampal neurons transfected with dCas-p300 and gRNAs. (G) Observed distribution of Fos protein levels in cultured mouse neurons co-transfected with dCas-p300 and either control plasmid or a pool of gRNAs targeted to *Fos* Enh2. Data were analyzed by Kolmogorov–Smirnov test. Ctrl n=43, Enh2 n=36 neurons from 3 biological replicates. Dashed lines show average protein expression for each group. scale bar= 5µm.

neurons was translated into increases in Fos protein (**Fig. 49**, $p=0.03$). Because Fos is a transcription factor, once its expression is induced Fos binds AP-1 elements across the genome to regulate the expression of secondary response genes in a cell-type specific manner. In N2A cells co-transfected with a 3xAP-1 firefly luciferase reporter plasmid and dCas9-p300 we found significantly more firefly luciferase (*FLuc*) mRNA in cells in which *Fos* Enh2 gRNAs had been used to drive *Fos* expression compared to control transfected cells (**Fig. 50B**, $p<0.01$). Thus these data show that the activation of *Fos* transcription induced by enhancer histone acetylation is sufficient to increase Fos-dependent transcription. What might be the consequences of increasing Fos transcription in neurons? Though the precise cell-autonomous consequences of Fos induction in hippocampal neurons remain to be determined, a recent RNA-seq of dentate granule neurons overexpressing Fos in vivo revealed both increased and decreased expression of a large number

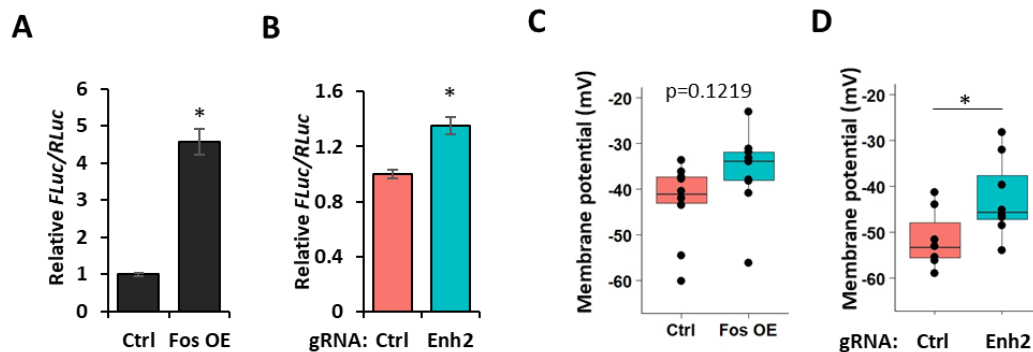


Figure 50: (A) FLuc mRNA to RLuc mRNA levels in N2A cells co-transfected with 3xAP1-FLuc, pTKrenilla luciferase and control (Ctrl) or Fos overexpression plasmid (Fos OE). (B) Firefly luciferase (FLuc) mRNA to Renilla luciferase (RLuc) mRNA levels in N2A cells co-transfected with 3xAP1-FLuc, pTK-renilla luciferase, dCas-p300 and either control gRNA plasmid or a pool of gRNAs targeted to *Fos* Enh 2. The FLuc mRNA levels were normalized for each well to co-transfected RLuc mRNA levels. n=6/condition. Data are represented as mean \pm SEM. (C) Box and whiskers plot of resting membrane potential (mV) in mouse hippocampal neurons that were transfected with either control (Ctrl) or Fos overexpression plasmid (Fos OE). Ctrl n=10, Fos OE n=9 neurons from 2 biological replicates. (D) Box and whiskers plot of resting membrane potential (mV) in mouse hippocampal neurons that were transfected with dCas-p300 and either control plasmid or a pool of gRNAs targeted to *Fos* Enh 2. Ctrl n=7, Enh2 n=8 neurons from 2 biological replicates. The lower and upper hinges correspond to the first and third quartiles. The whiskers extend from the hinges to the values no further than 1.5 * the inter-quartile range(IQR) from the hinges. Dots are data points of individual neurons. Two-tailed Student's t test, * $p<0.05$ compared with Ctrl. (C) and (D) data from Breanna Kalmeta and Jörg Grandl.

of genes encoding ion channels, suggesting that Fos overexpression might change the membrane properties of hippocampal neurons (Su et al., 2017). Consistent with this possibility, and similar to the effects of *Fos* overexpression (**Fig. 50A, C**) we found that hippocampal neurons co-transfected with dCas9-p300 and Enh2 gRNAs showed significantly higher resting membrane potentials compared with control-transfected neurons (**Fig. 50D**, $p=0.04$). In summary, these data show that induction of histone acetylation at *Fos* enhancers plays a causative role in the induction of Fos-dependent neuronal adaptations.

4.5 Discussion

Epigenome profiling studies have yielded substantial data on the distribution of chromatin marks across the genome and their correlative relationship to gene expression. These data have driven the formation of intriguing hypotheses of the functional consequences of chromatin regulation, including the speculation that the priming of histone modifications or DNA methylation at regulatory elements controlling stimulus-regulated genes could modulate behavioral responses to the environment (Day and Sweatt, 2011; Graff and Tsai, 2013). Epigenome editing offers an opportunity to test the causative role of chromatin modifications for gene transcription via the local recruitment of histone modifying enzymes to specific gene regulatory elements (Thakore et al., 2016). Here we have used this methodology to study the transcriptional consequences of histone acetylation at enhancers of the canonical neuronal activity-inducible gene *Fos*. Not only do our data show that enhancer histone acetylation is sufficient to increase the expression and function of Fos in neurons, they also offer mechanistic insight into how this enhancer modification changes the dynamics of activity-inducible gene transcription.

At the level of a single gene allele, transcription is a probabilistic process driven by the biophysics of interactions between DNA and the transcriptional machinery. One important consequence of this biology is that most if not all genes are transcribed in a pulsatile fashion,

called bursts, with variable periods of transcriptional inactivity followed by typically short periods when RNA is actively transcribed. Prior single-cell studies of steroid- and serum-inducible genes have indicated that the increases in RNA expression that follow cellular stimulation arise due to an increase in the frequency of bursts (Larson et al., 2013; Senecal et al., 2014). Our single-neuron smFISH data for *Fos* and *Npas4* (Gómez-Schiavon et al., 2017) are well fit by similar bursting model in which membrane depolarization decreases the time until a given promoter transitions to the ON state, which would result in more frequent bursts (**Fig. 48B**). This model matches well with the known molecular mechanisms used by calcium-dependent intracellular signal pathways to turn on gene expression, in which the phosphorylation of transcription factors enhances recruitment of the transcriptional machinery to activity-inducible gene promoters, mediating their activation (Lyons and West, 2011). Importantly, although the time scale (order of minutes) of the stimulus we used in this study was commensurate with the burst kinetics we observed, it would be valuable in the future to examine activity-dependent gene induction over a continuous time course following temporally complex patterned stimuli like those known to induce synaptic plasticity, since differences in the induction of neuronal activity-regulated genes have been linked to distinct patterns of upstream stimuli (Lee et al., 2017). Engineered RNA tags are beginning to be used to image RNA expression and localization in single living neurons (Park et al., 2014), and the application of these methods to study the impact of synaptic activity patterns on the kinetics of transcriptional bursting will allow us to more precisely define the input-output relationship between neuronal activity and the transcriptional induction of plasticity genes.

Enhancers are functionally defined regions of the genome that promote the expression of a given gene. Enhancers serve as binding sites for transcription factors, and as such they regulate gene promoters by increasing the local likelihood of the intermolecular interactions that underlie the formation of active transcriptional regulatory complexes (Levine et al., 2014). However modified histones can also serve as docking sites for transcriptional regulatory proteins,

suggesting a potential causative mechanism by which these chromatin marks can impact transcriptional processes (Andrews et al., 2016). The challenge for testing the functional importance of protein interactions with histones has been finding a way to isolate the modification of histones at regulatory elements independent of the changes in transcription factor binding and/or activation that normally accompany the induction of these modifications. Here we achieve that goal by using CRISPR-dCas9 to engineer increased histone acetylation at *Fos* enhancers. In the context of neuronal activity-induced *Fos* transcription, our model suggests that enhancer histone acetylation increases burst duration by inhibiting the transition of active promoters to the OFF state (**Fig. 48B**). Although the precise transcriptional mechanisms that are associated with the ON and OFF promoter states in our neurons are not known, these data on promoter state kinetics are compatible with a primary effect of enhancer acetylation on transcriptional elongation. Specifically, paused PolII has been shown to inhibit new transcriptional initiation at genes (Shao and Zeitlinger, 2017), and transcriptional bursts are characterized by the rapid successive initiation of multiple PolII complexes at gene promoters (Larson et al., 2011). If these two processes are in dynamic equilibrium, then relief of pausing could favor additional rounds of initiation, lengthening the duration of transcriptional bursts as we observe.

Finally our data show that enhancer chromatin modifications play a role in fine-tuning the dynamic features of stimulus-inducible *Fos* transcription. These effects are modulatory and indeed they are of a smaller magnitude than the transcription changes induced by membrane depolarization (**Fig. 47B**). Nonetheless, we show that the changes in *Fos* expression induced by enhancer histone acetylation alone are sufficient to shift neuronal membrane potential (**Fig. 50D**), revealing a mechanism by which chromatin regulation could impact neuroplasticity. Consistent with this possibility, small molecule inhibition of Brd4 binding in neurons with the drug JQ1 has been shown both to blunt stimulus-dependent induction of genes including *Fos* and to impair behavioral performance in memory tasks (Korb et al., 2015). Might the variance in *Fos* induction

between neurons have a functional role in enabling aspects of neuronal plasticity? Here we have used a relatively robust stimulus that is capable of inducing *Fos* in the majority of cells in our culture. However *in vivo* most physiologically relevant stimuli (e.g. sensory stimulation, novel environment/object exploration, task learning) are associated with sparse induction of activity-inducible genes within activated brain regions (Barth et al., 2004; Guzowski et al., 2006; Wang et al., 2006). Forcing some cells to have more or less activity-inducible transcription, for example by manipulating CREB function, can influence the probability that specific neurons are brought into a memory trace (Han et al., 2007), and *in vivo* imaging studies of the activity-inducible gene *Arc* have shown that the neurons making the most *Arc* during the early stages of a learning task are the ones most likely to be recruited to the ensemble that mediates the expression of the memory (Cao et al., 2015). If enhancer histone acetylation were to be present in some neurons and not others, this could contribute to the kind of differences in activity-inducible gene expression that drive the formation of these neuronal ensembles. The challenge for fully addressing this hypothesis is advancing methods for the single-neuron analysis of histone modifications. A few innovative studies using high-resolution imaging have managed to see H3K27ac at single genes either in live or fixed cells (Khan et al., 2017; Stasevich et al., 2014) and single cell ChIP for histone marks has been reported (Rotem et al., 2015) though these biochemical methods remain highly inefficient at the single cell level. Importantly, strategies are just beginning to emerge that will allow the application of CRISPR to manipulate chromatin state *in vivo* (Liu et al., 2016) and these will present an exciting opportunity to carry the findings revealed here to a circuit level of analysis.

5. Conclusion and Discussion

The timing and magnitude of transcriptional response following neuronal activity must be precisely regulated to form proper neuronal connections. For example, transgenic mice which overexpressing BDNF in the forebrain show an accelerated maturation of cortical inhibition (Huang et al., 1999). In my dissertation research, I have identified and characterized several novel mechanisms of specificity in neuronal activity-regulated transcription. In Chapter 2, I show that transcription factor, CaRF limits NMDARs dependent gene transcription in the developing brain via a developmental regulated NMDAR subunit, GluN3A. Following this work, in Chapter 3, I find that GluN3A inhibits both NMDAR-induced nuclear translocation of the p38 MAP kinase and activation of the transcription factor MEF2C. These two works reveal a novel mechanism that confers the temporal specificity on the transcription of activity-regulated genes in the developing brain. In Chapter 4, I reveal the causative relationship between enhancer histone acetylation and neuronal activity-regulated gene transcription via the combination of CRISPR mediated epigenome editing and single cell analysis. In this chapter, I will further discuss my findings regarding the significance and future directions that could be pursued.

5.1 CaRF: a context-specific regulator of *Bdnf* transcription and GABAergic synapse formation

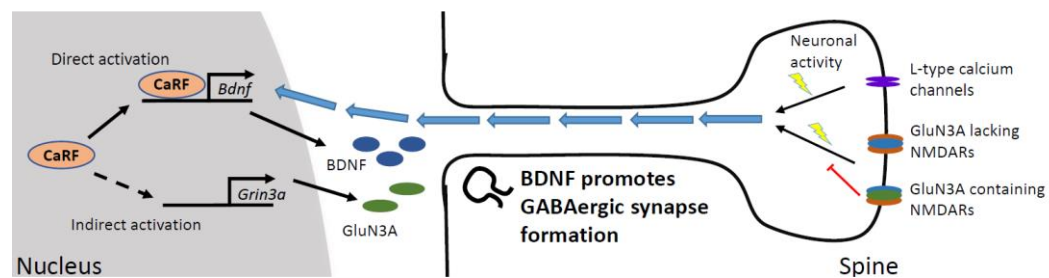


Figure 51: Calcium-response factor (CaRF) binds to *Bdnf* IV promoter and activates basal *Bdnf* transcription. It also inhibits activity-dependent *Bdnf* transcription via indirect activation of *Grin3a* expression, which encodes the NMDA receptor (NMDAR) subunit GluN3A. GluN3A inhibits NMDAR-induced *Bdnf* transcription without impairing the ability of L-type voltage-gated calcium channels to activate *Bdnf* transcription.

Calcium-response factor (CaRF) was initially discovered as a transcriptional activator of *Brain-Derived Neurotrophic Factor (Bdnf)*, which it directly induces by binding to a 10-bp

calcium response element (CaRE1) in the proximal region of *Bdnf* promoter IV (McDowell et al., 2010; Tao et al., 2002) (**Fig. 51**). Expression of exon IV-containing forms of *Bdnf* is significantly reduced in the cortex of CaRF-knockout mice, demonstrating that CaRF contributes to transcriptional activation of *Bdnf* promoter IV in vivo (McDowell et al., 2010). Surprisingly, although the CaRE1 element is required for transcriptional induction of *Bdnf* upon membrane depolarization, and the transcriptional activity of CaRF is induced by the subsequent calcium influx, CaRF is not required for the induction of *Bdnf* transcription that is driven by this stimulus (McDowell et al., 2010; Tao et al., 2002). Instead, membrane depolarization-mediated activation of *Bdnf* promoter IV requires the transcription factor MEF2C, which binds CaRE1 independently of CaRF and acts together with CREB to drive the calcium-inducible component of *Bdnf* transcription (Hong et al., 2008; Lyons et al., 2012).

Following up previous works in the lab, in Chapter 2, we found that CaRF inhibits the induction of *Bdnf* promoter IV following activation of NMDA-type glutamate receptors. Membrane depolarization promotes the activation of *Bdnf* transcription via the opening of L-type voltage-gated calcium channels (Tao et al., 1998). By contrast, treatment of neurons with the sodium channel inhibitor tetrodotoxin (TTX) silences action potentials and induces homeostatic synaptic plasticity such that upon TTX withdrawal there is rebound excitation, release of synaptic glutamate, activation of synaptic glutamate receptors, and the NMDA receptor (NMDAR)-dependent induction of transcription from genes including *Bdnf* promoter IV (Ghiretti et al., 2014; Turrigiano and Nelson, 2004). We show that after TTX withdrawal-induced activation of NMDARs, neurons lacking CaRF show significantly higher induction of exon IV-containing forms of *Bdnf* mRNA and BDNF protein compared with CaRF-expressing control neurons (**Fig. 9**). Unlike the direct activation of *Bdnf* transcription by CaRF, which requires binding of CaRF to *Bdnf* promoter IV, the CaRF-dependent inhibition of *Bdnf* transcription is proposed to occur through an indirect mechanism that involves CaRF-dependent induction of the unusual NMDAR subunit GluN3A. Incorporation of GluN3A into functional NMDARs with GluN1 and GluN2

subunits reduces receptor currents, including the influx of calcium (Das et al., 1998; Kehoe et al., 2013). Levels of GluN3A are reduced in the brains of CaRF-knockout mice, and restoration of GluN3A expression in CaRF-knockdown neurons restores *Bdnf* inducibility to wild-type levels (**Fig. 12B**). Thus although CaRF is a direct activator of basal *Bdnf* transcription via its binding to *Bdnf* promoter elements, it acts as an indirect inhibitor of NMDAR inducible *Bdnf* transcription by its ability to modulate the subunit composition of neuronal NMDARs (**Fig. 51**).

The link between CaRF and GluN3A is important because it suggests a potential mechanism by which CaRF could regulate the timing of synapse development. Both CaRF and GluN3A are most highly expressed during the first two postnatal weeks of brain development, after which time their expression declines (McDowell et al., 2010; Sucher et al., 1995). This decline parallels the onset of the critical period for sensory-dependent synapse development in the cortex, and, notably, prolonging the expression of GluN3A inhibits critical period maturation of synapses in visual cortex, suggesting an essential function for the changing NMDAR composition in this process (Roberts et al., 2009). BDNF expression is strongly induced in sensory cortex during the critical period, and it drives critical period closure by promoting the formation of inhibitory GABAergic synapses (Huang et al., 1999). Consistent with a role for CaRF-dependent repression of NMDAR-inducible *Bdnf* expression in the regulation of GABAergic synapse development in vivo, adult CaRF-knockout mice show substantially increased synaptic expression of GABAergic synapse markers (McDowell et al., 2010). This appears to be a cell-autonomous effect of CaRF, because we found that single-cell knockdown of CaRF in cultured mouse hippocampal neurons significantly enhances the formation of GABAergic synapses onto that neuron in a manner that can be rescued by simultaneous knockdown of BDNF (**Fig. 20**). Taken together, these data establish CaRF as a novel regulator of the formation of GABAergic synapses in the developing brain and suggest that, via its regulation of GluN3A, it could contribute to the timing of the synaptic changes that underlie critical period closure.

5.2 Single cell analysis of neuronal activity-regulated gene transcription

In recent years, technological advances in imaging methodologies have made it possible to quantify endogenous gene transcription at the single-cell and single-molecule levels, greatly increasing our understanding of transcription dynamics. Fluorescent in situ hybridization (FISH) relies on fluorescently labeled DNA oligos hybridized to RNA in fixed cells. This methodology is capable of detecting single RNAs, allowing one both to count the number of total mRNA in the cell and determine the number of nascent pre-mRNA at the active transcription site. One major advantage of FISH is that, by using multiple primers, one can measure transcripts from multiple endogenous genes at one time (Femino et al., 1998). It also can record the probability distribution of gene expression, which contains a great deal of information about the dynamics of transcription (Raj and van Oudenaarden, 2009). However FISH can only report transcription at a single time point (the time of fixation) in any given cell. Much more temporal information can be derived from live imaging studies such as those using the MS2 system. The MS2 protein is a bacteriophage capsid protein that binds a specific RNA stem-loop structure with high affinity. The MS2 system has been co-opted for imaging RNA in living cells (Bertrand et al., 1998). This system contains two parts: 1) a reporter gene that contains a DNA cassette coding for multimerized RNA stem loops (typically 24 stem loops) and 2) the constitutively expressed MS2 capsid protein tagged with a fluorescent protein. When the reporter gene stem loop region is transcribed, the capsid protein binds the RNA with high affinity, resulting in an active transcription site that appears as a bright fluorescent spot above the background. The advantage of this system is that pre-mRNA synthesis dynamics can be directly observed at the single-gene, single-RNA level. The limitations of MS2 system are that the long preparation time for knocking MS2 sequence into the targeting region in genome and one can only measure one or two genes in few cells at one time.

Single-cell imaging in both living and fixed cells has revealed two major principles of gene expression: 1) many interactions between upstream regulatory molecules and chromatin are

transient (on the order of seconds) (Darzacq et al., 2009) and 2) downstream gene expression products display considerable variation from cell to cell (Raj and van Oudenaarden, 2008). Furthermore, the dynamics of transcription have been observed to fall into two classes: either 1) a continuous transcription, in which transcription events occur randomly over time but with a constant probability or 2) bursting, in which the expression of individual genes is highly variable and transcription is irregular with strong variable duration periods of activity interspersed by variable duration periods of inactivity (Zenklusen et al., 2008). For example, in yeast, housekeeping genes display a robust, constitutive expression, whereas cell-cycle-regulated and stress-response genes display much higher variability, consistent with bursting (Zenklusen et al., 2008). The two-state model of gene expression derived from these data offers a unified description of transcription dynamics. In this model, a gene randomly switches between periods in which it is permissive for transcription ('on') and periods of inactivity ('off'). When the gene is 'on', transcription events fire randomly over time. This model is attractive because it captures a vast range of transcriptional dynamics within a single mathematical framework: 'bursty' transcription corresponds to infrequent transitions to the permissive state, but the permissive gene initiates transcription at a high frequency; on the other hand, continuous expression can also be described within the same scheme such that the gene is continuously 'on' with very infrequent transitions to the 'off' state. The two-state model has now been broadly used to classify gene expression, resulting in descriptions where the frequency varies, the burst size varies, both vary, or the transcription rate varies (Larson, 2011). These studies have increased our mechanistic understanding of the transcriptional machinery. For example, the origin of bursting transcription has been suggested to come from chromatin remodeling, weak interactions between the initiation complex and promoter, or DNA topology, depending on the organism and gene of study.

What might similar single cell kinetic analyses reveal about neuronal IEG expression, in which genes are primed but not on until driven by a very rapid upstream stimulus? Previous studies of inducible transcription have yielded different results in different systems. For example,

bacteria have been shown to increase the frequency (Locke et al., 2011) or the total number of transcription pulses (Friedman et al., 2005) in response to increased extracellular signaling, suggesting that transcription is directly graded with inducer concentration. By contrast, in *Dictyostelium*, a cAMP-responsive gene showed remarkable stability in bursting kinetics over a range of doses. A 1000-fold range of cAMP caused an increase in the number of cells responding, but no change in pulse length, intensity or frequency, indicating that the transcription is an all-or-none response which occurs only above a threshold inducer concentration and once transcription turns on, the transcription machinery works at full speed (Stevense et al., 2010). Recent studies of stimulus-inducible genes in mammalian cells show that the induction of RNA expression following cellular stimulation arise due to an increase in the frequency of bursts (Larson et al., 2013; Senecal et al., 2014). While RNA tagging by MS2 based method has been applied in neurons (Buxbaum et al., 2015; Park et al., 2014), it is a relative low throughput method, compared to smFISH, making it is harder to use.

We developed BayFish, a computational pipeline, that allows us to estimate the kinetic parameters of promoter state transitions for any given gene from smFISH data gathered over a time course following stimulus (Gómez-Schiavon et al., 2017) and applied it to infer parameters for multiple gene regulation models from our smFISH data. Consistent with previous findings, our single cell analysis in neuronal activity-induced *Fos* transcription indicates that membrane depolarization drives *Fos* expression mainly by increasing the frequency of bursts (**Fig. 48B**). We investigated the role of enhancer histone acetylation in transcriptional dynamics of neuronal activity gene expression and our BayFish results suggested that histone acetylation at enhancer decreases k_{OFF} meaning that increasing histone acetylation at enhancer prolongs *Fos* promoter in on state once it is activated (**Fig. 48B**). We are the first group to apply single cell analysis in neuronal activity-regulated gene transcription and there are a lot more to explore. Studies in other cell types have suggested that the transcript copy-number distribution is greatly affected by transcriptional parameters. For example, even with the same average number of transcripts, the

transcription systems with long On and Off periods show bimodal distributions of transcript whereas systems with short Off periods show continuous production and more graded unimodal distributions. (Munsky et al., 2012). Given that many of neuronal activity-regulated genes encode protein products that important for synapse functions and formation (West and Greenberg, 2011), distinct expression patterns in a population of neurons could lead to different configuration of neuronal networks. The work in Chapter 4 provides a good platform to investigate the source of variability in neuronal activity-regulated gene transcription. In the future, by studying the role of each biochemical steps within transcriptional machinery, such as eRNA production and promoter-enhancer looping, in transcriptional dynamics, will increase our understanding of how neurons control and use transcriptional variability to form proper neuronal connection.

5.3 Epigenome editing in neuronal activity-regulated gene transcription

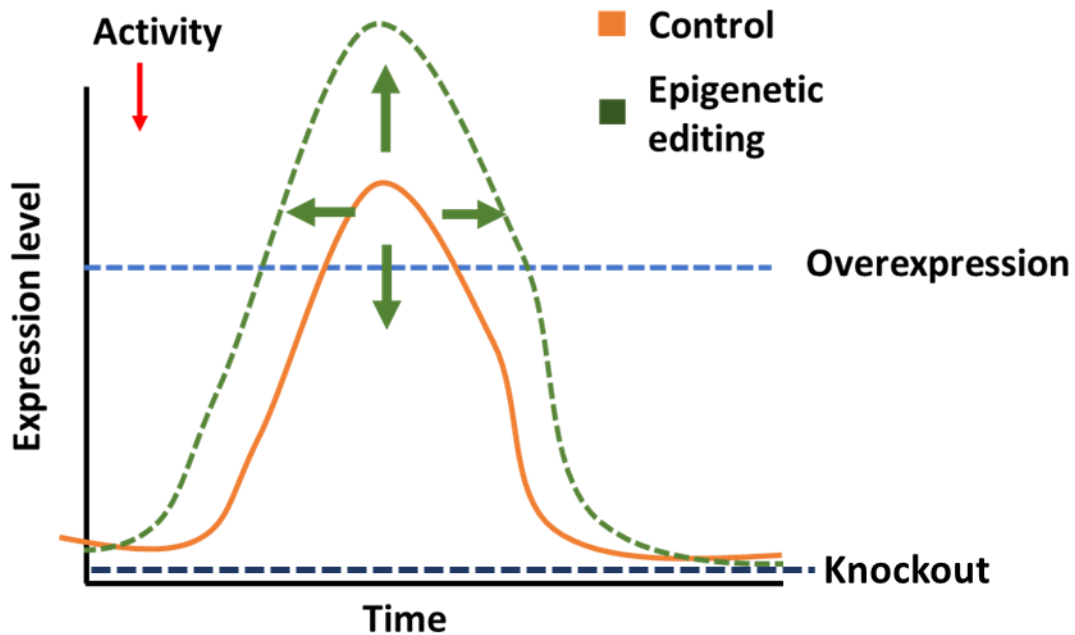


Figure 52: Diagram of control activity-regulated gene transcription by epigenetic editing

Epigenetic marks at chromatin have been long known that regulate gene transcription. In Chapter 4, using CRISPR mediated epigenome editing, we induce histone acetylation at endogenous *Fos* enhancers. Increasing enhancer histone acetylation not only enhances the

expression of *Fos* but also effects the temporal dynamics of neuronal activity-induced *Fos* transcription (**Fig. 47B**). This result suggests that by manipulating chromatin state at neuronal activity-regulated enhancers, we could potentially control the timing and magnitude of neuronal activity-regulated gene transcription (**Fig. 52**). Compared to overexpression of activity-regulated genes, which lead to a constantly expression in the certain level, manipulating chromatin state at enhancers could enhance or repress gene transcription in a neuronal activity-regulated manner. This ability to preserve the neuronal activity-dependent component in transcription can largely reduce the side effects that drive from the high expression level without neuronal activity. It is also different than enhance neuronal activity-regulated gene transcription by reducing intrinsic excitability such as overexpression CREB (Benito and Barco, 2010). While reducing intrinsic excitability could lead to a higher expression level following neuronal activity, it also increases the number of neurons that response to stimuli. Given that neuronal activity-regulated genes are important for synapse plasticity, different in the number of neurons that response to stimuli could lead to a distinct neuronal network configuration. CRISPR mediated epigenome editing provides a feasible but powerful tool to manipulate chromatin state. This neuronal activity dependent enhancement or repression of gene transcription by CRISPR-based method provides a new and better way to help in treating neurological diseases or improving cognitive performance.

Appendix A

Real time primers:

Mouse *Arc* F: 5'- GAGCCTACAGAGCAGGAGA -3'
R: 5'- TGCCTTGAAAGTGTCTTGGA -3'

Mouse *Bdnf* exon I F: 5'- AGTCTCCAGGACAGCAAAGC -3'
R: 5'-GCCTTCATGCAACCGAAGTA -3'

Mouse *Bdnf* exon IV: F: 5'- CGCCATGCAATTTCCACTATCAATAA -3'
R: 5'- GCCTTCATGCAACCGAAGTATG -3'

Mouse *Carf* F: 5'- GCATTGACAAATGGGATTCCGTC -3',
R: 5'- GTTGAAGAACCTTTGCTGGCTC -3'

Mouse/Rat *Carf* F: 5'-TGCCGTCTTAGGAGTTGTGA-3'
R: 5'-CTCGACTTCCTGCATTGACA-3'

Mouse *cFos* F: 5'- TTTATCCCCACGGTGACAGC -3'
R: 5'- CTGCTCTACTTTGCCCTTCT -3'

Mouse *Gapdh* F: 5'- CATGGCCTTCCGTGTTCT -3
R: 5'- TGATGTCATCATACTTGGCAGGTT-3'

Mouse *Grin1* F: 5'- GCTCAGAAACCCCTCAGACA -3'
R: 5'- GGCATCCTTGTGTCGCTTGTAG -3'

Mouse *Grin2a* F: 5'- TACTCCAGCGCTGAACATTG -3'
R: 5'- TCAGCTGGACCTGTGTCTTG -3'

Mouse *Grin2b* F: 5'- GAGCATAATCACCCGCATCT -3'
R: 5'- AAGGCACCGTGTCCGTATCC -3'

Mouse *Grin2c* F: 5'- GCAGAACTTCCTGGACTTGC -3'
R: 5'- CTCTTCACGGGAGCAGTAGG -3'

Mouse *Grin2d* F: 5'- TTTTGAGGTGCTGGAGGAGT -3'
R: 5'- GTCTCGGTTATCCCAGGTGA -3';

Mouse *Grin3a* F: 5'- AAAGCCATTTGCCATTGAAG -3'
R: 5'- GAATCCTATGCACAGCAGCA -3'

Mouse *Grin3b* F: 5'- CTACATCAAGGCGAGCTTCC -3'
R: 5'- AGCTTGCAGTCCGCATCTAT -3'

Mouse *Npas4* F: 5'-GCTATACTCAGAAGGTCCAGAAGGC-3'
R: 5'-TCAGAGAATGAGGGTAGCACAGC-3'

firefly luciferase F: 5'-GAGGTGAACATCACGTACGCG-3'
F: 5'-GAGGTGGACATCACTTACGCT-3'
R: 5'-AAGAGAGTTTTCACTGCATACGACG-3'

renilla luciferase F: 5'-GAAACTTCTTGGCACCTTCAACA-3'
R: 5'-GCTTATCTACGTGCAAGTGATGATTT-3'

ChIP primer:

Fos Promoter F 5'-CAAGACGGGGGTTGAAAGCC-3'
R 5'-TCACTGCTCGTTCCGCGGAAC-3'

Fos 3'UTR F 5'-TGACACCTGAGAGCTGGTAGTTAG-3'
R 5'-ATCAGCTGCACTAGATACAATCCA-3'

Fos Enh1 F 5'-TAAAGCCTATTGCCGTGACCTG-3'

R 5'-TCTTCCCTTACAATGCCCTTACC-3'
Fos Enh2 F 5'-GTCTACTGTCTGAGGAGAAGTGGTTAG-3'
R 5'-AGAACAGATTCTGGAACAGTGTCTAC-3'
Fos Enh4 F 5'-GGCCTAAATCCCACCAACATAAA-3'
R 5'-GAGGGCAGGGAGGCGGGGATTC-3'.

Appendix B

gRNA sequence:

Fos enh1 gRNA1 CATAACACACACGGCTCCGTC
Fos enh1 gRNA2 GCAATGCAGGTCACGGCAAT
Fos enh1 gRNA3 CTTGACTATACTATCCGGTA
Fos enh2 gRNA1 GGAACAGTGTCTACCGCCCC
Fos enh2 gRNA2 ACGTCTATGCGTTTTAGCCA
Fos enh2 gRNA3 AGATCTTGGAGGCTGCGGTC
Fos enh2 gRNA4 GTGCTACCCCCTGCAGGATC
Fos enh2 gRNA5 TACGCCGGCTAGAAGAAATC
Fos enh3 gRNA1 CGGGCGTGGGATTCTGCCGC
Fos enh3 gRNA2 CTTGCACTAATTAGTCGCGG
Fos enh3 gRNA3 GCCCAACACAGGGTCTTAGT
Fos enh4 gRNA1 TCCACTCATAACTGCGTCTC
Fos enh4 gRNA2 AGGCGGGGATTCGTGGAAAT
Fos enh4 gRNA3 CGAGGGTGATGTCAGTCGGC
Fos enh5 gRNA1 CTGTTCCCGGTGGACGATCC
Fos enh5 gRNA2 TGATTAATAATCGCGCGGCA
Fos enh5 gRNA3 TTGCGGGATCGGACTTATGA
Fos promoter gRNA1 TCCGAAATCCTACACGCGGA
Fos promoter gRNA2 GGATGGACTTCCTACGTCAC
Fos promoter gRNA3 GGGTTTCAACGCCGACTACG.

Reference

- Abrahams, B.S., and Geschwind, D.H. (2008). Advances in autism genetics: on the threshold of a new neurobiology. *Nat Rev Genet* 9, 341–355.
- Agostino, P. V, Cheng, R.-K., Williams, C.L., West, A.E., and Meck, W.H. (2013). Acquisition of response thresholds for timed performance is regulated by a calcium-responsive transcription factor, CaRF. *Genes. Brain. Behav.* 12, 633–644.
- Aizawa, H. (2004). Dendrite Development Regulated by CREST, a Calcium-Regulated Transcriptional Activator. *Science* (80-.). 303, 197–202.
- Al-Hallaq, R.A., Jarabek, B.R., Fu, Z., Vicini, S., Wolfe, B.B., and Yasuda, R.P. (2002). Association of NR3A with the N-methyl-D-aspartate receptor NR1 and NR2 subunits. *Mol. Pharmacol.* 62, 1119–1127.
- Andrews, F.H., Strahl, B.D., and Kutateladze, T.G. (2016). Insights into newly discovered marks and readers of epigenetic information. *Nat Chem Biol* 12, 662–668.
- Bading, H. (2013). Nuclear calcium signalling in the regulation of brain function. *Nat. Rev. Neurosci.* 14, 593–608.
- Bading, H., Ginty, D.D., and Greenberg, M.E. (1993). Regulation of gene expression in hippocampal neurons by distinct calcium signaling pathways. *Science* 260, 181–186.
- Balkowiec, a, and Katz, D.M. (2000). Activity-dependent release of endogenous brain-derived neurotrophic factor from primary sensory neurons detected by ELISA in situ. *J. Neurosci.* 20, 7417–7423.
- Banerji, J., Rusconi, S., and Schaffner, W. (1981). Expression of a beta-globin gene is enhanced by remote SV40 DNA sequences. *Cell* 27, 299–308.
- Barbosa, A.C., Kim, M.S., Ertunc, M., Adachi, M., Nelson, E.D., McAnally, J., Richardson, J.A., Kavalali, E.T., Monteggia, L.M., Bassel-Duby, R., et al. (2008). MEF2C, a transcription factor that facilitates learning and memory by negative regulation of synapse numbers and function. *Proc Natl Acad Sci U S A* 105, 9391–9396.
- Bargmann, C.I., and Marder, E. (2013). From the connectome to brain function. *Nat. Methods* 10, 483–490.
- Barrangou, R., Fremaux, C., Deveau, H., Richards, M., Boyaval, P., Moineau, S., Romero, D.A., and Horvath, P. (2007). CRISPR Provides Acquired Resistance Against Viruses in Prokaryotes. *Science* (80-.). 315, 1709–1712.
- Barth, A.L., Gerkin, R.C., and Dean, K.L. (2004). Alteration of Neuronal Firing Properties after. *Corpus* 24, 6466–6475.
- Bassell, G.J., and Warren, S.T. (2008). Fragile X syndrome: loss of local mRNA regulation alters synaptic development and function. *Neuron* 60, 201–214.
- Ben-Levy, R., Hooper, S., Wilson, R., Paterson, H.F., and Marshall, C.J. (1998). Nuclear export of the stress-activated protein kinase p38 mediated by its substrate MAPKAP kinase-2. *Curr. Biol.* 8, 1049–1057.
- Benito, E., and Barco, A. (2010). CREB's control of intrinsic and synaptic plasticity: implications for CREB-dependent memory models. *Trends Neurosci.* 33, 230–240.
- Bertrand, E., Chartrand, P., Schaefer, M., Shenoy, S.M., Singer, R.H., and Long, R.M. (1998). Localization of ASH1 mRNA particles in living yeast. *Mol. Cell* 2, 437–445.

- Bhatt, D.M., Pandya-Jones, A., Tong, A.J., Barozzi, I., Lissner, M.M., Natoli, G., Black, D.L., and Smale, S.T. (2012). Transcript dynamics of proinflammatory genes revealed by sequence analysis of subcellular RNA fractions. *Cell* 150, 279–290.
- Bito, H., Deisseroth, K., and Tsien, R.W. (1996). CREB phosphorylation and dephosphorylation: a Ca(2+)- and stimulus duration-dependent switch for hippocampal gene expression. *Cell* 87, 1203–1214.
- Bito, H., Deisseroth, K., and Tsien, R.W. (1997). Calcium-dependent regulation in neuronal gene expression. *Curr. Opin. Neurobiol.* 7, 419–429.
- Bloodgood, B.L., Sharma, N., Browne, H.A., Trepman, A.Z., and Greenberg, M.E. (2013). The activity-dependent transcription factor NPAS4 regulates domain-specific inhibition. *Nature* 503, 121–125.
- Blow, M.J., McCulley, D.J., Li, Z., Zhang, T., Akiyama, J.A., Holt, A., Plajzer-Frick, I., Shoukry, M., Wright, C., Chen, F., et al. (2010). CHIP-Seq identification of weakly conserved heart enhancers. *Nat Genet* 42, 806–810.
- Boch, J., Scholze, H., Schornack, S., Landgraf, A., Hahn, S., Kay, S., Lahaye, T., Nickstadt, A., and Bonas, U. (2009). Breaking the Code of DNA Binding Specificity of TAL-Type III Effectors. *Science* (80-.). 326, 1509–1512.
- Brunet, A., Park, J., Tran, H., Hu, L.S., Hemmings, B.A., and Greenberg, M.E. (2001). Protein kinase SGK mediates survival signals by phosphorylating the forkhead transcription factor FKHL1 (FOXO3a). *Mol Cell Biol* 21, 952–965.
- Buxbaum, A.R., Yoon, Y.J., Singer, R.H., and Park, H.Y. (2015). Single-molecule insights into mRNA dynamics in neurons. *Trends Cell Biol.* 1–8.
- Cao, V.Y., Ye, Y., Mastwal, S., Ren, M., Coon, M., Liu, Q., Costa, R.M., and Wang, K.H. (2015). Motor Learning Consolidates Arc-Expressing Neuronal Ensembles in Secondary Motor Cortex. *Neuron* 86, 1385–1392.
- Castrén, E., Zafra, F., Thoenen, H., and Lindholm, D. (1992). Light regulates expression of brain-derived neurotrophic factor mRNA in rat visual cortex. *Proc. Natl. Acad. Sci. U. S. A.* 89, 9444–9448.
- Chan, S.F., and Sucher, N.J. (2001). An NMDA receptor signaling complex with protein phosphatase 2A. *J. Neurosci.* 21, 7985–7992.
- Chen, Z.-Y., Jing, D., Bath, K.G., Ieraci, A., Khan, T., Siao, C.-J., Herrera, D.G., Toth, M., Yang, C., McEwen, B.S., et al. (2006). Genetic variant BDNF (Val66Met) polymorphism alters anxiety-related behavior. *Science* 314, 140–143.
- Cholewa-Waclaw, J., Bird, A., von Schimmelmann, M., Schaefer, A., Yu, H., Song, H., Madabhushi, R., and Tsai, L.-H. (2016). The Role of Epigenetic Mechanisms in the Regulation of Gene Expression in the Nervous System. *J. Neurosci.* 36.
- Chrivia, J.C., Kwok, R.P., Lamb, N., Hagiwara, M., Montminy, M.R., and Goodman, R.H. (1993). Phosphorylated CREB binds specifically to the nuclear protein CBP. *Nature* 365, 855–859.
- Ciabarra, A.M., Sullivan, J.M., Gahn, L.G., Pecht, G., Heinemann, S., and Sevarino, K.A. (1995). Cloning and characterization of chi-1: a developmentally regulated member of a novel class of the ionotropic glutamate receptor family. *J. Neurosci.* 15, 6498–6508.
- Clapham, D.E. (2007). Calcium signaling. *Cell* 131, 1047–1058.

- Cong, L., Ran, F.A., Cox, D., Lin, S., Barretto, R., Habib, N., Hsu, P.D., Wu, X., Jiang, W., Marraffini, L.A., et al. (2013). Multiplex Genome Engineering Using CRISPR/Cas Systems. *Science* (80-.). 339, 819–823.
- Cosma, M.P., Tanaka, T., and Nasmyth, K. (1999). Ordered recruitment of transcription and chromatin remodeling factors to a cell cycle- and developmentally regulated promoter. *Cell* 97, 299–311.
- Cull-Candy, S.G., and Leszkiewicz, D.N. (2004). Role of distinct NMDA receptor subtypes at central synapses. *Sci. STKE* 2004, re16.
- Darzacq, X., Yao, J., Larson, D.R., Causse, S.Z., Bosanac, L., de Turris, V., Ruda, V.M., Lionnet, T., Zenklusen, D., Guglielmi, B., et al. (2009). Imaging transcription in living cells. *Annu. Rev. Biophys.* 38, 173–196.
- Das, S., Sasaki, Y.F., Rothe, T., Premkumar, L.S., Takasu, M., Crandall, J.E., Dikkes, P., Conner, D.A., Rayudu, P. V, Cheung, W., et al. (1998). Increased NMDA current and spine density in mice lacking the NMDA receptor subunit NR3A. *Nature* 393, 377–381.
- Day, J.J., and Sweatt, J.D. (2011). Epigenetic mechanisms in cognition. *Neuron* 70, 813–829.
- DeFelipe, J. (2010). From the connectome to the synaptome: an epic love story. *Science* 330, 1198–1201.
- Dietrich, J.-B. (2013). The MEF2 family and the brain: from molecules to memory. *Cell Tissue Res.* 352, 179–190.
- Dingledine, R., Borges, K., Bowie, D., and Traynelis, S.F. (1999). The glutamate receptor ion channels. *Pharmacol. Rev.* 51, 7–61.
- Dolmetsch, R.E., Pajvani, U., Fife, K., Spotts, J.M., and Greenberg, M.E. (2001). Signaling to the nucleus by an L-type calcium channel-calmodulin complex through the MAP kinase pathway. *Science* 294, 333–339.
- Dorigi, K.M., Swigut, T., Henriques, T., Bhanu, N. V, Scruggs, B.S., Nady, N., Still 2nd, C.D., Garcia, B.A., Adelman, K., and Wysocka, J. (2017). Mll3 and Mll4 Facilitate Enhancer RNA Synthesis and Transcription from Promoters Independently of H3K4 Monomethylation. *Mol Cell* 66, 568–576 e4.
- Femino, A.M., Fay, F.S., Fogarty, K., and Singer, R.H. (1998). Visualization of single RNA transcripts in situ. *Science* 280, 585–590.
- Fiuza, M., González-González, I., and Pérez-Otaño, I. (2013). GluN3A expression restricts spine maturation via inhibition of GIT1/Rac1 signaling. *Proc. Natl. Acad. Sci. U. S. A.* 110, 20807–20812.
- Flavell, S.W., Cowan, C.W., Kim, T.-K., Greer, P.L., Lin, Y., Paradis, S., Griffith, E.C., Hu, L.S., Chen, C., and Greenberg, M.E. (2006). Activity-dependent regulation of MEF2 transcription factors suppresses excitatory synapse number. *Science* 311, 1008–1012.
- Freund, T.F., and Buzsáki, G. (1996). Interneurons of the hippocampus. *Hippocampus* 6, 347–470.
- Friedman, N., Vardi, S., Ronen, M., Alon, U., and Stavans, J. (2005). Precise temporal modulation in the response of the SOS DNA repair network in individual bacteria. *PLoS Biol.* 3, e238.
- Ge, B., Gram, H., Di Padova, F., Huang, B., New, L., Ulevitch, R.J., Luo, Y., and Han, J. (2002). MAPKK-independent activation of p38alpha mediated by TAB1-dependent autophosphorylation

of p38alpha. *Science* 295, 1291–1294.

Genoud, C., Knott, G.W., Sakata, K., Lu, B., and Welker, E. (2004). Altered synapse formation in the adult somatosensory cortex of brain-derived neurotrophic factor heterozygote mice. *J. Neurosci.* 24, 2394–2400.

Gersbach, C.A. (2014). Genome engineering: the next genomic revolution. *Nat. Methods* 11, 1009–1011.

Ghiretti, A.E., Moore, A.R., Brenner, R.G., Chen, L.-F., West, A.E., Lau, N.C., Van Hooser, S.D., and Paradis, S. (2014). Rem2 is an activity-dependent negative regulator of dendritic complexity in vivo. *J. Neurosci.* 34, 392–407.

Ghosh, A., Carnahan, J., and Greenberg, M.E. (1994). Requirement for BDNF in activity-dependent survival of cortical neurons. *Science* 263, 1618–1623.

Gilbert, L.A., Larson, M.H., Morsut, L., Liu, Z., Brar, G.A., Torres, S.E., Stern-Ginossar, N., Brandman, O., Whitehead, E.H., Doudna, J.A., et al. (2013). CRISPR-mediated modular RNA-guided regulation of transcription in eukaryotes. *Cell* 154, 442–451.

Ginty, D.D. (1997). Calcium regulation of gene expression: isn't that spatial? *Neuron* 18, 183–186.

Gomez-Ospina, N., Tsuruta, F., Barreto-Chang, O., Hu, L., and Dolmetsch, R. (2006). The C terminus of the L-type voltage-gated calcium channel Ca(V)1.2 encodes a transcription factor. *Cell* 127, 591–606.

Gomez-Ospina, N., Panagiotakos, G., Portmann, T., Pasca, S.P., Rabah, D., Budzillo, A., Kinet, J.P., and Dolmetsch, R.E. (2013). A promoter in the coding region of the calcium channel gene CACNA1C generates the transcription factor CCAT. *PLoS One* 8, e60526.

Gómez-Schiavon, M., Chen, L.-F., West, A.E., and Buchler, N.E. (2017). BayFish: Bayesian inference of transcription dynamics from population snapshots of single-molecule RNA FISH in single cells. *Genome Biol.* 18, 164.

Gong, X., Ming, X., Deng, P., and Jiang, Y. (2010). Mechanisms regulating the nuclear translocation of p38 MAP kinase. *J. Cell. Biochem.* 110, 1420–1429.

Gossett, L.A., Kelvin, D.J., Sternberg, E.A., and Olson, E.N. (1989). A new myocyte-specific enhancer-binding factor that recognizes a conserved element associated with multiple muscle-specific genes. *Mol Cell Biol* 9, 5022–5033.

Graff, J., and Tsai, L.H. (2013). Histone acetylation: molecular mnemonics on the chromatin. *Nat Rev Neurosci* 14, 97–111.

Graff, J., Joseph, N.F., Horn, M.E., Samiei, A., Meng, J., Seo, J., Rei, D., Bero, A.W., Phan, T.X., Wagner, F., et al. (2014). Epigenetic priming of memory updating during reconsolidation to attenuate remote fear memories. *Cell* 156, 261–276.

Gräff, J., and Tsai, L.-H. (2013). Histone acetylation: molecular mnemonics on the chromatin. *Nat. Rev. Neurosci.* 14, 97–111.

Gray, J.M., Kim, T.-K., West, A.E., Nord, A.S., Markenscoff-Papadimitriou, E., and Lomvardas, S. (2015). Genomic Views of Transcriptional Enhancers: Essential Determinants of Cellular Identity and Activity-Dependent Responses in the CNS. *J. Neurosci.* 35, 13819–13826.

Greenberg, M.E., Ziff, E.B., and Greene, L.A. (1986). Stimulation of neuronal acetylcholine receptors induces rapid gene transcription. *Science* (80-.). 234, 80–83.

Greer, P.L., and Greenberg, M.E. (2008). From synapse to nucleus: calcium-dependent gene

- transcription in the control of synapse development and function. *Neuron* 59, 846–860.
- Greer, P.L., Hanayama, R., Bloodgood, B.L., Mardinly, A.R., Lipton, D.M., Flavell, S.W., Kim, T.-K., Griffith, E.C., Waldon, Z., Maehr, R., et al. (2010). The Angelman Syndrome protein Ube3A regulates synapse development by ubiquitinating arc. *Cell* 140, 704–716.
- Gu, X., and Spitzer, N.C. (1997). Breaking the Code: Regulation of Neuronal Differentiation by Spontaneous Calcium Transients. *Dev. Neurosci.* 19, 33–41.
- Gu, Y., Huang, S., Chang, M.C., Worley, P., Kirkwood, A., and Quinlan, E.M. (2013). Obligatory role for the immediate early gene NARP in critical period plasticity. *Neuron* 79, 335–346.
- Gu, Y.Z., Hogenesch, J.B., and Bradfield, C.A. (2000). The PAS superfamily: sensors of environmental and developmental signals. *Annu Rev Pharmacol Toxicol* 40, 519–561.
- Guzowski, J.F., Miyashita, T., Chawla, M.K., Sanderson, J., Maes, L.I., Houston, F.P., Lipa, P., McNaughton, B.L., Worley, P.F., and Barnes, C. a (2006). Recent behavioral history modifies coupling between cell activity and Arc gene transcription in hippocampal CA1 neurons. *Proc. Natl. Acad. Sci. U. S. A.* 103, 1077–1082.
- Han, J., Jiang, Y., Li, Z., Kravchenko, V. V, and Ulevitch, R.J. (1997). Activation of the transcription factor MEF2C by the MAP kinase p38 in inflammation. *Nature* 386, 296–299.
- Han, J.H., Kushner, S.A., Yiu, A.P., Cole, C.J., Matynia, A., Brown, R.A., Neve, R.L., Guzowski, J.F., Silva, A.J., and Josselyn, S.A. (2007). Neuronal competition and selection during memory formation. *Science* (80-.). 316, 457–460.
- Hardingham, G.E., and Bading, H. (2010). Synaptic versus extrasynaptic NMDA receptor signalling: implications for neurodegenerative disorders. *Nat. Rev. Neurosci.* 11, 682–696.
- Hardingham, G.E., Chawla, S., Johnson, C.M., and Bading, H. (1997). Distinct functions of nuclear and cytoplasmic calcium in the control of gene expression. *Nature* 385, 260–265.
- Hardingham, G.E., Fukunaga, Y., and Bading, H. (2002). Extrasynaptic NMDARs oppose synaptic NMDARs by triggering CREB shut-off and cell death pathways. *Nat. Neurosci.* 5, 405–414.
- Hargreaves, D.C., and Crabtree, G.R. (2011). ATP-dependent chromatin remodeling: genetics, genomics and mechanisms. *Cell Res.* 21, 396–420.
- Harrington, A.J., Raissi, A., Rajkovich, K., Berto, S., Kumar, J., Molinaro, G., Raduazzo, J., Guo, Y., Loerwald, K., Konopka, G., et al. (2016). MEF2C regulates cortical inhibitory and excitatory synapses and behaviors relevant to neurodevelopmental disorders. *Elife* 5, 1–26.
- Heintzman, N.D., Hon, G.C., Hawkins, R.D., Kheradpour, P., Stark, A., Harp, L.F., Ye, Z., Lee, L.K., Stuart, R.K., Ching, C.W., et al. (2009). Histone modifications at human enhancers reflect global cell-type-specific gene expression. *Nature* 459, 108–112.
- Hensch, T.K. (2005). Critical period mechanisms in developing visual cortex. *Curr. Top. Dev. Biol.* 69, 215–237.
- Henson, M.A., Larsen, R.S., Lawson, S.N., Pérez-Otaño, I., Nakanishi, N., Lipton, S.A., and Philpot, B.D. (2012). Genetic deletion of NR3A accelerates glutamatergic synapse maturation. *PLoS One* 7, e42327.
- Henson, M. a, Roberts, A.C., Pérez-Otaño, I., and Philpot, B.D. (2010). Influence of the NR3A subunit on NMDA receptor functions. *Prog. Neurobiol.* 91, 23–37.
- Hilton, I.B., and Gersbach, C.A. (2015). Enabling functional genomics with genome engineering.

Genome Res. 25, 1442–1455.

Hilton, I.B., Ippolito, A.M.D., Vockley, C.M., Thakore, P.I., Crawford, G.E., Reddy, T.E., and Gersbach, C. a (2015). Epigenome editing by a CRISPR-Cas9-based acetyltransferase activates genes from promoters and enhancers. *Nat. Biotechnol.*

Ho, L., and Crabtree, G.R. (2010). Chromatin remodelling during development. *Nature.*

Hong, E.J., McCord, A.E., and Greenberg, M.E. (2008). A biological function for the neuronal activity-dependent component of Bdnf transcription in the development of cortical inhibition. *Neuron* 60, 610–624.

Hu, G., Cui, K., Northrup, D., Liu, C., Wang, C., Tang, Q., Ge, K., Levens, D., Crane-Robinson, C., and Zhao, K. (2013). H2A.Z facilitates access of active and repressive complexes to chromatin in embryonic stem cell self-renewal and differentiation. *Cell Stem Cell* 12, 180–192.

Hu, J.-H., Park, J.M., Park, S., Xiao, B., Dehoff, M.H., Kim, S., Hayashi, T., Schwarz, M.K., Huganir, R.L., Seeburg, P.H., et al. (2010). Homeostatic scaling requires group I mGluR activation mediated by Homer1a. *Neuron* 68, 1128–1142.

Huang, Z.J., Kirkwood, a, Pizzorusso, T., Porciatti, V., Morales, B., Bear, M.F., Maffei, L., and Tonegawa, S. (1999). BDNF regulates the maturation of inhibition and the critical period of plasticity in mouse visual cortex. *Cell* 98, 739–755.

Ibata, K., Sun, Q., and Turrigiano, G.G. (2008). Rapid Synaptic Scaling Induced by Changes in Postsynaptic Firing. *Neuron* 57, 819–826.

Impey, S., Obrietan, K., Wong, S.T., Poser, S., Yano, S., Wayman, G., Deloulme, J.C., Chan, G., and Storm, D.R. (1998). Cross talk between ERK and PKA is required for Ca²⁺ stimulation of CREB-dependent transcription and ERK nuclear translocation. *Neuron* 21, 869–883.

Jonkers, I., and Lis, J.T. (2015). Getting up to speed with transcription elongation by RNA polymerase II. *Nat. Rev. Mol. Cell Biol.* 16, 167–177.

Joo, J.-Y., Schaukowitch, K., Farbiak, L., Kilaru, G., and Kim, T.-K. (2015). Stimulus-specific combinatorial functionality of neuronal c-fos enhancers. *Nat. Neurosci.* 19.

Joo, J.Y., Schaukowitch, K., Farbiak, L., Kilaru, G., and Kim, T.K. (2016). Stimulus-specific combinatorial functionality of neuronal c-fos enhancers. *Nat Neurosci* 19, 75–83.

Kadoch, C., and Crabtree, G.R. (2015). Mammalian SWI/SNF chromatin remodeling complexes and cancer: Mechanistic insights gained from human genomics. *Sci. Adv.* 1, e1500447.

Karpova, A., Mikhaylova, M., Bera, S., Bär, J., Reddy, P.P., Behnisch, T., Rankovic, V., Spilker, C., Bethge, P., Sahin, J., et al. (2013). Encoding and transducing the synaptic or extrasynaptic origin of NMDA receptor signals to the nucleus. *Cell* 152, 1119–1133.

Katz, L.C., and Shatz, C.J. (1996). Synaptic activity and the construction of cortical circuits. *Science* 274, 1133–1138.

Kawasaki, H., Morooka, T., Shimohama, S., Kimura, J., Hirano, T., Gotoh, Y., and Nishida, E. (1997). Activation and involvement of p38 mitogen-activated protein kinase in glutamate-induced apoptosis in rat cerebellar granule cells. *J. Biol. Chem.* 272, 18518–18521.

Kawashima, T., Okuno, H., Nonaka, M., Adachi-Morishima, A., Kyo, N., Okamura, M., Takemoto-Kimura, S., Worley, P.F., and Bito, H. (2009). Synaptic activity-responsive element in the Arc/Arg3.1 promoter essential for synapse-to-nucleus signaling in activated neurons. *Proc. Natl. Acad. Sci. U. S. A.* 106, 316–321.

Kehoe, L.A., Bellone, C., De Roo, M., Zanduetta, A., Dey, P.N., Pérez-Otaño, I., and Muller, D.

- (2014). GluN3A promotes dendritic spine pruning and destabilization during postnatal development. *J. Neurosci.* *34*, 9213–9221.
- Kehoe, L. a, Bernardinelli, Y., and Muller, D. (2013). GluN3A: an NMDA receptor subunit with exquisite properties and functions. *Neural Plast.* *2013*, 145387.
- Kewley, R.J., Whitelaw, M.L., and Chapman-Smith, A. (2004). The mammalian basic helix-loop-helix/PAS family of transcriptional regulators. *Int J Biochem Cell Biol* *36*, 189–204.
- Khan, D.H., Healy, S., He, S., Lichtensztejn, D., Klewes, L., Sharma, K.L., Lau, V., Mai, S., Delcuve, G.P., and Davie, J.R. (2017). Mitogen-induced distinct epialleles are phosphorylated at either H3S10 or H3S28, depending on H3K27 acetylation. *Mol Biol Cell* *28*, 817–824.
- Kim, T.-K., Hemberg, M., Gray, J.M., Costa, A.M., Bear, D.M., Wu, J., Harmin, D. a, Laptewicz, M., Barbara-Haley, K., Kuersten, S., et al. (2010). Widespread transcription at neuronal activity-regulated enhancers. *Nature* *465*, 182–187.
- Köhr, G. (2006). NMDA receptor function: subunit composition versus spatial distribution. *Cell Tissue Res.* *326*, 439–446.
- Korb, E., and Finkbeiner, S. (2011). Arc in synaptic plasticity: from gene to behavior. *Trends Neurosci* *34*, 591–598.
- Korb, E., Herre, M., Zucker-Scharff, I., Darnell, R.B., and Allis, C.D. (2015). BET protein Brd4 activates transcription in neurons and BET inhibitor Jq1 blocks memory in mice. *Nat Neurosci* *18*, 1464–1473.
- Korte, M., Carroll, P., Wolf, E., Brem, G., Thoenen, H., and Bonhoeffer, T. (1995). Hippocampal long-term potentiation is impaired in mice lacking brain-derived neurotrophic factor. *Proc. Natl. Acad. Sci. U. S. A.* *92*, 8856–8860.
- Kuzniewska, B., Nader, K., Dabrowski, M., Kaczmarek, L., and Kalita, K. (2016). Adult Deletion of SRF Increases Epileptogenesis and Decreases Activity-Induced Gene Expression. *Mol Neurobiol* *53*, 1478–1493.
- Larsen, R.S., Corlew, R.J., Henson, M.A., Roberts, A.C., Mishina, M., Watanabe, M., Lipton, S.A., Nakanishi, N., Pérez-Otaño, I., Weinberg, R.J., et al. (2011). NR3A-containing NMDARs promote neurotransmitter release and spike timing-dependent plasticity. *Nat. Neurosci.* *14*, 338–344.
- Larson, D.R. (2011). What do expression dynamics tell us about the mechanism of transcription? *Curr. Opin. Genet. Dev.* *21*, 591–599.
- Larson, D.R., Zenklusen, D., Wu, B., Chao, J.A., and Singer, R.H. (2011). Real-time observation of transcription initiation and elongation on an endogenous yeast gene. *Science (80-)*. *332*, 475–478.
- Larson, D.R., Fritsch, C., Sun, L., Meng, X., Lawrence, D.S., and Singer, R.H. (2013). Direct observation of frequency modulated transcription in single cells using light activation. *Elife* *2*, e00750.
- Lau, C.G., and Zukin, R.S. (2007). NMDA receptor trafficking in synaptic plasticity and neuropsychiatric disorders. *Nat. Rev. Neurosci.* *8*, 413–426.
- Lee, P.R., Cohen, J.E., Iacobas, D.A., Iacobas, S., and Fields, R.D. (2017). Gene networks activated by specific patterns of action potentials in dorsal root ganglia neurons. *Sci. Rep.* *7*, 43765.
- Leifer, D., Krainc, D., Yu, Y.T., McDermott, J., Breitbart, R.E., Heng, J., Neve, R.L., Kosofsky,

- B., Nadal-Ginard, B., and Lipton, S.A. (1993). MEF2C, a MADS/MEF2-family transcription factor expressed in a laminar distribution in cerebral cortex. *Proc Natl Acad Sci U S A* *90*, 1546–1550.
- Leslie, J.H., and Nedivi, E. (2011). Activity-regulated genes as mediators of neural circuit plasticity. *Prog. Neurobiol.* *94*, 223–237.
- Lessard, J., Wu, J.I., Ranish, J.A., Wan, M., Winslow, M.M., Staahl, B.T., Wu, H., Aebersold, R., Graef, I.A., Crabtree, G.R., et al. (2007). An essential switch in subunit composition of a chromatin remodeling complex during neural development. *Neuron* *55*, 201–215.
- Levine, M., Cattoglio, C., and Tjian, R. (2014). Looping back to leap forward: transcription enters a new era. *Cell* *157*, 13–25.
- Lin, Y., Bloodgood, B.L., Hauser, J.L., Lapan, A.D., Koon, A.C., Kim, T.K., Hu, L.S., Malik, A.N., and Greenberg, M.E. (2008). Activity-dependent regulation of inhibitory synapse development by Npas4. *Nature* *455*, 1198–1204.
- Liu, X.S., Wu, H., Ji, X., Stelzer, Y., Wu, X., Czauderna, S., Shu, J., Dadon, D., Young, R.A., and Jaenisch, R. (2016). Editing DNA Methylation in the Mammalian Genome. *Cell* *167*, 233–247 e17.
- Locke, J.C.W., Young, J.W., Fontes, M., Hernández Jiménez, M.J., and Elowitz, M.B. (2011). Stochastic pulse regulation in bacterial stress response. *Science* *334*, 366–369.
- Loe-Mie, Y., Lepagnol-Bestel, A.M., Maussion, G., Doron-Faigenboim, A., Imbeaud, S., Delacroix, H., Aggerbeck, L., Pupko, T., Gorwood, P., Simonneau, M., et al. (2010). SMARCA2 and other genome-wide supported schizophrenia-associated genes: regulation by REST/NRSF, network organization and primate-specific evolution. *Hum Mol Genet* *19*, 2841–2857.
- Lois, C., Hong, E.J., Pease, S., Brown, E.J., and Baltimore, D. (2002). Germline transmission and tissue-specific expression of transgenes delivered by lentiviral vectors. *Science* *295*, 868–872.
- Lu, G., Kang, Y.J., Han, J., Herschman, H.R., Stefani, E., and Wang, Y. (2006). TAB-1 modulates intracellular localization of p38 MAP kinase and downstream signaling. *J. Biol. Chem.* *281*, 6087–6095.
- Lyons, M.R., and West, A.E. (2011). Mechanisms of specificity in neuronal activity-regulated gene transcription. *Prog. Neurobiol.* *94*, 259–295.
- Lyons, G.E., Micales, B.K., Schwarz, J., Martin, J.F., and Olson, E.N. (1995). Expression of *mef2* genes in the mouse central nervous system suggests a role in neuronal maturation. *J. Neurosci.* *15*, 5727–5738.
- Lyons, M.R., Schwarz, C.M., and West, A.E. (2012). Members of the myocyte enhancer factor 2 transcription factor family differentially regulate *Bdnf* transcription in response to neuronal depolarization. *J. Neurosci.* *32*, 12780–12785.
- Lyons, M.R., Chen, L.F., Deng, J. V., Finn, C., Pfenning, A.R., Sabhlok, A., Wilson, K.M., and West, A.E. (2016). The transcription factor calcium-response factor limits NMDA receptor-dependent transcription in the developing brain. *J. Neurochem.* *137*, 164–176.
- Maeder, M.L., Linder, S.J., Cascio, V.M., Fu, Y., Ho, Q.H., and Joung, J.K. (2013). CRISPR RNA-guided activation of endogenous human genes. *Nat. Methods* *10*, 977–979.
- Majdan, M., and Shatz, C.J. (2006). Effects of visual experience on activity-dependent gene regulation in cortex. *Nat. Neurosci.* *9*, 650–659.
- Mali, P., Aach, J., Stranges, P.B., Esvelt, K.M., Moosburner, M., Kosuri, S., Yang, L., and

- Church, G.M. (2013). CAS9 transcriptional activators for target specificity screening and paired nickases for cooperative genome engineering. *Nat. Biotechnol.* *31*, 833–838.
- Malik, A.N., Vierbuchen, T., Hemberg, M., Rubin, A. a, Ling, E., Couch, C.H., Stroud, H., Spiegel, I., Farh, K.K.-H., Harmin, D. a, et al. (2014). Genome-wide identification and characterization of functional neuronal activity–dependent enhancers. *Nat. Neurosci.*
- Mao, Z. (1999). Neuronal Activity-Dependent Cell Survival Mediated by Transcription Factor MEF2. *Science* (80-.). *286*, 785–790.
- Martel, M.-A., Ryan, T.J., Bell, K.F.S., Fowler, J.H., McMahon, A., Al-Mubarak, B., Komiyama, N.H., Horsburgh, K., Kind, P.C., Grant, S.G.N., et al. (2012). The subtype of GluN2 C-terminal domain determines the response to excitotoxic insults. *Neuron* *74*, 543–556.
- Matsuda, K., Kamiya, Y., Matsuda, S., and Yuzaki, M. (2002). Cloning and characterization of a novel NMDA receptor subunit NR3B: a dominant subunit that reduces calcium permeability. *Brain Res. Mol. Brain Res.* *100*, 43–52.
- McBain, C.J., and Mayer, M.L. (1994). N-methyl-D-aspartic acid receptor structure and function. *Physiol. Rev.* *74*, 723–760.
- McCurry, C.L., Shepherd, J.D., Tropea, D., Wang, K.H., Bear, M.F., and Sur, M. (2010). Loss of Arc renders the visual cortex impervious to the effects of sensory experience or deprivation. *Nat. Neurosci.* *13*, 450–457.
- McDowell, K. a, Hutchinson, A.N., Wong-Goodrich, S.J.E., Presby, M.M., Su, D., Rodriguiz, R.M., Law, K.C., Williams, C.L., Wetsel, W.C., and West, A.E. (2010). Reduced cortical BDNF expression and aberrant memory in Carf knock-out mice. *J. Neurosci.* *30*, 7453–7465.
- McKinsey, T. a, Zhang, C.L., and Olson, E.N. (2002). MEF2: a calcium-dependent regulator of cell division, differentiation and death. *Trends Biochem. Sci.* *27*, 40–47.
- Miranti, C.K., Ginty, D.D., Huang, G., Chatila, T., and Greenberg, M.E. (1995). Calcium activates serum response factor-dependent transcription by a Ras- and Elk-1-independent mechanism that involves a.
- Morgan, J.I., Cohen, D.R., Hempstead, J.L., and Curran, T. (1987). Mapping patterns of c-fos expression in the central nervous system after seizure. *Science* (80-.). *237*, 192–197.
- Morrow, E.M., Yoo, S.Y., Flavell, S.W., Kim, T.K., Lin, Y., Hill, R.S., Mukaddes, N.M., Balkhy, S., Gascon, G., Hashmi, A., et al. (2008). Identifying autism loci and genes by tracing recent shared ancestry. *Science* (80-.). *321*, 218–223.
- Moscou, M.J., and Bogdanove, A.J. (2009). A Simple Cipher Governs DNA Recognition by TAL Effectors. *Science* (80-.). *326*, 1501–1501.
- Mueller, F., Senecal, A., Tantale, K., Marie-Nelly, H., Ly, N., Collin, O., Basyuk, E., Bertrand, E., Darzacq, X., and Zimmer, C. (2013). FISH-quant: automatic counting of transcripts in 3D FISH images. *Nat Methods* *10*, 277–278.
- Munsky, B., Neuert, G., and van Oudenaarden, A. (2012). Using Gene Expression Noise to Understand Gene Regulation. *Science* (80-.). *336*, 183–187.
- Nedivi, E., Hevroni, D., Naot, D., Israeli, D., and Citri, Y. (1993). Numerous candidate plasticity-related genes revealed by differential cDNA cloning. *Nature* *363*, 718–722.
- Nelson, S.B., and Turrigiano, G.G. (2008). Strength through diversity. *Neuron* *60*, 477–482.
- Nguyen, P. V, Abel, T., and Kandel, E.R. (1994). Requirement of a critical period of transcription for induction of a late phase of LTP. *Science* (80-.). *265*, 1104–1107.

- Nishi, M., Hinds, H., Lu, H.P., Kawata, M., and Hayashi, Y. (2001). Motoneuron-specific expression of NR3B, a novel NMDA-type glutamate receptor subunit that works in a dominant-negative manner. *J. Neurosci.* *21*, RC185.
- Nord, A.S., Blow, M.J., Attanasio, C., Akiyama, J.A., Holt, A., Hosseini, R., Phouanavong, S., Plajzer-Frick, I., Shoukry, M., Afzal, V., et al. (2013). Rapid and pervasive changes in genome-wide enhancer usage during mammalian development. *Cell* *155*, 1521–1531.
- Okamoto, S., Krainc, D., Sherman, K., and Lipton, S.A. (2000). Antiapoptotic role of the p38 mitogen-activated protein kinase-myocyte enhancer factor 2 transcription factor pathway during neuronal differentiation. *Proc. Natl. Acad. Sci. USA* *97*, 7561–7566.
- Ooe, N., Saito, K., Mikami, N., Nakatuka, I., and Kaneko, H. (2004). Identification of a novel basic helix-loop-helix-PAS factor, NXF, reveals a Sim2 competitive, positive regulatory role in dendritic-cytoskeleton modulator drebrin gene expression. *Mol Cell Biol* *24*, 608–616.
- Park, H.Y., Lim, H., Yoon, Y.J., Follenzi, a., Nwokafor, C., Lopez-Jones, M., Meng, X., and Singer, R.H. (2014). Visualization of Dynamics of Single Endogenous mRNA Labeled in Live Mouse. *Science (80-.)*. *343*, 422–424.
- Park, S., Park, J.M., Kim, S., Kim, J.A., Shepherd, J.D., Smith-Hicks, C.L., Chowdhury, S., Kaufmann, W., Kuhl, D., Ryazanov, A.G., et al. (2008). Elongation factor 2 and fragile X mental retardation protein control the dynamic translation of Arc/Arg3.1 essential for mGluR-LTD. *Neuron* *59*, 70–83.
- Partch, C.L., and Gardner, K.H. (2010). Coactivator recruitment: a new role for PAS domains in transcriptional regulation by the bHLH-PAS family. *J Cell Physiol* *223*, 553–557.
- Pérez-Otaño, I., Luján, R., Tavalin, S.J., Plomann, M., Modregger, J., Liu, X.-B., Jones, E.G., Heinemann, S.F., Lo, D.C., and Ehlers, M.D. (2006). Endocytosis and synaptic removal of NR3A-containing NMDA receptors by PACSIN1/syndapin1. *Nat. Neurosci.* *9*, 611–621.
- Perez-Pinera, P., Kocak, D.D., Vockley, C.M., Adler, A.F., Kabadi, A.M., Polstein, L.R., Thakore, P.I., Glass, K.A., Ousterout, D.G., Leong, K.W., et al. (2013). RNA-guided gene activation by CRISPR-Cas9-based transcription factors. *Nat. Methods* *10*, 973–976.
- Pfeiffer, B.E., Zang, T., Wilkerson, J.R., Taniguchi, M., Maksimova, M.A., Smith, L.N., Cowan, C.W., and Huber, K.M. (2010). Fragile X mental retardation protein is required for synapse elimination by the activity-dependent transcription factor MEF2. *Neuron* *66*, 191–197.
- Pfenning, A.R., Kim, T.-K., Spotts, J.M., Hemberg, M., Su, D., and West, A.E. (2010). Genome-wide identification of calcium-response factor (CaRF) binding sites predicts a role in regulation of neuronal signaling pathways. *PLoS One* *5*, e10870.
- Pilli, J., and Kumar, S.S. (2012). Triheteromeric N-methyl-D-aspartate receptors differentiate synaptic inputs onto pyramidal neurons in somatosensory cortex: involvement of the GluN3A subunit. *Neuroscience* *222*, 75–88.
- Plotnikov, A., Zehorai, E., Procaccia, S., and Seger, R. (2011). The MAPK cascades: signaling components, nuclear roles and mechanisms of nuclear translocation. *Biochim. Biophys. Acta* *1813*, 1619–1633.
- Pon, J.R., and Marra, M.A. (2016). MEF2 transcription factors: developmental regulators and emerging cancer genes. *Oncotarget* *7*, 2297–2312.
- Qian, Z., Gilbert, M.E., Colicos, M.A., Kandel, E.R., and Kuhl, D. (1993). Tissue-plasminogen activator is induced as an immediate-early gene during seizure, kindling and long-term potentiation. *Nature* *361*, 453–457.

- Qiu, Z., and Ghosh, A. (2008). A calcium-dependent switch in a CREST-BRG1 complex regulates activity-dependent gene expression. *Neuron* 60, 775–787.
- Qiu, Z., Ghosh, A., Aizawa, H., Hu, S.C., Bobb, K., Balakrishnan, K., Ince, G., Gurevich, I., Cowan, M., Ghosh, A., et al. (2008). A calcium-dependent switch in a CREST-BRG1 complex regulates activity-dependent gene expression. *Neuron* 60, 775–787.
- Raj, A., and van Oudenaarden, A. (2008). Nature, nurture, or chance: stochastic gene expression and its consequences. *Cell* 135, 216–226.
- Raj, A., and van Oudenaarden, A. (2009). Single-molecule approaches to stochastic gene expression. *Annu. Rev. Biophys.* 38, 255–270.
- Raj, A., van den Bogaard, P., Rifkin, S.A., van Oudenaarden, A., and Tyagi, S. (2008). Imaging individual mRNA molecules using multiple singly labeled probes. *Nat Methods* 5, 877–879.
- Rajkovich, K.E., Loerwald, K.W., Hale, C.F., Hess, C.T., Gibson, J.R., and Huber, K.M. (2017). Experience-Dependent and Differential Regulation of Local and Long-Range Excitatory Neocortical Circuits by Postsynaptic Mef2c. *Neuron* 93, 48–56.
- Ran, F.A., Cong, L., Yan, W.X., Scott, D.A., Gootenberg, J.S., Kriz, A.J., Zetsche, B., Shalem, O., Wu, X., Makarova, K.S., et al. (2015). In vivo genome editing using *Staphylococcus aureus* Cas9. *Nature* 520, 186–191.
- Rao, V.R., Pintchovski, S.A., Chin, J., Peebles, C.L., Mitra, S., and Finkbeiner, S. (2006). AMPA receptors regulate transcription of the plasticity-related immediate-early gene *Arc*. *Nat. Neurosci.* 9, 887–895.
- Roberts, A.C., Díez-García, J., Rodriguiz, R.M., López, I.P., Luján, R., Martínez-Turrillas, R., Picó, E., Henson, M. a., Bernardo, D.R., Jarrett, T.M., et al. (2009). Downregulation of NR3A-Containing NMDARs Is Required for Synapse Maturation and Memory Consolidation. *Neuron* 63, 342–356.
- Ronan, J.L., Wu, W., and Crabtree, G.R. (2013). From neural development to cognition: unexpected roles for chromatin. *Nat. Rev. Genet.* 14, 347–359.
- Rotem, A., Ram, O., Shores, N., Sperling, R.A., Goren, A., Weitz, D.A., and Bernstein, B.E. (2015). Single-cell ChIP-seq reveals cell subpopulations defined by chromatin state. *Nat Biotechnol* 33, 1165–1172.
- Saha, R.N., and Dudek, S.M. (2013). Splitting Hares and Tortoises: a classification of neuronal immediate early gene transcription based on poised RNA polymerase II. *Neuroscience* 247, 175–181.
- Saha, R.N., Wissink, E.M., Bailey, E.R., Zhao, M., Fargo, D.C., Hwang, J.-Y., Daigle, K.R., Fenn, J.D., Adelman, K., and Dudek, S.M. (2011). Rapid activity-induced transcription of *Arc* and other IEGs relies on poised RNA polymerase II. *Nat. Neurosci.* 14, 848–856.
- Sasaki, Y.F., Rothe, T., Premkumar, L.S., Das, S., Cui, J., Talantova, M. V, Wong, H.-K., Gong, X., Chan, S.F., Zhang, D., et al. (2002). Characterization and comparison of the NR3A subunit of the NMDA receptor in recombinant systems and primary cortical neurons. *J. Neurophysiol.* 87, 2052–2063.
- Schaukowitz, K., Joo, J.-Y., Liu, X., Watts, J.K., Martinez, C., and Kim, T.-K. (2014). Enhancer RNA Facilitates NELF Release from Immediate Early Genes. *Mol. Cell* 56, 29–42.
- Scheetz, A.J., and Constantine-Paton, M. (1994). Modulation of NMDA receptor function: implications for vertebrate neural development. *FASEB J.* 8, 745–752.

- Senecal, A., Munsky, B., Proux, F., Ly, N., Braye, F.E., Zimmer, C., Mueller, F., and Darzacq, X. (2014). Transcription Factors Modulate c-Fos Transcriptional Bursts. *Cell Rep.* 8, 75–83.
- Shalizi, A., Gaudilliere, B., Yuan, Z.Q., Stegmuller, J., Shirogane, T., Ge, Q.Y., Tan, Y., Schulman, B., Harper, J.W., and Bonni, A. (2006). A calcium-regulated MEF2 sumoylation switch controls postsynaptic differentiation. *Science* (80-). 311, 1012–1017.
- Shao, W., and Zeitlinger, J. (2017). Paused RNA polymerase II inhibits new transcriptional initiation. *Nat Genet* 49, 1045–1051.
- Sheffield, N.C., Thurman, R.E., Song, L., Safi, A., Stamatoyannopoulos, J.A., Lenhard, B., Crawford, G.E., and Furey, T.S. (2013). Patterns of regulatory activity across diverse human cell types predict tissue identity, transcription factor binding, and long-range interactions. *Genome Res* 23, 777–788.
- Sheng, M., Thompson, M.A., and Greenberg, M.E. (1991). CREB: a Ca(2+)-regulated transcription factor phosphorylated by calmodulin-dependent kinases. *Science* 252, 1427–1430.
- Shyu, A.B., Greenberg, M.E., and Belasco, J.G. (1989). The c-fos transcript is targeted for rapid decay by two distinct mRNA degradation pathways. *Genes Dev* 3, 60–72.
- Sim, S., Antolin, S., Lin, C.W., Lin, Y., and Lois, C. (2013). Increased cell-intrinsic excitability induces synaptic changes in new neurons in the adult dentate gyrus that require Npas4. *J. Neurosci.* 33, 7928–7940.
- Soliman, F., Glatt, C.E., Bath, K.G., Levita, L., Jones, R.M., Pattwell, S.S., Jing, D., Tottenham, N., Amso, D., Somerville, L.H., et al. (2010). A genetic variant BDNF polymorphism alters extinction learning in both mouse and human. *Science* 327, 863–866.
- Spiegel, I., Mardinly, A.R., Gabel, H.W., Bazinet, J.E., Couch, C.H., Tzeng, C.P., Harmin, D.A., and Greenberg, M.E. (2014). Npas4 regulates excitatory-inhibitory balance within neural circuits through cell-type-specific gene programs. *Cell* 157, 1216–1229.
- Stasevich, T.J., Hayashi-Takanaka, Y., Sato, Y., Maehara, K., Ohkawa, Y., Sakata-Sogawa, K., Tokunaga, M., Nagase, T., Nozaki, N., McNally, J.G., et al. (2014). Regulation of RNA polymerase II activation by histone acetylation in single living cells. *Nature* 516, 272–275.
- Stevenson, M., Muramoto, T., Müller, I., and Chubb, J.R. (2010). Digital nature of the immediate-early transcriptional response. *Development* 137, 579–584.
- Su, Y., Shin, J., Zhong, C., Wang, S., Roychowdhury, P., Lim, J., Kim, D., Ming, G.L., and Song, H. (2017). Neuronal activity modifies the chromatin accessibility landscape in the adult brain. *Nat Neurosci* 20, 476–483.
- Sucher, N.J., Akbarian, S., Chi, C.L., Leclerc, C.L., Awobuluyi, M., Deitcher, D.L., Wu, M.K., Yuan, J.P., Jones, E.G., and Lipton, S.A. (1995). Developmental and regional expression pattern of a novel NMDA receptor-like subunit (NMDAR-L) in the rodent brain. *J. Neurosci.* 15, 6509–6520.
- Sucher, N.J., Yu, E., Chan, S.F., Miri, M., Lee, B.J., Xiao, B., Worley, P.F., and Jensen, F.E. (2010). Association of the small GTPase Rheb with the NMDA receptor subunit NR3A. *Neurosignals.* 18, 203–209.
- Sweatt, J.D. (2013). The Emerging Field of Neuroepigenetics. *Neuron* 80, 624–632.
- Symmons, O., and Raj, A. (2016). What’s Luck Got to Do with It: Single Cells, Multiple Fates, and Biological Nondeterminism. *Mol. Cell* 62, 788–802.
- Tao, X., Finkbeiner, S., Arnold, D.B., Shaywitz, A.J., and Greenberg, M.E. (1998). Ca²⁺ influx

regulates BDNF transcription by a CREB family transcription factor-dependent mechanism. *Neuron* 20, 709–726.

Tao, X., West, A.E., Chen, W.G., Corfas, G., and Greenberg, M.E. (2002a). A Calcium-Responsive Transcription Factor, CaRF, that Regulates Neuronal Activity-Dependent Expression of BDNF. *Neuron* 33, 383–395.

Tao, X., West, A.E., Chen, W.G., Corfas, G., and Greenberg, M.E. (2002b). A calcium-responsive transcription factor, CaRF, that regulates neuronal activity-dependent expression of BDNF. *Neuron* 33, 383–395.

Thakore, P.I., Black, J.B., Hilton, I.B., and Gersbach, C.A. (2016). Editing the epigenome: technologies for programmable transcription and epigenetic modulation. *Nat Methods* 13, 127–137.

Tsai, N.P., Wilkerson, J.R., Guo, W., Maksimova, M.A., DeMartino, G.N., Cowan, C.W., and Huber, K.M. (2012). Multiple autism-linked genes mediate synapse elimination via proteasomal degradation of a synaptic scaffold PSD-95. *Cell* 151, 1581–1594.

Turrigiano, G.G., and Nelson, S.B. (2004). Homeostatic plasticity in the developing nervous system. *Nat. Rev. Neurosci.* 5, 97–107.

Urnov, F.D., Miller, J.C., Lee, Y.-L., Beausejour, C.M., Rock, J.M., Augustus, S., Jamieson, A.C., Porteus, M.H., Gregory, P.D., and Holmes, M.C. (2005). Highly efficient endogenous human gene correction using designed zinc-finger nucleases. *Nature* 435, 646–651.

Vasanwala, F.H., Kusam, S., Toney, L.M., and Dent, A.L. (2002). Repression of AP-1 function: a mechanism for the regulation of Blimp-1 expression and B lymphocyte differentiation by the B cell lymphoma-6 protooncogene. *J Immunol* 169, 1922–1929.

Vera, M., Biswas, J., Senecal, A., Singer, R.H., and Park, H.Y. (2016). Single-Cell and Single-Molecule Analysis of Gene Expression Regulation. *Annu Rev Genet* 50, 267–291.

Visel, A., Taher, L., Girgis, H., May, D., Golonzhka, O., Hoch, R. V, McKinsey, G.L., Pattabiraman, K., Silberberg, S.N., Blow, M.J., et al. (2013). A high-resolution enhancer atlas of the developing telencephalon. *Cell* 152, 895–908.

Vogel-Ciernia, A., and Wood, M.A. (2014). Neuron-specific chromatin remodeling: A missing link in epigenetic mechanisms underlying synaptic plasticity, memory, and intellectual disability disorders. *Neuropharmacology* 80, 18–27.

Vogel-Ciernia, A., Matheos, D.P., Barrett, R.M., Kramar, E.A., Azzawi, S., Chen, Y., Magnan, C.N., Zeller, M., Sylvain, A., Haettig, J., et al. (2013). The neuron-specific chromatin regulatory subunit BAF53b is necessary for synaptic plasticity and memory. *Nat Neurosci* 16, 552–561.

Wang, K.H., Majewska, A., Schummers, J., Farley, B., Hu, C., Sur, M., and Tonegawa, S. (2006). In vivo two-photon imaging reveals a role of arc in enhancing orientation specificity in visual cortex. *Cell* 126, 389–402.

West, A.E., and Greenberg, M.E. (2011). Neuronal activity-regulated gene transcription in synapse development and cognitive function. *Cold Spring Harb. Perspect. Biol.* 3, 1–21.

West, A.E., Griffith, E.C., and Greenberg, M.E. (2002). Regulation of transcription factors by neuronal activity. *Nat. Rev. Neurosci.* 3, 921–931.

West, A.E., Pruunsild, P., and Timmusk, T. (2014). *Neurotrophic Factors* (Berlin, Heidelberg: Springer Berlin Heidelberg).

Whitney, O., Pfenning, a. R., Howard, J.T., Blatti, C. a., Liu, F., Ward, J.M., Wang, R., Audet,

- J.-N., Kellis, M., Mukherjee, S., et al. (2014). Core and region-enriched networks of behaviorally regulated genes and the singing genome. *Science* (80-). *346*, 1256780–1256780.
- Wiesel, T.N. (1982). Postnatal development of the visual cortex and the influence of environment. *Nature* *299*, 583–591.
- Wijayatunge, R., Chen, L.-F., Cha, Y.M., Zannas, A.S., Frank, C.L., and West, A.E. (2014). The histone lysine demethylase Kdm6b is required for activity-dependent preconditioning of hippocampal neuronal survival. *Mol. Cell. Neurosci.* *61*, 187–200.
- Wilkerson, J.R., Tsai, N.-P., Maksimova, M.A., Wu, H., Cabalo, N.P., Loerwald, K.W., Dictenberg, J.B., Gibson, J.R., and Huber, K.M. (2014). A role for dendritic mGluR5-mediated local translation of Arc/Arg3.1 in MEF2-dependent synapse elimination. *Cell Rep.* *7*, 1589–1600.
- Winter, G.E., Mayer, A., Buckley, D.L., Erb, M.A., Roderick, J.E., Vittori, S., Reyes, J.M., di Iulio, J., Souza, A., Ott, C.J., et al. (2017). BET Bromodomain Proteins Function as Master Transcription Elongation Factors Independent of CDK9 Recruitment. *Mol Cell.*
- Wong, H.-K., Liu, X.-B., Matos, M.F., Chan, S.F., Pérez-Otaño, I., Boysen, M., Cui, J., Nakanishi, N., Trimmer, J.S., Jones, E.G., et al. (2002). Temporal and regional expression of NMDA receptor subunit NR3A in the mammalian brain. *J. Comp. Neurol.* *450*, 303–317.
- Wu, J.I., Lessard, J., Olave, I.A., Qiu, Z., Ghosh, A., Graef, I.A., and Crabtree, G.R. (2007). Regulation of dendritic development by neuron-specific chromatin remodeling complexes. *Neuron* *56*, 94–108.
- Wyatt, R.M., Tring, E., and Trachtenberg, J.T. (2012). Pattern and not magnitude of neural activity determines dendritic spine stability in awake mice. *Nat. Neurosci.* *15*, 949–951.
- Wyllie, D.J.A., Livesey, M.R., and Hardingham, G.E. (2013). Influence of GluN2 subunit identity on NMDA receptor function. *Neuropharmacology* *74*, 4–17.
- Xia, Z., Dudek, H., Miranti, C.K., and Greenberg, M.E. (1996). Calcium influx via the NMDA receptor induces immediate early gene transcription by a MAP kinase/ERK-dependent mechanism. *J. Neurosci.* *16*, 5425–5436.
- Yamada, T., Yang, Y., Hemberg, M., Yoshida, T., Cho, H.Y., Murphy, J.P., Fioravante, D., Regehr, W.G., Gygi, S.P., Georgopoulos, K., et al. (2014). Promoter Decommissioning by the NuRD Chromatin Remodeling Complex Triggers Synaptic Connectivity in the Mammalian Brain. *Neuron* *83*, 122–134.
- Yang, Y., Yamada, T., Hill, K.K., Hemberg, M., Reddy, N.C., Cho, H.Y., Guthrie, A.N., Oldenborg, A., Heiney, S.A., Ohmae, S., et al. (2016). Chromatin remodeling inactivates activity genes and regulates neural coding. *Science* (80-). *353*.
- Zehorai, E., and Seger, R. (2014). Beta-like importins mediate the nuclear translocation of mitogen-activated protein kinases. *Mol. Cell. Biol.* *34*, 259–270.
- Zenklusen, D., Larson, D.R., and Singer, R.H. (2008). Single-RNA counting reveals alternative modes of gene expression in yeast. *Nat. Struct. Mol. Biol.* *15*, 1263–1271.
- Zhai, S., Ark, E.D., Parra-Bueno, P., and Yasuda, R. (2013). Long-distance integration of nuclear ERK signaling triggered by activation of a few dendritic spines. *Science* (80-). *342*, 1107–1111.
- Zhan, X., Shi, X., Zhang, Z., Chen, Y., and Wu, J.I. (2011). Dual role of Brg chromatin remodeling factor in Sonic hedgehog signaling during neural development. *Proc. Natl. Acad. Sci. U. S. A.* *108*, 12758–12763.
- Zhang, H., Roberts, D.N., and Cairns, B.R. (2005). Genome-wide dynamics of Htz1, a histone

H2A variant that poises repressed/basal promoters for activation through histone loss. *Cell* 123, 219–231.

Zhang, Z., Cao, M., Chang, C.-W., Wang, C., Shi, X., Zhan, X., Birnbaum, S.G., Bezprozvanny, I., Huber, K., and Wu, J.I. (2015). Autism-Associated Chromatin Regulator Brg1/SmadA4 is Required for Synapse Development and MEF2-mediated Synapse Remodeling. *Mol. Cell. Biol.* 36, MCB.00534-15.

Zhu, B., and Gulick, T. (2004). Phosphorylation and alternative pre-mRNA splicing converge to regulate myocyte enhancer factor 2C activity. *Mol. Cell. Biol.* 24, 8264–8275.

Zhu, Y., Pak, D., Qin, Y., McCormack, S.G., Kim, M.J., Baumgart, J.P., Velamoor, V., Auberson, Y.P., Osten, P., van Aelst, L., et al. (2005). Rap2-JNK removes synaptic AMPA receptors during depotentiation. *Neuron* 46, 905–916.

Zippo, A., Serafini, R., Rocchigiani, M., Pennacchini, S., Krepelova, A., and Oliviero, S. (2009). Histone crosstalk between H3S10ph and H4K16ac generates a histone code that mediates transcription elongation. *Cell* 138, 1122–1136.

Biography

Liang-Fu Chen

Date of Birth:	January 07, 1984
Place of Birth:	Hsinchu City, Taiwan
Education:	
Graduate Student, Neurobiology, Duke University, USA	2011.08- present
M.S., Biochemical Science, National Taiwan University, Taiwan	2006.09-2008.06
B.S., Psychology, National Taiwan University, Taiwan	2002.09-2006.06

Publications:

1. Gomez-Schiavon M, **Chen LF**, West AE, Buchler NE. (2017). *Genome Biol.* 18(1):164.
2. **Chen LF**, Zhou AS, West AE. (2017). *J. Neurophysiol.* 118(2):755-770. Review.
3. Chakraborty M, **Chen LF**, Fridel EE, Klein ME, Senft RA, Sarkar A, Jarvis ED. (2017). *Sci Rep.* 7(1):942.
4. Lyons MR*, **Chen LF***, Deng JV, Finn C, Pfenning AR, Sabhlok A, Wilson KM, West AE. (2016). *J Neurochem.* 137(2):164-76. *equal contribution
5. Norris KL, Hao R, **Chen LF**, Lai CH, Kapur M, Shaughnessy PJ, Chou D, Yan J, Taylor JP, Engelender S, West AE, Lim KL, Yao TP. (2015). *J Biol Chem.* 290(22):13862-74.
6. Wijayatunge R, **Chen LF**, Cha YM, Zannas AS, Frank CL, West AE. (2014). *Mol Cell Neurosci.* 61:187-200.
7. Ghiretti A, Moore A, Brenner R, **Chen LF**, West AE, Lau N, Hooser SV, Paradis S. (2014). *J. Neurosci.* 34(2):392– 407.
8. Liang CY, Wang LJ, Chen CP, **Chen LF**, Chen YH, Chen H. (2010). *Biol Reprod.* 83(3):387-95.
9. Chiang MH*, **Chen LF***, Chen H. (2008). *Biol Reprod.* 79(5):914-20. *equal contribution
10. Chen CP, **Chen LF**, Yang SR, Chen CY, Ko CC, Chang GD, Chen H. (2008). *Biol Reprod.* 79(5):815-23.
11. Chou CC, Chang C, Liu JH, **Chen LF**, Hsiao CD, Chen H. (2007). *J Biol Chem.* 282(37):27239-49.

Funding and Awards:

Duke Graduate School Conference Travel Award	2014, 2016
Hung Taiwan-Duke University Fellowship	2011-2012
Top Master's Thesis Award	2008